Performance Evaluation of Powerline Technology on Low Voltage Distribution Networks

Thesis

PERFORMANCE EVALUATION OF POWERLINE TECHNOLOGY ON LOW VOLTAGE DISTRIBUTION NETWORKS

Lister Wills BEng. CEng. MIET

A thesis submitted to the Open University Faculty of Mathematics, Computing and Technology for the degree of Doctor of Philosophy

JULY 2013

DATE of SUBMISSION: 28 JUNE 2013
DATE of AWARD: 18 FEBRUARY 2014

ProQuest LLC.
789 East Eisenhower Parkway
P.O. Box 1346
Ann Arbor, MI 48106 – 1346

ABSTRACT

Powerline technology (PLT) employs the electrical distribution network to transmit data in addition to supplying power. PLT is currently employed to provide data networking in many domestic environments, and is expected to play a major part in the development of the forthcoming Smart Grid.

Given that the electrical distribution network was not designed with data transmission in mind, electromagnetic radiation from the network can give rise to interference. Regulators and researchers have considered the impact of such widespread radiation, and investigations of the various aspects of powerline have been conducted over the last decade. Despite this prolonged period, however, there remains a lack of agreement on the typical performance of such networks or the implications for regulation policy.

An accurate model of the radio frequency (RF) properties of the typical electrical distribution network would be extremely valuable in developing standards and informing policy. The aim of this thesis is to provide a cohesive approach to determining the RF characteristics of a typical domestic property and applying such parameters to model the performance of PLT.

The thesis reviews the recent development of broadband PLT, the progress made by the more prominent regulators, and the trials undertaken to define the key parameters affecting propagation. A detailed experimental programme carried out both in the laboratory and at typical sites is described.

An empirical model of the RF performance of a UK domestic low voltage distribution network (LVDN) is developed from analysis of the experimental

results. It is shown via this analysis that discrete measurements of the conducted and radiated parameters can be related and that the RF performance of the LVDN can be described by Conversion and Radiated Loss. The radiated field is shown to comprise the combined common mode current to the LVDN and common bonding network (CBN).

The thesis concludes with consideration of the future development of powerline technology, particularly in support of the Smart Grid development.

ACKNOWLEDGEMENT

Thank you jet stream .. I owe you ... having a thesis submission date at the end of June was never ideal but the British summer has not let me down and here we are in the nick of time.

My sincere gratitude goes first to Sandie and the girls for their extreme patience in allowing me the opportunity to complete this work, I appreciate that summer 2013 has not been fun so far and we shall make amends.

I am also greatly indebted to my supervisors at the Open University for their patience and support over the years. Dr John Newbury has remained an unswerving source of enthusiasm and has provided a regular insight on the progress of the international powerline community, whilst Dr Adrian Poulton has provided the guidance so often needed.

Finally, I would like to thank the Open University for providing some of the equipment used within the measurements described below, and especially Fraser Robertson, for his advice when things went wrong.

LIST OF ABBREVIATIONS

ADSL	Asymmetric Digital Subscriber Link
BALUN	Balanced to unbalanced impedance transformer
CENELEC	European Committee for Electro technical Standardisation
CISPR	International Special Committee on Radio Interference
CM	Common Mode
CMC	Common Mode Current
CMZ	Common Mode Impedance
CBN	Common Bonding Network
CPD	Circuit Protective Device
CUT	Circuit under Test
DM	Differential Mode
DMC	Differential Mode Current
DMZ	Differential Mode Impedance
EMC	Electromagnetic Compatibility
EMI	Electromagnetic Interference
ETSI	European Telecommunications Standards Institute
HF	High Frequency
IEEE	Institute of Electrical and Electronics Engineers
ITU	International Telecommunication Union
L-ISN	Line Impedance Stabilisation Network
LCL	Longitudinal Conversion Loss
LV	Low Voltage
LVDN	Low voltage distribution network
OFDM	Orthogonal Frequency Division Multiplexing
OU	Open University
OUPLTRG	Open University PLT Research Group
NSO	National Standards Organisation
PAPR	Peat to Average Power Ratio
PVC	Polyvinylchloride

PLT	Powerline Technology
PME	Permanent Multiple Earthing
PSD	Power Spectral Density
QP	Quasi-peak
REC	Regional Electricity Company
RF	Radio Frequency
RBW	Resolution Bandwidth
SA	Spectrum Analyser
TCL	Transverse Conversion Loss
TG	Tracking Generator
TN-C-S	Combined Neutral Earth Earthing System
VoP	Velocity of Propagation
VSWR	Voltage Standing Waves Ratio

LIST OF SYMBOLS

α	Attenuation Coefficient
β	Propagation Coefficient
δ	Skin Depth
ε	Permittivity
λ	Wavelength
μ	Permeability
ρ	Density
σ	Conductivity
ω	Angular frequency
Ω.	Ohms
Γ	Reflection Coefficient
B	Bandwidth
C	Capacitance
d	Distance
d_{NF}	Distance near field transition
L	Inductance
r	Radius
Z	Impedance
S_{11}	Return Loss (dB)
S_{21}	Efield (dBμV/m)

CONTENTS

1 INTRODUCTION

1.1 Introduction to Powerline 1

1.2 History of Broadband PLT Development 3

1.3 Commercial Opportunities for PLT 3

1.4 Widespread Implementation 7

1.5 Regulation is Required 8

1.6 How to Regulate 9

1.7 A future for PLT 10

1.8 Thesis Structure 11

1.9 Summary of Broadband PLT 12

2 LITERATURE REVIEW

2.1 Introduction to Literature Review 14

2.2 Regulation Review 14

2.3 Review of CISPR Standards 16

2.4 OPEN PLC European Research Alliance (OPERA) D84 18

2.5 CENELEC/ETSI Code of Practice 19

2.6 Draft Standard prEN 50471 20

2.7 IEEE Std 1775-2010 21

2.8 Review of ITU-R SM.2158-2 22

2.9 Draft Standard prEN 50561-1 22

2.10 Review of Modelling 23

2.11 Review of Field Trials 24

2.12 PA Consulting (OFCOM) 25

2.13 NATO – Research Task Group 26

2.14 Communications Research Centre (CRC) of Canada 27

2.15 Open University PLT Research Group (OUPLTRG) 28

2.16 Trial Methodology 29

2.17 Summary & Research Questions 31

3 THEORY

3.1 Introduction to Theory 33

3.2 PLT Signal Injection 33

3.3 PLT Signal Distribution 37

3.4 Physical Arrangement of the LVDN 38

3.5 Wiring Installation 41

3.6 Earthing & Bonding 42

3.7 Characteristic Impedance 43

3.8 Low Voltage Distribution Network (LVDN) Impedances 46

3.9 Transverse and Longitudinal Conversion Loss (TCL & LCL) 51

3.10 Reflections & Discontinuities 54

3.11 Skin Depth 55

3.12 Common Mode Transfer 56

3.13 Field Generation 57

3.14 Basis for Measurement 64

3.15 Ingress & Conducted Noise Floor 67

3.16 RF Noise floor 68

3.17 k Factor, Antenna Factor & Emission Factor 71

3.18 Near Field/Far Field Transition & Regression 73

3.19 Isotropic Equivalent Field 74

3.20 Summary 75

4 MEASUREMENTS

4.1 Introduction 77

4.2 Test Methodology 78

4.3 Characteristic Impedance (Twin & Earth Cabling) 81

4.4 BALUN 82

4.5 Directional Coupler 82

4.6 Spectrum Analyser & Tracking Generator 83

4.7 Current Probe 85

4.8 TCL Probe 88
4.9 Signal Level 89
4.10 S_{21} Radiated Field 89
4.11 Mains Coupler 92
4.12 Line Impedance Stabilisation Network (L-ISN) 93
4.13 Measurements 95
4.14 Test Cable – Unterminated 96
4.15 Test Cable – Terminated 100Ω 103
4.16 Bramble – LVDN Measurements 113
4.17 Summary of Initial Measurements 124
4.18 Bramble – Individual Circuits 127
4.19 Lighting Radial –All luminaires off 128
4.20 Lighting Radial – All luminaires on 134
4.21 Cooker Radial – OFF 139
4.22 Cooker Radial - On 146
4.23 Ring Main 149
4.24 Summary of Circuit Tests 155
4.25 PLT Measurements 159
4.26 L-ISN – PLT Measurements 160
4.27 BRAMBLE – PLT Measurements 164
4.28 Measurement Uncertainty 167

5 CONCLUSIONS

5.1 Introduction 169
5.2 Model 169
5.3 Conversion Loss 171
5.4 Radiated Loss 172
5.5 Earthing 175
5.6 Overall Conclusion 177

6 FURTHER WORK

6.1 Introduction 180

6.2 Areas of further study 180

6.3 Future Design 181

6.4 Smart Grid and Powerline of the Future 182

FIGURES

Figure 1.3.1 Develo DLAN 200 (Develo, 2009) 4

Figure 1.6.1 Limits of Radiated Disturbances below 30MHz (BSI, 2006) 10

Figure 2.16.1 Diagram of Local Distribution Cabling (OFCOM, 2010) 29

Figure 3.4.1 REC Service Head at Mains Intake (IET, 2008) 39

Figure 3.4.2 Detail of the UK Standard 'twin and earth' Cable (Eland, 2009) 40

Figure 3.6.1 Impression to indicate the Principle of a CBN (Williams, 2000) 43

Figure 3.7.1 Calculation of cable characteristics for 2.5mm^2 'twin and earth' 46

Figure 3.8.1 Sketch identifying the Extent of the Differential Signal Circuit 47

Figure 3.8.2 Calculation of Transmission Factors for 2.5mm^2 'twin and earth' 49

Figure 3.8.3 Sketch identifying the Extent of the Asymmetrical Circuit 50

Figure 3.13.1 Geometrical Arrangement for the Common Mode Circuit (Donohoe, 2012) 58

Figure 3.13.2 Image of Array Factor for Common Mode Circuit (Donohoe, 2012) 59

Figure 3.13.3 Image of Field Generation from CMC and DMC (Donohoe, 2012) 61

Figure 3.14.1 Indicative Arrangement for Test Cell 'setup' (EN 55016) 65

Figure 3.15.1 Typical ingress noise floor at GLEBE, 2010 68

Figure 3.16.1 Typical 'rural' noise floor, 2010 71

Figure 3.20.1 Predicted Performance of a PLT system 75

Figure 4.2.1 S Parameters 79

Figure 4.2.2 Measurement Setup 80

Figure 4.6.1 Image of spectrum analyser sample processing (RS, 2008) 84

Figure 4.7.1 HF Current probe on ring main recording Comtrend DMC 86

Figure 4.10.1 Antenna Factor for Wellbrook Loop 90

Figure 4.11.1Circuit Diagram for mains coupler 92

Figure 4.11.1 Image of completed coupler 93

Figure 4.12.1 TCL Measured for the Rohde & Schwarz L-ISN 95

Figure 4.14.1 S_{11} for Unterminated Test Cable 96

Figure 4.14.2 DMC for Unterminated Test Cable 97

Figure 4.14.3 CMC for Unterminated Test Cable 98

Figure 4.14.4 Reduction in Electrical Length to Differential Mode Path 99
Figure 4.14.5 Current Graph for Unterminated Test Cable 99
Figure 4.14.6 S_{21} for Unterminated Test Cable 101
Figure 4.14.7 Radiated Graph for Unterminated Test Cable 102
Figure 4.14.8 Transfer Factor Graph for Unterminated Test Cable 103
Figure 4.15.1 S_{11} on Terminated Test Cable 104
Figure 4.15.2 DMC(Left) and CMC(Right) on Terminated Test Cable 105
Figure 4.15.3 TCL for Terminated Test Cable 106
Figure 4.15.4 LCL for Cat 3 Cabling 107
Figure 4.15.5 Impedance Graphs for Terminated Test Cable 108
Figure 4.15.6 Current Graph for Terminated Test Cable 109
Figure 4.15.7 S_{21} for Terminated Test Cable 110
Figure 4.15.8 Radiated Graph for Terminated Test Cable 111
Figure 4.15.9 Transfer Factor Graph for Terminated Test Cable 112
Figure 4.16.1 Bramble Layout and Outlet Positions 114
Figure 4.16.2 S_{11} for Bramble 115
Figure 4.16.3 TCL for Bramble 116
Figure 4.16.4 S_{21} for Bramble 117
Figure 4.16.5 Current Graph for Bramble 117
Figure 4.16.6 Current Graph for Bramble 118
Figure 4.16.7 S_{21} for Bramble with PME Disconnected 119
Figure 4.16.8 Impedance Graph for Bramble 121
Figure 4.16.9 Radiated Graph for Bramble 122
Figure 4.16.10 Transfer Graph for Bramble 123
Figure 4.17.1 Power Diagram 124
Figure 4.17.2 Factor Graph for Bramble 125
Figure 4.17.3 Image of Wellbrook Antenna at 10 metre range 127
Figure 4.19.1 Current Graph for Lighting Circuit – OFF 129
Figure 4.19.2 VSWR Graph for Lighting Circuit – OFF 130
Figure 4.19.3 Impedance Graph for Lighting Circuit – OFF 131

Figure 4.19.4 Radiated Graph for Lighting Circuit – OFF 132
Figure 4.19.5 Radiated Graph for Lighting OFF and Earthed 134
Figure 4.20.1 Current Graph for Lighting Circuit – ON & OFF 135
Figure 4.20.2 TCL Variation for Lighting Circuit– ON & OFF 136
Figure 4.20.3 Radiation Graph for Lighting Circuit– ON & OFF 137
Figure 4.20.4 Gain Graph for Lighting Circuit – ON & OFF 137
Figure 4.20.5 Measured and Calculated Efield 139
Figure 4.21.1 10mm^2 Cable Characteristics 140
Figure 4.21.2 Current Graph for Cooker OFF 141
Figure 4.21.3 Power Loss to TCL Comparison for Cooker OFF 142
Figure 4.21.4 Radiated Graph for Cooker OFF 143
Figure 4.21.5 Graph indicating CM Power & Efield for Lighting & Cooker 145
Figure 4.22.1 Current Graph for Cooker - On 147
Figure 4.22.2 Gain Graph for Cooker - On 148
Figure 4.22.3 Power and Efield Graph for Cooker - On 149
Figure 4.23.1 Power Graph for Ring Main 150
Figure 4.23.2 TCL measurement along Ring Main 151
Figure 4.23.3 TCL Measurement on Ring Main at Mains Position 152
Figure 4.23.4 Gain Graph for Cooker, Lighting and Ring Main 153
Figure 4.23.5 Transfer Graph for Ring Main 154
Figure 4.24.1 TCL to Conversion Loss Comparison per circuit type 156
Figure 4.24.2 Gain Graph for Bramble 158
Figure 4.25.1 Comtrend Conducted Voltage and Current Measurements 159
Figure 4.26.1 Image of the Comtrend modems operating via the L-ISN 162
Figure 4.26.2 Profile of Comtrend radiated field via L-ISN 164
Figure 4.27.1 DMC & CMC for Comtrend on Bramble 165
Figure 4.27.2 Graph of Efield with Noise Floor 167
Figure 5.3.1 Power Graph for Bramble 172
Figure 5.4.1 Power Density Graph for Bramble 173
Figure 5.4.2 – Power Density Graph for Comtrend 174

Figure 5.5.1 TCL and PME current for Bramble 175
Figure 5.5.2 Comparison of LVDN CMC & PME CMC 176
Figure 5.5.3 CMC Distribution Diagram 177

TABLES

Table 2.3.1 Conducted Mode Voltage at PLT ports (BSI, 2006) 17

Table 2.6.1 Limits of Conducted Current on Network Cable (BSI, 2006) 20

Table 2.12.1 Verification for Household Wiring Performance (OFCOM, 2010) 25

Table 3.13.1 Attenuation of HF signals within structures (Ishigami, 2007) 63

Table 3.16.1 Value of constants c & d 70

Table 3.17.1 Emission Factors for several OUPLCRG Test Sites (Brannon, 2005) ... 72

Table 4.3.1 Characteristic Impedance Measurements 81

Table 4.15.1 Average Values for Test Cable 113

Table 4.19.1 Power Values for Lighting Circuit – OFF & Bramble 133

Table 4.21.1 Average Values for Light OFF & Cooker OFF 146

Table 4.24.1 Table of Average Parameter Values for Circuit Type 155

Table 4.24.2 Gain Comparison per circuit type 157

Table 4.26.1 Values of Comtrend conducted parameters via L-ISN 161

Table 4.26.2 Comtrend S_{21} via L-ISN 164

Table 4.27.1 Bramble Average Values 166

EQUATIONS

Equation 3.2.1 34

Equation 3.2.2 34

Equation 3.2.3 35

Equation 3.2.4 35

Equation 3.2.5 36

Equation 3.3.1 37

Equation 3.3.2 38

Equation 3.7.1 44

Equation 3.7.2 44

Equation 3.7.3 44

Equation 3.7.4 44

Equation 3.7.5 45

Equation 3.7.6 45

Equation 3.8.1 47

Equation 3.8.2 48

Equation 3.8.3 48

Equation 3.8.4 51

Equation 3.9.1 52

Equation 3.9.2 53

Equation 3.10.1 55

Equation 3.10.2 55

Equation 3.11.1 55

Equation 3.11.2 56

Equation 3.13.1 58

Equation 3.13.2 58

Equation 3.13.3 60

Equation 3.13.4 60

Equation 3.13.5 60

Equation 3.13.6 61
Equation 3.13.7 61
Equation 3.13.8 62
Equation 3.13.9 62
Equation 3.13.10 62
Equation 3.16.1 69
Equation 3.16.2 69
Equation 3.16.3 70
Equation 3.17.1 71
Equation 3.17.2 72
Equation 3.17.3 72
Equation 3.18.1 74
Equation 3.19.1 74
Equation 4.2.1 79
Equation 4.3.1 81
Equation 4.6.1 85
Equation 4.7.1 86
Equation 4.7.2 87
Equation 4.8.1 88
Equation 4.10.1 90
Equation 4.10.2 92
Equation 4.10.3 92
Equation 4.14.1 97
Equation 4.14.2 100
Equation 4.15.1 107
Equation 4.5.11 126
Equation 4.26.1 162
Equation 4.26.2 163

CHAPTER 1- INTRODUCTION

1.1 Introduction to Powerline

Powerline technology (PLT) is the generic name used throughout this thesis to describe the simultaneous transmission of mains power and 'broadband' communications data via the medium and low voltage electrical distribution networks (LVDN). Given the international application of PLT it is also often referred to as powerline carrier or communications (PLC), broadband for power lines (BPL) and more often simply as powerline, however, all these terms are generally interchangeable.

Powerline technology is currently employed to provide limited connectivity in many domestic environments and is expected to play a major part in the development of the forth coming Smart Grid, through connectivity and control of appliances, metering plant and embedded energy generators. Many researchers, including institutions such as ETSI and the ITU, have therefore considered the impact of such widespread implementation and investigations of the various aspects of PLT have been conducted over the last decade.

Whilst most researchers agree that the LVDN is not the ideal medium for the propagation of high frequency broadband signals there is little agreement on the typical RF performance for such networks nor how to regulate any subsequent electromagnetic interference (EMI) resulting from such networks.

A dichotomy for regulators exists; should EMI from powerline be limited by imposing power limits to the injected signal, by imposing conducted limits to

common mode current or through limitation of the permissible radiated field from the LVDN? There is much debate but no clear policy.

This thesis aims to progress these issues with the development of this research to provide an overall model of the LVDN performance.

- Chapter 1 therefore commences with a historical overview of the recent development of broadband PLT and discusses modem development for use on the LVDN.

- Chapter 2 reviews progress made by the more prominent regulators and considers some of the field trials undertaken to define the key parameters affecting propagation. A technical description of the parameters and metrics for defining the LVDN and PLT performance is provided in Chapter 3.

- Chapter 4 provides details of the measurements undertaken as part of this thesis, whilst Chapter 5 extrapolates the measurements via analysis and development of a model, depicting the 'standard' UK domestic LVDN.

- Chapter 6 concludes with consideration of the future development of powerline technology, particularly in support of Smart Grid development, and gives an indication of expected LVDN performance issues and areas for further research.

1.2 History of Broadband PLT Development

The commercial use of powerline technology has been in existence since the 1870s (Dostert, 2001) when electrical utilities companies in the United States used their electrical distribution systems to provide network monitoring and control functions. Whilst the need for such monitoring was the driving force for PLT development, the additional advantages of providing communication between remote parts of the network were soon considered a significant benefit.

Traditionally PLT technology has used the frequencies below 150 kHz and this form of PLT was eventually formalised via CENELEC within the standard EN50065-1. By the 1950s low frequency powerline technology was widely used on medium and low voltage networks for the transmission of controls and signalling information associated with the protection and inter-tripping equipment.

Gradual expansion of PLT usage by the utilities led to various communication techniques being employed in remote network areas, where alternative forms of communication were not available; however for the first 30 years PLT technology was essentially the preserve of the utility companies, having little other commercial potential.

1.3 Commercial Opportunities for PLT

During the decades leading up to the millennium, the development of PLT had concentrated primarily on distribution functions, such as automatic meter reading, selective load control and demand side management for Utility Companies. However, in parallel to these developments a plethora of

communication networking technologies, with associated IEEE standards such as 802.3 'Ethernet' & 802.11 'wireless', also emerged to satisfy the rapidly growing commercial and domestic IT infrastructure needs.

Given that both these developments occurred during the time that many of the Utility Companies had become privatised, a realisation spread that opportunities for further commercial revenue may exist via the application of PLT to the electricity supply of domestic consumers providing alternative high speed broadband connectivity.

Equally the application of PLT to the domestic wiring within a property, providing a direct alternative to some of the networking technologies described above, was also considered to be a significant market for PLT devices. This was realised by the marketing of several stand-alone plug and play products, such as the Develo DLAN 200 shown in Figure 1.3.1.

Figure 1.3.1 Develo DLAN 200 (Develo, 2009)

The DLAN 200 typifies the majority of PLT devices for the domestic market, providing a throughput data rate of 200 megabits per second via the injection of high frequency (HF) communication signals, nominally between 1.6–

30MHz. These signals are directly coupled onto the low voltage distribution network (LVDN) at the low voltage (LV) source or at the incoming supply position to the installation. Signals are therefore distributed throughout the LVDN and may be liable to propagate beyond it, resulting in electromagnetic radiation and possible subsequent electromagnetic interference (EMI).

Such EMI is generally quoted to occur due to the unsymmetrical nature of the cabling, the circuit topology, the changes that occur in the network impedance with load switching, and through electromagnetic coupling with other radiators.

Coincident with these first generation domestic PLT devices a number of EMI problems were noted by various amateur radio organisations, as recorded by Hansen (2002), whose comments are summarized below and recount the political landscape for PLT at the time:

> "Early field trials in the UK, Germany and Switzerland have shown excessive radiated emissions (up to 40dB) above the German NB30 Reg TP limits, which are already around 20dB more relaxed than the 4/2000 RA version of UK MPT 1570 limits for the HF spectrum.
>
> Broadcast, military, commercial as well as licensed amateur radio services started seriously objecting to a nationwide implementation of PLT. Far field effects and underestimated PLT system antenna factors lead to HF signal mirroring at the ionosphere. These sky wave propagation effects might lead to background noise increase also outside Europe. Sensitive receiving sites in Germany may experience,

based on first simulations, degradations of 10 to 40dB. This is unacceptable for security agencies in the present political scenario.
The introduction of power reduction in broadcasting, due to digital technologies, reducing transmit power and therefore lowering electromagnetic pollution or health hazards, become useless if at the same time the signal noise ratio will be PLT degraded.

Reports on publicly available, new measurements data from PLT modems/systems indicate serious legal and technical trouble in wide spread PLT field trials systems. Suspicion arouses, due to questionable promoter companies, seemingly forcing contracts with non-discloser agreements to be signed by their clients.

PLT signal level, modulation and existing line noise are important to bridge the distance without costly repeaters. The PLT community is therefore fighting for "better" i.e. less stringent regulations and want new electromagnetic compatibility standards (EMC). Little attention was formerly given to commercial System EMC as box testing was rather dominant. Finally, the commercial EMC community is forced into Systems Thinking!

Typical test problems involve identifying PLT Interference in bands <30 MHz, receiver jamming, time variant EMI. It takes wireless experts to be sure that interference is generated from PLT and not other EMI. Normally at CW, AM, SSB, the whole received spectrum is experiencing a massive noise floor increase and there is very little willingness of the PLT people to talk technical even today.

On the official side 100 serious, professional NB30 objections, some demanding even lower limits, were filed to RegTP and politically ignored by the 78 ministry of economic affairs last year when NB30 came out."

1.4 Widespread Implementation

However, despite the concerns raised above, one such example of the manner in which PLT has been employed on a large scale in the UK, since the release of these first generation broadband devices, is the well documented case of British Telecom and BT Vision.

Following the removal of the restriction on British Telecom in January 2001, the company re-entered the highly competitive cable television market with the launch of BT Vision in December 2006. As part of this campaign British Telecom included a range of PLT products, initially based on the Comtrend 902 unit, allowing consumers to utilise their electrical distribution system to provide an audio/visual link between their set-top box and HomeHub broadband unit.

It was believed (OFCOM, 2010) that by September 2009 some 423,000 units were deployed across the UK and there are now estimated to be around 1.8 million pairs of PLT apparatus in use.

Since July 2008 until the end of May 2010 it was stated by OFCOM (2010) that a total of 272 cases of electromagnetic interference, thought to be PLT related, had been reported of which 223 cases have been referred directly to British Telecom for further investigation and resolution.

1.5 Regulation is Required

It appeared that a groundswell of complaints generated by schemes such as BT Vision was inevitable and yet despite the near decade of research into PLT based interference there remained no regulatory framework to deal with such complaints formally. In light of these concerns, expressed by both the amateur and regulatory bodies across the EU and North America, a progressive programme for the development and introduction of standards was now eagerly commenced.

To develop and implement such a standard, whether for national or international use, clearly requires consensus from a wide range of relevant technical experts, and this task was impeded with such experts already divided as to the benefits versus problems created by broadband PLT.

An early response was to try and use existing high frequency (2-30MHz) RF emissions standards such as the German NB30 or the UK based MPT1570 which were principally developed for the introduction of VDSL and ADSL technologies. For several years the performance of PLT installations was compared to the emissions limits provided by these standards and largely found to exceed such limits by at least 40dB. It was therefore clear that specific legislation was needed to allow powerline technology to co-exist with other users of the spectrum, and would therefore arguably require more exhaustive field trials and communication with interested parties. Equally an understanding of PLT performance in all operational environments may allow such specific legislation to utilise some of the processes developed for other 'balanced' technologies, such as VDSL.

1.6 How to Regulate

In June 2003 CENELEC released a questionnaire (EU, 2003) for completion by the National Standards Organisations (NSOs) within the ETSI member countries which sought comments on the proposal for PLT field trial measurements to be conducted in line with the current standard, i.e. BS EN 55022:2006, and whether the preferred test arrangement should be via conducted or radiated emissions.

Table 1.6.1 below is an example of the proposed radiated limits for selection by the NSOs, and the majority of respondents appear to conclude that the use of a radiated emissions standard brings with it several additional complications, which are summarised as;

- It is more difficult to achieve repeatable and verifiable measurement of radiated emissions below 30MHz than it is for measurements of common mode current.
- The relationship between the measured H field and E field close to the radiating network cables is unknown.
- It is considered almost impossible to include for the effects of local topography of the network cabling, conducting objects and other RF structures.
- The quantification of the reduction of radiated field with distance from the network cabling is not understood, i.e. the application of regression is unknown.
- A reliable method for specifying appropriate receiving equipment sensitivity is not available.

- Testing would require a clear methodology for accounting for any interference from external signals to be developed.

Such an indictment of the radiated emission method, that had formed the basis of all PLT measurements previously, highlights the practitioners concerns that the implementation of a PLT standard would require further understanding of these unique powerline issues.

Frequency range (MHz)	Field strength limit (dB(μA/m))			Standard measurement distance	Measurement bandwidth
	Quasi-peak	Average	Peak		
0,15 to 0,5	14 to 4)[1]	4 to -6)[1]	---	3 m	9 kHz
0,5 to 30	4	-6	---	3 m	9 kHz
NOTE 1 In the frequency range 0,15 MHz to 0,5 MHz, the limit decreases linearly with the logarithm of frequency.					

Figure 1.6.1 Limits of Radiated Disturbances below 30MHz (BSI, 2006)

To many regulators it was becoming clear that central to this understanding is a need to quantify the RF performance of the low voltage distribution network (LVDN), which had largely been discounted by previous researchers, due mainly to the infinite variation encountered in the arrangement of the LVDN and uncertainty as to which parameters related to powerline EMI.

1.7 A future for PLT

As described above the implementation of PLT has not followed a conventional process and in 2013 there remain key concerns over the continued and long term implications of PLT deployment to urban areas.

It is believed that the following now summarises the key issues facing PLT, which if not resolved, will continue to prevent the formal acceptance of

powerline technology as a mainstream network technology and prevent the fulfilment of its full commercial potential in the Smart Grid markets of tomorrow. Areas to be overcome are:

- the definition of a 'typical' LVDN with typical (maximum) known EMI performance parameters.
- the definition of a clear test methodology to accommodate the above and allow PLT system specific emissions standards to be created.

1.8 Thesis Structure

This thesis therefore aims to provide a cohesive approach to determining the RF properties of the typical domestic property and apply such parameters to determine a model for the performance of PLT in this environment. As a result of such modelling the following key questions are to be resolved.

- Is it possible to accurately determine the RF performance of the LVDN through a number of discrete and unobtrusive measurements?
- Can the benefit of a LVDN transfer factor be confirmed within a proposed model? Is the commonly accepted figure of -30dBi appropriate to the employment of powerline within the UK housing stock?
- Would such modelling discern technical benefit or resolution to the stalemate of regulation, and should the use of applied conducted or radiated limits take precedence?

- Finally, can it be shown which parameters influence most greatly the EMI generated?

In order to describe this work this thesis has been structured in the following manner;

- Chapter 2 commences with a review of the various attempts to gain a consensus of understanding to produce PLT specific legislation and considers some of the more notable site trials, as undertaken by academic and commercial bodies

- Chapter 3 considers the physical parameters of the LVDN and the mechanics of the EMI production

- Chapter 4 reviews the testing undertaken as part of this thesis and the wider test results obtained within the Open University (OU) PLT Research Group campaigns

- Chapter 5 discusses the consequences of the testing and concludes with the development of a model for the standard LVDN

- Chapter 6 concludes with details of future powerline technology performance and further works to be considered.

1.9 Summary of Broadband PLT

High bandwidth PLT has come of age and has been extensively deployed within the UK in recent years. Despite formal complaints and the lack of both legislation and product standards, PLT continues to gain in market share with

new products offering increased network performance and further potential EMI concerns.

Despite more than a decade of field trials and varying degrees of analysis there remains little clear understanding of the significant PLT performance parameters and their direct correlation to the EMI produced.

Such uncertainty explains why little progress has been made at the national and international standards committees and why equally there is still little common ground between the proponents and critics of PLT on how to measure emissions and ultimately control and limit such EMI to an acceptable level.

It is within the context of this situation that the aims of this thesis are to demonstrate the correlation between specific parameters of the LVDN and the resulting EMI produced. The following chapter therefore commences with a review of both the moves made to legislate PLT performance and the site trials conducted to determine such performance.

2.1 Introduction to Literature Review

It was concluded in the previous chapter that broadband PLT has become commercially viable, and that whilst the deployment of these systems has now commenced in large numbers there remains little regulation or widespread agreement for the manner in which modelling or measurement is to be undertaken to allow the determination of resulting EMI.

This chapter reviews the attempts made on behalf of both the Regulators, at a national and international level to either revise existing standards or produce new PLT specific standards, and considers those efforts made by several leading commercial and academic institutions in realising PLT field trials.

It shall be seen that the various trials have been completed under the auspices of different bodies for different purposes and the results published therefore vary considerably. This inconsistency in reporting the outcome of trials has made the task of utilising this information for the purposes of regulation more difficult still.

2.2 Regulation Review

Prior to 1999 there was little regulation directly applicable to PLT operation. The national standards of the UK (proposed as MPT1570) and the German NB30 provided radiated limits from telecoms equipment below 30MHz and become the two most referenced benchmarks. EN 55022 also provided conducted limits below 30MHz to the mains port of telecoms equipment, but was arguably not applicable to devices intentionally propagating data via the

mains port. The principal argument for not applying EN 55022 to PLT devices is that the conducted performance criteria given for mains ports suggested limits far lower than that of conventional telecommunication ports and far too low to allow compliance or even operation of any broadband PLT device.

This arrangement was clearly not ideal and the European Commission acknowledged this problem in 2001 and mandated, via Mandate M313 (European Commission, 2001) that ETSI & CENELEC establish a working group to determine a standard for the permitted emissions from data networks utilising electrical distribution cables as passive networks. The mandate specifically stated the need to address the EMC aspects of the LVDNs and not the equipment compatibility issues, which were generally considered to be dealt with via the EMC product standards.

Several working groups were established and April 2004 saw the release of the Final Draft of TS 50437 which proposed both limits and measurement methods for conducted and radiated emissions for 'access' PLT systems. Although 'access' is generally used to define PLT transmission between the regional electricity company (REC) and the consumer, the draft standard makes references to the performance of indoor and outdoor radiated measurements.

In 2004, the EU also released a revised EMC Directive 2004/108/EC which further clarified the concept EMC performance for a 'fixed installation'. In particular, the new Directive clarified that no direct assessment or testing of the installation is necessary if the user could demonstrate the use of compliant components assembled according to good EMC engineering practices.

It therefore became more prudent that agreement be reached on good EMC engineering practices relating to PLT installations and finally in 2008, under the M313 Mandate the EU published the following three part standard.

- EN 50529-1: Conducted Transmission Networks - Part 1: Telecommunication Lines
- EN 50529-1: Conducted Transmission Networks - Part 2: Coaxial cables (CaTV-based)
- EN 50529-3: Conducted Transmission Networks - Part 3: Power line Communications

In addition to these European network-based initiatives the IEC, via its technical committee responsible for the EMC performance of IT equipment, CISPR/I, also prepared multiple draft standards to accommodate PLT.

2.3 Review of CISPR Standards

The starting point for these standards was the universally accepted and much referenced CISPR 22:2005, which is the international source standard for EN 55022. CISPR 22 is titled ITE Radio Disturbance Characteristics and was formally used to provide both limits and measurement methods relating to RF emissions from all IT equipment. CISPR had spent many years trying to include for an amendment specifically named 'PLT port' which would ensure that PLT devices could not be excluded from this encompassing standard. However, gaining consensus from all members for such an amendment had proven impossible. This was largely due to the opinion that the existing limits for both conducted (symmetric) to the mains port and conducted (asymmetric) to the telecommunications port, as given in Tables 2 and 3 respectively of the

standard were sufficient to encompass the performance of all powerline devices.

Instead CISPR/I initiated the CISPR/I PT PLT working groups which produced several draft standards. CISPR/I 257 standard was initiated to specifically consider the measurement methods and emission limits relating to PLT devices and issues of the symmetrical performance of the PLT device versus the asymmetric nature of the network. This resulted in a proposed methodology of measurement based on the asymmetric (common mode) current to the PLT port. The limits for operation when in transmission mode are show in Table 2.3.1 and rely on the use of an impedance stabilisation network (ISN). ISNs had been previously used in Japan and Germany, which allowed both repeatability of results and a means to directly compare results through having a known, stable mains network connection.

Frequency range MHz	Voltage limits dB(μV)		Current limits dB(μA)	
	Quasi-peak	Average	Quasi-peak	Average
1,605 to 5	56	46	28	18
5 to 30	60	50	32	22
NOTE 1 The lower limit shall apply at the transition frequencies.				
NOTE 2 The current and voltage disturbance limits are derived for use with an impedance stabilization network (ISN) which presents a common mode (asymmetric mode) impedance of 25 Ω to the PLT port under test. (conversion factor is 20 $\log_{10}$ 25 Ω = 28 dB)				

Table 2.3.1 Conducted Mode Voltage at PLT ports (BSI, 2006)

CISPR/I 258 introduced the concept of frequency notching to the amateur radio bands with the final draft of CISPR/I 301, issued in 2009, extending notching up to 28MHz. Power management schemes were also introduced to reduce power during periods between data transmissions and to limit devices operating power to a power spectral density of -55dBm/Hz.

Finally CISPR/I 44 took the approach of removing the need for field testing altogether and proposed the use of an artificial mains network arranged to be unbalanced, with impedance and longitudinal conversion loss (LCL) values representative of the LVDN, allowing laboratory based conducted measurements to demonstrate compliance with EN 55022.

Despite these multiple drafts, with the European surveillance authorities repeatedly stating an urgent need for a standard and powerline appliances being widely deployed across Europe, none were formally adopted by CISPR.

Therefore ETSI did not have a good starting position but fairly rapidly produced a code of practice and draft EN 50471, which as we shall see essentially replicated the proposals of CISPR 257.

2.4 OPEN PLC European Research Alliance (OPERA) D84

Although this document is titled D84: Field Test Design, Implementation and Testing (2005) it is essentially a discussion of the PLT components available circa 2005. The field tests described are arranged to determine the Quality of Service (QoS) provided by PLT in various LV environments. The performance parameters of data transfer, namely bit error rate and latency were considered the primary data to be measured.

Unfortunately, other than recording the signal to noise ratio observed on the networks to be tested, this document did not consider that any of the environmental parameters or emissions created as a result of such signal injection were to be recorded.

2.5 CENELEC/ETSI Code of Practice

It was generally accepted throughout Europe that a Code of Practice for the measurement of PLT emissions would be beneficial, and in 2004 the Joint Working Group on EMC in Conducted Transmission Networks produced the first issue.

The scope for this publication was stated as "to ensure a common approach to the measurement of emissions from PLT systems and to facilitate comparable and quantifiable information which Member States can report to the Communications Committee of the European Commission." In addition the authors clearly expected this code of practice to be used by regulatory bodies, PLT system owners and other RF interested parties to complete impartial evaluation of the systems under test. This was to be achieved via the Emission Measurement Methodology, which centred mainly on external radiated testing locations.

Although it was acknowledged that indoor measurements for frequencies less than 30MHz would be within the near field, the code of practice recommends that self-powered, unearthed measurement equipment is used to prevent earth loops which may distort the measurement. It does not however give any prescriptive methodology for conducting indoor radiated tests and gives no reference to conducted measurement, other than those affecting adjacent telecommunications networks.

Pre-measurements are to be conducted to determine the location indicating the highest field strength and full documentation to record of all parameters relating to the test site. Finally the code of practice also recommends the use

of swept measurements in place of spot frequency measurements and proposes a method for processing measurements during subsequent analysis.

2.6 Draft Standard prEN 50471

A further document, produced by the CENELEC/ETSI Joint Working Group on EMC in Conducted Transmission Networks in 2005, is the draft standard prEN 50471 named EMC – Emission Standard for Wire-line Telecommunication Networks.

Whilst this standard is principally centred around the process for making radiated field measurements it also includes for the measurement of the conducted common mode currents below 30MHz, via the application of a high frequency (HF) current probe to the network or LVDN.

Frequency range MHz	Current limits dB(μA)		Measurement bandwidth
	Quasi-peak	Average	
0,15 to 0,5	40 to 30 [1]	30 to 20 [1]	9 kHz
0,5 to 30	30	20	9 kHz
NOTE 1 In the frequency range 0,15 MHz to 0,5 MHz, the limit decreases linearly with the logarithm of frequency.			

Table 2.6.1 Limits of Conducted Current on Network Cable (BSI, 2006)

Maximum conducted measurements are given as Table 2.6.1, which are slightly reduced than those proposed by CISPR/I 257, and further detail of the testing process is given.

2.7 IEEE Std 1775-2010

In 2010 the IEEE Std 1775 was issued and is comprehensive on the extent of the areas covered it is again light on the actual testing regime and particular issues relating to in-house emissions. Section 7 of the standard makes reference to the contribution of both the circuit type and the wiring type, but does not suggest an actual effect or a method to normalise these differences. It does note that mains wiring shall not be installed within metal cable containment such as conduit, offering RF attenuation.

Where it includes for emission testing in situ at in-house PLT systems the directions given are minimal and relate only to radiated emission measurements.

This is the first standard to attempt to address a normalised LVDN and by clearly preventing that test site utilise steel conduit it is dictating an environment having 'soft skin' cables such as those used in UK domestic wiring. This assertion is made without reference to any experimental data, which is interesting as the effect of an extensive network of conduit, which is earthed, may serve to both increase the common mode current and radiated field.

As discussed below the area of trying to understand and normalise the LVDN is difficult and forms part of the proposed RF model for such electrical installations.

2.8 Review of ITU-R SM.2158-2

After several years ITU-R Working Party 1A approved Report ITU-R SM.2158 (ITU, 2011) on the "Impact of Power Line Telecommunication Systems on Radio-Communication Systems Operating in the LF, MF, HF and VHF bands below 80 MHz." Whilst this provides some detail of the various modem types and their performance, the document is centred on the need to maintain appropriate signal to noise ratio for intended signal reception and provides criteria to assess both the impact of individual and cumulative PLT generated EMI.

2.9 Draft Standard prEN 50561-1

Having being proposed by CENELEC Working Group 11 some years previously the approval of the draft standard known as prEN 50561-1 occurred in November 2012.. The majority of the European NSOs including the UK voted in favour of its adoption.

This draft standard, which has significant similarity to CISPR/I 257, is essentially a product performance standard for PLT in-house devices. The term PLT port is now firmly defined, the need for dynamic power reduction on detection of a valid radio broadcast is also required and a 15 minute time limit is given for the abatement of conducted disturbances at all frequencies post data transfer.

According to Pink (2012) the specific requirements placed on new products by prEN 50561-1 are that they must;

- Provide permanent notching of the HF amateur bands, and aeronautical bands, down to the level of the EN 55022 standard
- Provide adaptive notching of the HF broadcast bands
- Reduced emissions from the modem, when the attenuation caused by the mains connection between units is low
- A reduction of transmitted power to below the level of EN 55022 when there is no user data.

This draft standard essentially formalises the requirement for the employment of techniques used by most modem manufacturers and helps overcome the regulatory mess resulting from not having an applicable product standard. However, despite the use of these additional techniques, such as adaptive notching, which clearly reduces EMI to certain defined frequency bands, the EMC community (RSGB, 2012) has already suggested that this proposed standard does not follow the intent of the EMC Regulations, citing "Equipment shall be so designed and manufactured as to ensure that the electromagnetic disturbance generated does not exceed the level above which radio and telecommunications equipment cannot operate as intended".

2.10 Review of Modelling

It could be expected that with the current computational techniques available that PLT emissions would be most easily modelled. Whilst numerous electromagnetic computational models have been produced as Pang (2008) to model the PLT environment, it has become apparent that given the variety of

in-house wiring connections, the unique arrangement of national wiring practices and the unknown variation of instantaneous load conditions, the creation of a universal model is not possible.

As found by Zheng (2006), the LVDN does not permit analysis through application of transmission line theory alone and requires supplementary measurement of real networks to allow numerical modelling. Catrysse (2008) equally found that numerical analysis of all but the simplest circuits introduced significant error when compared to the equivalent measurement data.

Finally Zhang et al (2008) attempted to describe and analyse individual circuits via use of numerical electromagnetic codes such as NEC2 to illustrate the current distributions and disturbances. However, it was found impractical to derive quantitative results in such a way that could be applied to all cases.

Therefore most researchers have favoured to determine and understand PLT related emissions via field measurements based on testing campaigns alone and use such data to derive qualitative models.

2.11 Review of Field Trials

Despite the voracious engagement in this area and the numerous field trials that have been conducted around the world, in both the low and medium voltage mediums, there are few examples of published results providing comprehensive analysis. Of those available the more significant, and therefore reviewed here, are trials undertaken by OFCOM (via PA Consulting Group), NATO and the Communications Research Centre of Canada.

2.12 PA Consulting (OFCOM)

The PA Consulting study was conducted in 2009 (OFCOM, 2010) and opted to review the likelihood of PLT generated interference affecting an adjacent user through a statistical probability assessment method based on current and projected deployment figures for PLT installations. Whilst they considered the various mechanisms through which interference would result, and provided link budgets identifying the anticipated field strength for such interference, they did not undertake any works on the performance or principal features of the LVDN within either the PLT source or victims installation.

Expected versus Measured Values of PLT Emissions (In 9kHz measurement bandwidth)	Value
Quasi peak PLT transmit power (-57.3dBm/Hz in 9kHz as per the UPA devices used in the Canadian field trials)	-17.8dBm
Assumed household wiring antenna gain	-30dBI
Convert quasi peak to peak (to match Canadian measurement technique)	-5.8
Expected peak EIRP at PLT house	-42dBm
Expected peak field strength at 3m (EIRP converted using ITU-R P368.7 for isotropic radiator)	53.2dBµV/m
Expected peak field strength at 10m (EIRP converted using ITU-R P368.7 for isotropic radiator)	42.8dBµV/m
Measured peak field strength at 3m	53dBµV/m
Measured peak field strength at 10m	41dBµV/m

Table 2.12.1 Verification for Household Wiring Performance (OFCOM, 2010)

In order to therefore enable a numerical analysis PA Consulting assumed that all premises, irrespective of the source frequency, have an antenna gain or k factor of -30dBi. Justification for the use of this figure, which was referenced as being derived from the Canadian Communications Research Centre, was given in the results presented in Table 2.3, which shows that the theoretical field strength calculation when using -30dBi provides similar results to the measured values.

In conclusion PA Consulting did not consider that the current deployment of widespread PLT would render significant effects to the HF spectrum for the next decade.

2.13 NATO – Research Task Group

The NATO Research Task Group (NATO, 2008) conversely concluded that PLT has the ability to 'cause appreciable degradation of the HF spectrum' through its cumulative modelling of the Effective Isotropic Radiated Power (EIRP) produced from each PLT installation.

However, as with PA Consulting they also did not undertake a review of the performance of an in-house PLT installation but opted to assume that each installation has an inherent 'Wire Line Antenna Gain' of -30dBi.

They defined antenna gain of a wire-line transmission system as the ratio between EIRP and injected power and suggest that a review by the Research Task Group (RTG) concluded the following gains:

- –30 dBi for in-house systems
- –15 dBi for overhead access systems
- –50 dBi for underground access systems.

The RTG did recognize the level of uncertainty in these systems with gains of ±10dB due to statistical spread, and in the case of overhead access system power lines an increase in antenna gain of up to 13dB was recorded at resonant frequencies.

The NATO report acknowledged the assistance of the Canadian Communications Research Centre and concluded that there was a high probability that PLT would increase the noise levels at sensitive sites, which would have an adverse effect on HF military communications.

2.14 Communications Research Centre (CRC) of Canada

The North American Broadcasters Association contracted CRC (2009) to carry out a far more exhaustive trial involving multiple PLT modems over three months and assessing seventeen distinct property types.

In addition to recording the radiated field produced from the LVDN when used as the PLT medium, CRC also carried out in situ conducted emission measurements on two of the sites. The intention of these measurements was to allow the development of further correlation between the differential mode current produced by the modem, the common mode current observed within the installation and the radiated field strength.

Ultimately the CRC report concluded that individual properties can have up to 20dB variation in emissions when using the same modem, and that there was no discernible relationship between the measured common mode current and the radiated field values. Other observations noted were;

- No correlation seen between injected power, differential mode current (DMC) and common mode current (CMC)
- There was no discernible relationship between EMI and CMC

- Longitudinal Conversion Loss (LCL) was also introduced but despite showing a consistent value on all LVDNs tested, the observation that no discernible relationship existed between the LCL and the CMC was made.

2.15 Open University PLT Research Group (OUPLTRG)

The OUPLTRG has undertaken extensive in situ testing around the world during the past eight years on a large number of residential and commercial buildings. Having emissions measurements from such a range of installations, incorporating all LVDN wiring types, geometries and local wiring practices provides a unique database to allow identification of the prominent features of such emissions.

Typical testing methodology for the testing completed by the OUPLTRG involved a number of discrete tests which when considered in totality describe the electrical characteristics of the LVDN and the electromagnetic environment of the locality.

- Swept measurements of the noise floor were taken using tuned antenna
- Spot frequencies measurements of the LVDN impedance
- Longitudinal Conversion Loss (LCL) of the LVDN
- Ingress measurements on the LVDN between 1.6–30MHz

- Internal and external radiated emissions were conducted utilising a magnetic loop antenna
- Injected tests were conducted using the signal generator to provide injection of a 20dBm signal at 5MHz on the LVDN whilst recording with the loop antenna and a receiver at each corner of the building, 3 metres from the perimeter.

Much of the data presented in Chapter 4 has been collated as a result of this on-going measurement campaign. Equally the data derived from these measurements has been included in various papers (Newbury, 2007) and (Brannon, 2005) and other PhD theses, such as Haq (2012), however, no overriding analysis of these measurements has been concluded to demonstrate key findings.

2.16Trial Methodology

Despite the same base data being used for the assumed performance of the LVDN the above field trials have not concluded the same long term effects of PLT implementation.

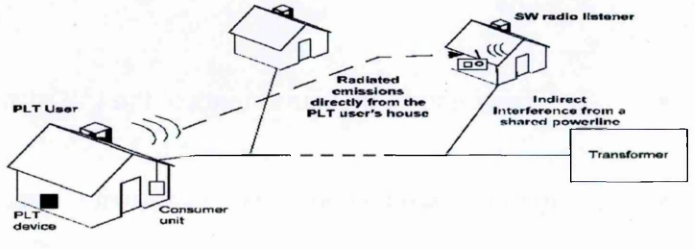

Figure 2.16.1 Diagram of Local Distribution Cabling (OFCOM, 2010)

It is also to be noted that whilst all parties made recognition that the LVDN was unbounded, only PA Consulting included the effects of the electrical 'consumer unit' and propagation beyond the test property itself.

Figure 2.16.1 above highlights this issue, whereby the victim is either affected through the directly radiated field or via their own locally radiated field. This local field results from the unbounded PLT conducted emission which propagates via the common electrical distribution system, i.e. the LV cabling from the local transformer. The standard configuration within the UK, on three phase networks, is for approximately each third property to be connected via a direct and common supply. As the attenuation of power cables was assumed as 0.4dB/m, a value proposed by Koch (2009), it is extremely likely that the resulting radiated emission measured at 3, 10 or 30 metres from the source is a combination of emissions from multiple properties and from the electrical distribution system itself.

Filtering effects on the PLT signal by a domestic consumer unit are also unclear and whilst PA Consulting suggests that there is little data available on this subject, the draft report from the ITU-R Study Group 1A allowed the average loss across the consumer unit of 16dB to be derived.

Finally, it is to be noted that the term 'typical domestic property' assumes many factors in terms of the properties age, size, etc and application of the processes and measurements, as described within this thesis, will allow quantification of these factors. Following further testing on multiple properties of various ages, types will allow development of the model to accommodate such effects on the produced EMI.

We can see from above that whilst there was some common ground in the assumptions made, there was little correlation between the methodologies employed, and as none opted to identify the validity or scope of their assumptions there was consequently no overall conclusion resulting from these trials.

2.17 Summary & Research Questions

In summary we note that frustration on behalf of the EU in 2001 initiated a plethora of standards development work under mandate M313. The intended purpose of M313 was not to provide a PLT product standard but an operational performance standard, as product performance was felt to be covered in EN 55022. However, after eleven years we find prEN 50561-1 is the only standard to have been ratified for international use, and on examination it is largely a product standard that includes for specific modem performance features not described in EN 55022 but already employed by all PLT manufacturers.

Whilst prEN 50561-1 clearly improves the situation by defining the extent of notching and power management features, it is also questionable whether it fulfils the essence of the EMC regulations in requiring modems merely to limit their EMI production as opposed to 'being designed to prevent interference to other users'.

Equally, summarising the situation with regards to the field trials we see that a variety of approaches were used to record a range of both conducted and radiated emissions. Despite this inconsistency in approach these field trials have assumed the same base data for analysis, although the provenance of

which is not fully documented. Again it appears that the considerable efforts undertaken in this area have resulted in little progress towards the further application or regulation of PLT.

The CRC trial is however unique with the adoption of its recommendations by the ITU and subsequent influence on the EU and IEEE working groups. It is also surprising that such a trial, consisting of only 17 test sites and 8 modem types and employing an experimental nature to the data recorded, has gained such prominence.

There remains no consistent view as to how or what should be measured and equally those measurements made to date do not suggest any direct correlation between the measured parameter and that of performance or EMI production. Neither is there a consensus on the benefits of such testing or the employment of such data for regulatory benefit.

Despite the extensive efforts made by numerous researchers and the plethora of potential standards, there remains after more than a decade, no formal agreement on the performance nor methodology to record such performance of PLT systems.

The aims of this thesis, as described previously, attempt to address this situation and in doing so provide a cohesive approach to determining the RF properties of UK properties, via the establishment of an RF model.

3.1 Introduction to Theory

This chapter describes the environment in which PLT operates, the manner in which the signal is distributed and considers those parameters that affect such propagation.

In order that we may correlate these criteria to the field measurements data presented in the following chapter, a thorough understanding of these parameters is required, which also allows analysis and comparison with published trials undertaken by other parties.

The complexity of the PLT environment, employing the LVDN as the communication transmission network is significant, and can best be summarised by the following quotation from the PA Consulting Group (OFCOM, 2010):

> *"Interference mechanisms are difficult to quantify precisely as RF emissions from PLT devices may reach other spectrum users and create interference via a number of routes".*

3.2 PLT Signal Injection

Given the variation in the magnitude of RF signals, from transmitters emitting signal of several hundred kilowatts to the manipulation of micro-watt signals within distant receivers, the use of decibels within RF engineering is common place and provides several advantages.

The application of decibels to field measurements, such as voltage or current provides a ratio of the measured value to a reference value of one micro-volt (1μV) or one micro-amp (1μA). Therefore, as an example we can show that as a signal propagates and becomes attenuated the magnitude of that signal reduces from a source value of 4V to 10mV and 20μV respectively at intermediate and final stages of the transmission path as:

$$Voltage(dB\mu V) = 20\log(4V/1\mu V) = 132dB\mu V$$

$$Voltage(dB\mu V) = 20\log(10mV/1\mu V) = 80dB\mu V$$

$$Voltage(dB\mu V) = 20\log(20\mu V/1\mu V) = 26dB\mu V$$

Equation 3.2.1

Whilst the attenuation to each stage of the transmission path is found as the difference in voltage in (dB) between stages, i.e. 52dB and 54dB respectively, the total decibel loss or gain of a system comprising several stages can be simply calculated by summing the decibel losses of the individual stages. It can also be seen in the above example that just as the losses from the two stages can be compared so we can make direct comparison of the losses, in either of these stages to other systems, i.e. between various LVDNs.

As power is proportional to the square of the magnitude of the voltage and in order to maintain parity of voltage to power the following definition is used to calculate power ratios:

$$Power(dBm) = 10\log(Watts/1mW)$$

Equation 3.2.2

If the 20μV from the final stage above was presented across a 50Ω impedance the power in (dBm) can be shown as;

$$Power(dBm) = 10\log(\frac{(20\mu V)^2}{50\Omega}/1mW) = -81dBm$$

Equation 3.2.3

so it can be shown that for a 50Ω impedance system the power in dBm is found as 107dB less than the voltage and the current found as 34dB less than the voltage. Equally for systems based on other impedance values, such as the impedance of free space as 120π the voltage is again shown to be related to the power and current via reduction of 115.8dB and 51.5dB respectively.

Whilst dBm represents the total power measured across a given bandwidth, it does not allow us to directly compare the power output of various modems, which may operate with distinct bandwidths. To allow such a comparison we normalise the injected signal power of each modem, which is quantified as the Power Spectral Density (PSD) and derived by Clayton R Paul (Paul, 2006) as page 153 Equation 3.2.1, to a given resolution bandwidth (RBW) most often 9kHz.

$$PSD[dBm/RBW] = PSD[dBm@1Hz] + 10\log(RBW)$$

Equation 3.2.4

Whilst this would appear to be a simple manner in which to limit the EMI of PLT devices, and has been the subject of several draft editions of IEC standards, a maximum PSD has not been stipulated to date, although as

described earlier the consensus appears to wish to impose a future limit of -55dBm/Hz.

It is to be noted however, as observed in the ITU Radiocomms Doc. PT46(09)044 (ITU Radiocomms, 2009), that if Table 2 of EN 55022 is applied to the PLT modem then a quasi-peak limit of 56dBμV, when measured over a 9kHz bandwidth is permitted at the communications port. This translates, as shown by Equation 3.2.2 into an equivalent PSD of -93.5dBm/Hz.

$$PSD = 56\ dB\,\mu V - 10\log(9\,kHz) - 90 - 20\log(\sqrt{Z})$$

Equation 3.2.5

This assumes that Z, the system impedance, is 100Ω, which as we shall see in Chapter 4 is not untypical of the impedance seen at the LVDN.

It is therefore clear that PLT devices operating with a PSD of around -60dBm/Hz will generate disturbance voltage levels in the order of 90dBμV, which clearly exceeds the proposed CISPR conducted limits of 50dBμV average by several decades and has resulted in the legislative stalemate described in Chapter 2.

The body of results used within this thesis have been generated from trials using the Comtrend 902 devices used for all tests undertaken within the OU anechoic chamber and at the test site BRAMBLE. These modems operate with a PSD of -58dBm/Hz.

Therefore it is clear that a fundamental parameter to be recorded and normalised, where necessary, is that of PSD. Although all field measurements performed as part of this thesis have been based on the Comtrend 902 units care is exercised where measurements are compared to external field trials and/or third party results.

It is also to be noted that whilst most CISPR standards are prepared for use in both commercial and domestic environments, all limits and performance criteria relating to powerline devices stated within this thesis are based on Class B ITE products only, i.e. those intended for domestic use, and as such the often more lenient limits imposed for commercial environments have not been stipulated.

3.3 PLT Signal Distribution

Given the localised nature of the LVDN, which generally extends to a single property only, how much power is required to propagate the signal to all parts of the network?

Use of the Shannon-Hartley theorem (Shannon, 1949), as Equation 3.3.1, indicates that to achieve a given channel capacity (bits/second) the minimum signal to noise ratio required can be found as:

$$C = B\log_2\left(1+\frac{S}{N}\right)$$

Equation 3.3.1

Where *B* is the signal bandwidth, which we shall assume as 5MHz, and *S/N* is the signal to noise ratio. For high signal to noise environments Equation 3.3.1 is simplified to Equation 3.3.2;

$$C = 0.322B * 10\log\left(\frac{S}{N}\right)$$

Equation 3.3.2

To achieve the 100MBits/s as the Comtrend 902 units claim a minimum signal to noise ratio of 60dB is required (Ferriera, 2010). Equally, to overcome the signal loss due to attenuation with distance, and assuming a nominal property having circuit lengths no greater than 50m, we need to allow for the signal decay at the receiver. Testing undertaken by Koch (2009) indicates that an average loss of 0.4dB per metre run is typical for the mains power cabling used in the LVDN.

Therefore to achieve full data transfer across the physical extremes of a LVDN the injected signal will need to be 80dB greater than the conducted noise floor. Modems limited to -58dBm/Hz will suffer degradation of data throughput or a reduction in operating distance when operating in environments having a conducted noise floor greater than -95dBm. The OUPLCRG testing campaign has noted a significant number of installations with conducted noise floors in excess of this value.

3.4 Physical Arrangement of the LVDN

The majority of small to medium electrical installations within the UK are supplied via a single service from the Regional Electricity Company (REC)

which terminates in a service cut-out, as Figure 3.4.1 below indicates. The service cut-out is usually accompanied by a kilowatt-hour meter and consumer unit which provide energy metering, overcurrent protection and allows the formation of both separate circuits and neutral/earth conductors.

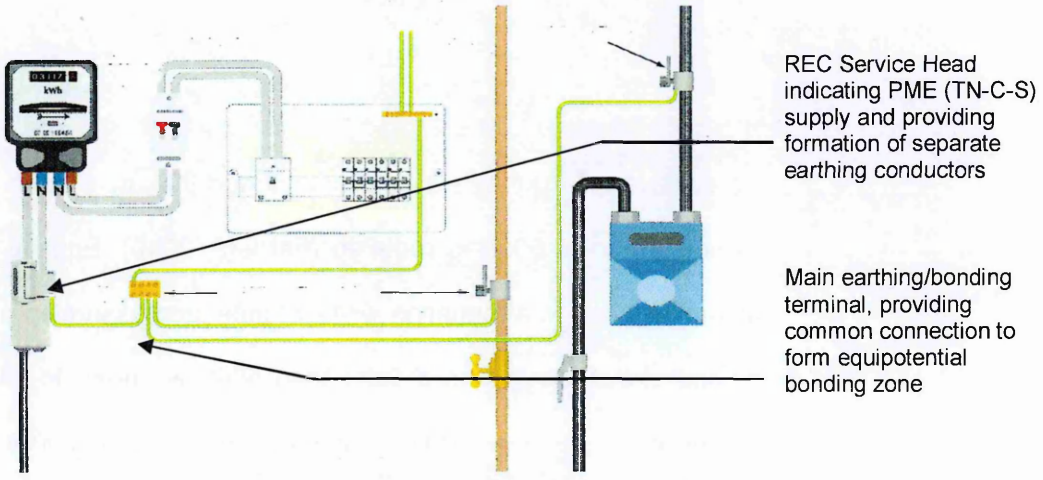

Figure 3.4.1 REC Service Head at Mains Intake (IET, 2008)

Assuming a single phase supply, all three conductors from the outgoing terminals of the cut-out are routed via the REC meter and supply power to the consumer unit. The individual circuits serving the installation emanate from this consumer unit and are provided with independent isolation, overcurrent protection and earth leakage protection where required.

Generally all circuits are defined as radials, i.e. each circuit consists of a single cable connecting one or more outlets in a linear fashion. The exception to this is the 'small power' circuitry which supplies the ubiquitous 13A socket outlets as a ring main. A ring main circuit consists of a pair of cables in which the phase conductor of each cable is connected to the same circuit protective

device (CPD) and the cables then arranged as a continuous loop, connected to multiple socket outlets covering a limited floor area.

Within the UK all electrical installations are designed and installed to meet the relevant edition of the IET Wiring Regulations or BS7671: Requirements for Electrical Installations (IET, 2008) which has evolved through seventeen editions since 1882, when the first edition was published principally to curb the number of house fires started by electric lighting.

These regulations document the development in wiring practices and have led not only to the principal forms of earthing, as described below, to be adopted but have also promoted the now nationally recognised and unique practices of ring main topology and 3-plate lighting circuitry.

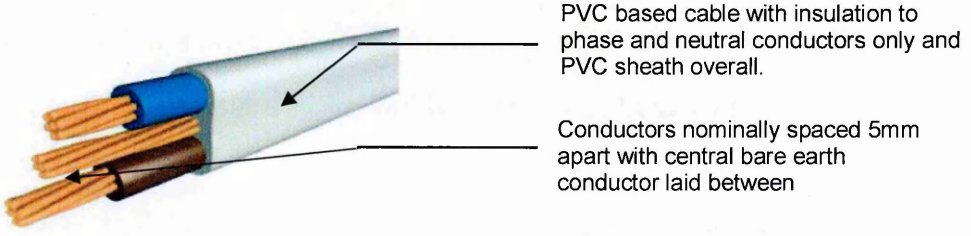

Figure 3.4.2 Detail of the UK Standard 'twin and earth' Cable (Eland, 2009)

Whilst it is generally accepted that all twenty seven countries of the EU now operate on a common voltage (230V AC ± 6% at 50Hz frequency) and with harmonised cable identification standards, there remain significant regional variations to the cable types employed. Within the UK the majority of light commercial and domestic installations comprise of flat polyvinylchloride (PVC) sheathed cable containing separately insulated phase and neutral conductors and a central bare copper earth conductor, as shown above in Figure 3.4.2.

These cables are generally known as twin and earth cables and constructed to comply with BS 6242Y. As described earlier the phase and neutral conductors are routed adjacent each other at a nominal 5mm of separation and provide a level of immunity to field generation due to symmetrical (differential) current flow. However, on lighting circuits specifically the common practice is to route the phase conductor only through the light switches. This means that all luminaires are provided with permanent neutral connections but are only made live on the closing of the respective light switch. Cabling between the light switch and luminaire therefore consists of a live phase conductor, i.e. the supply to the switch and a switched phase conductor, known as the switchwire, which is made live when the switch is on. Under such conditions both the symmetrical and asymmetrical currents are routed in isolation of the 'return' current and are liable to generate far greater radiated fields.

The implications of these physical parameters and the effects they have on the radiated and conducted EMI will be addressed in Chapter 5.

3.5 Wiring Installation

Within the small to medium installations we can see that the relatively recent introduction of earth leakage protection has meant that mechanical protection of cables is no longer afforded by the use of steel coverings such as conduit, capping and therefore most cables are now embedded within a plastic covering or routed within wall cavities, floor voids and roofspaces. From an EMC perspective these cables operate without a parallel earth conductor (PEC) as recommended by BSEN61000:5-2, and therefore any imbalance will be subject to the creation of a radiated field. Conversely some of the OUPLCRG testing has been undertaken in light commercial installations

where all cabling was installed within earthed metallic steel cable containment and the results presented in Chapter 4 discuss this.

3.6 Earthing & Bonding

All electrical installations must satisfy the requirements for earthing and bonding in accordance with the IET Regulations quoted above. In addition an electrical installation must be co-ordinated with the earthing arrangement of the incoming REC supply which is generally classified as those providing separate neutral and earth conductors throughout the system (TN-S), those providing a combined neutral and earth conductor to part of the system only (TN-C-S) and those in which the earth is locally derived via an independent source such as an earth electrode (TT).

Typical impedances given for such earth connections at 50Hz (IET, 2008) are 0.35Ω for TN-C-S and 0.8Ω for TN-S systems.

Equally, the internal installation requires all metallic 'exposed' conductive parts of the electrical installation to be earthed with all metallic 'extraneous' conductive parts not forming a direct part of the electrical installation bonded to the same, common earth system to create an equipotential zone. Whilst the equipotential zone ensures that all metallic components reside at the same potential, in the event of an electrical fault, it also forms a mesh arrangement, as shown in Figure 3.6.1, known as a Common Bonding Network (CBN) which inherently provides a low impedance path for currents to circulate.

As CBNs consist of earthing conductors and passive metalwork components, such as steel structures, pipework, etc the inductance of the CBN can be

lowered by reducing the size of the mesh. Earth electrodes also have inductance, although where employed in high-conductivity soil they exhibit a predominantly resistive connection up to several MHz.

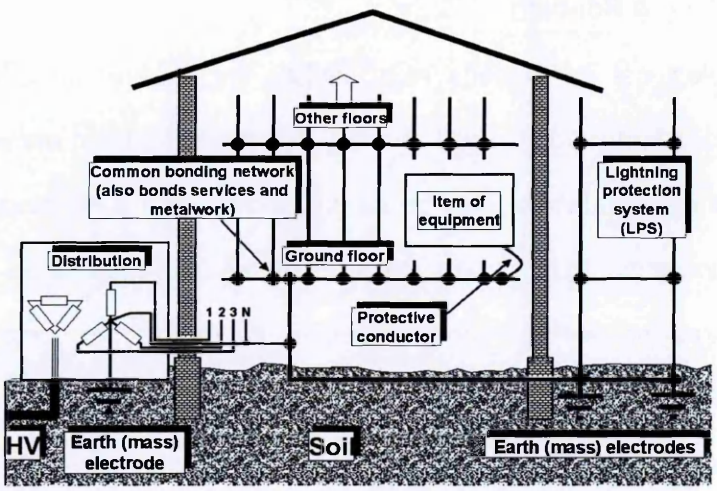

Figure 3.6.1 Impression to indicate the Principle of a CBN (Williams, 2000)

3.7 Characteristic Impedance

According to Hrasnica (2004) the impedance of the LVDN is mainly influenced by the characteristic impedance (Z_o) of the cables, the topology of the network under consideration and the nature of the connected electrical loads.

As detailed in Figure 3.4.2 above, twin and earth cabling has a defined construction which spatially maintains the conductors in position relative to each other along the entire cable length. This allows derivation of the cable as a parallel transmission line with characteristic impedance dependent on the conductor radius (r), distance between conductor centres (d) and the dielectric or relative permittivity (ε_r) of the insulating material. Also Dostert (2001) suggests that the high frequency performance of a cable is related to the insulation and conductor performance, together with temperature and frequency.

Calculation of the characteristic impedance of such cables, having a polyvinylchloride (PVC) dielectric with relative permittivity ε_r = 3.5 and copper conductors of relative permeability μ_r = 1 is given via the following equations.

Capacitance per unit length of cable, as page 194 of Paul (2006), and Equation 3.7.1:

$$\frac{C}{l} = \frac{\pi \varepsilon_r \varepsilon_o}{\ln\left[\frac{d}{2r} + \sqrt{\left(\frac{d}{2r}\right)^2 - 1}\right]}$$

Equation 3.7.1

$$\frac{C}{l} = \frac{\pi \varepsilon_r \varepsilon_o}{\cosh^{-1}(d/2r)}$$

Equation 3.7.2

where ε_0 is 8.85 $\times 10^{-12}$ F/m and the inductance, as Equation 3.7.2 and page 193 of Paul (2006), gives per unit length of cable;

$$\frac{L}{l} = \frac{\mu_r \mu_o}{\pi} \ln\left[\frac{d}{2r} + \sqrt{\left(\frac{d}{2r}\right)^2 - 1}\right]$$

Equation 3.7.3

$$\frac{L}{l} = \frac{\mu_r \mu_o}{\pi} \cosh^{-1}(d/2r)$$

Equation 3.7.4

where μ_0 is $4\pi\times10^{-7}$ $Hm^{-1} \approx 1.25 \times10^{-6}$ Hm^{-1}. Finally the HF resistance per unit length of cable is given by Verpoorte (2003) as Equation 3.7.5;

$$\frac{R}{l} = \frac{2R_s}{2\pi r} \frac{(d/2r)}{\sqrt{\left(\frac{d}{2r}\right)^2 - 1}}$$

Equation 3.7.5

Giving the characteristic impedance, Z_o, as Verpoorte (2003) and shown in Equation 3.7.6;

$$Z_o = \frac{\eta}{\pi} \cosh^{-1} \frac{d}{2r} \approx \sqrt{\frac{L}{C}}$$

Equation 3.7.6

where $\eta = \sqrt{\frac{\mu}{\varepsilon}}$

Applying the physical dimensions of the transmission line cable shown in Figure 3.4.2, which has conductors with a cross sectional area of $2.5mm^2$ indicates a nominal characteristic impedance of 108Ω, as shown in Figure 3.7.1.

If we assume that the characteristic impedance of the cable is the dominant feature, for lightly loaded circuits, we note in Chapter 4 that the results obtained from multiple UK based measurement trials generally correlate with this value. The measurements of DMZ are seen to be in the order of 90-120Ω.

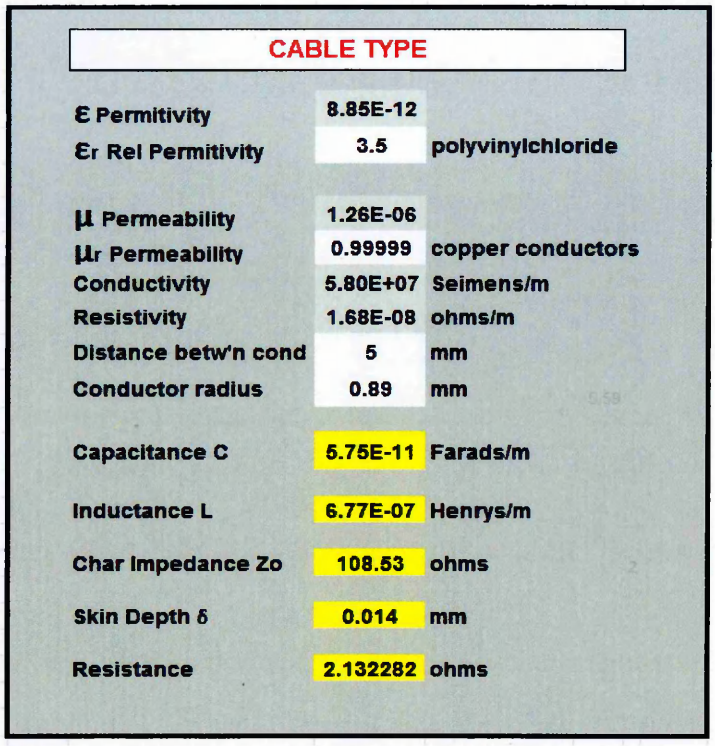

CABLE TYPE		
ε Permitivity	8.85E-12	
εr Rel Permitivity	3.5	polyvinylchloride
μ Permeability	1.26E-06	
μr Permeability	0.99999	copper conductors
Conductivity	5.80E+07	Seimens/m
Resistivity	1.68E-08	ohms/m
Distance betw'n cond	5	mm
Conductor radius	0.89	mm
Capacitance C	5.75E-11	Farads/m
Inductance L	6.77E-07	Henrys/m
Char Impedance Zo	108.53	ohms
Skin Depth δ	0.014	mm
Resistance	2.132282	ohms

Figure 3.7.1 Calculation of cable characteristics for 2.5mm^2 'twin and earth'

It is therefore reasonable to assume that domestic cabling internationally presents similar characteristic impedance and allows the direct comparison of results from such countries.

3.8 Low Voltage Distribution Network (LVDN) Impedances

Following time lapsed measurements Haq (2012) indicates that despite a significant variation in impedance over time and between circuit types given the variation in loads, an average differential impedance (DMZ) for the network can be derived.

Testing undertaken in North America by Martin (CISPR, 2003) and the PLT Committee of Japan (Oka, 2007) having conducted measurements on multiple

installations found that whilst DMZ showed a variation across the frequency range of 1–30MHz a median value of 100Ω resulted.

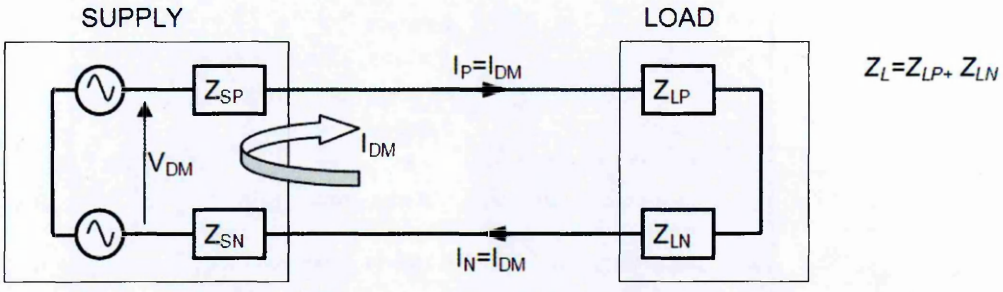

Figure 3.8.1 Sketch identifying the Extent of the Differential Signal Circuit

The relationship between characteristic impedance and DMZ is given as Equation 3.8.1, which requires the cable electrical length (*l*), load impedance and propagation coefficient (β) to be considered.

$$DMZ = Z_O \frac{Z_L + jZ_O \tan(\beta l)}{Z_O + jZ_L \tan(\beta l)}$$

Equation 3.8.1

where Z_O represents the characteristic impedance and Z_L the combined load impedance.

For a lossless line, where both *R* and *G* equal zero, the signal attenuation is negligible and the propagation coefficient equates the propagation constant, given as γ in Equation 3.8.2 and page 278 of Paul (2006), where α is the attenuation coefficient and β the propagation coefficient.

$$\gamma = \alpha + j\beta = \sqrt{(R + j\omega l)(G + j\omega C)}$$

Equation 3.8.2

For a distortionless transmission line the transverse electromagnetic wave of the signal is shown to propagate with a velocity v_p shown by Equation 3.8.3;

$$v_P = \frac{1}{\sqrt{LC}} = \frac{1}{\sqrt{\mu_O \mu_r \varepsilon_O \varepsilon_r}} = \frac{\omega}{\beta}$$

Equation 3.8.3

Application of the values derived in Figure 3.8.1 allow the transmission factors to be calculated, as Figure 3.8.2 below indicates. The velocity of propagation (VoP) is shown to be 0.53 due to the high permittivity, which delays EM propagation and has the effect of increasing the electrical length of the circuit. This allows us to note that whilst LVDN circuits within the domestic environment are typically no greater than 25m in length they are not considered as electrically 'short' for the frequencies of interest.

The propagation coefficient β is 0.587 radians per metre and allows DMZ, as Equation 3.8.1, to be derived as 107Ω when a load impedance Z_L =100Ω is assumed. Equally, we see that if the load impedance were to represent either a short circuit (0Ω) or an open circuit (1E+12Ω) the value of DMZ would vary between 29 - 404Ω.

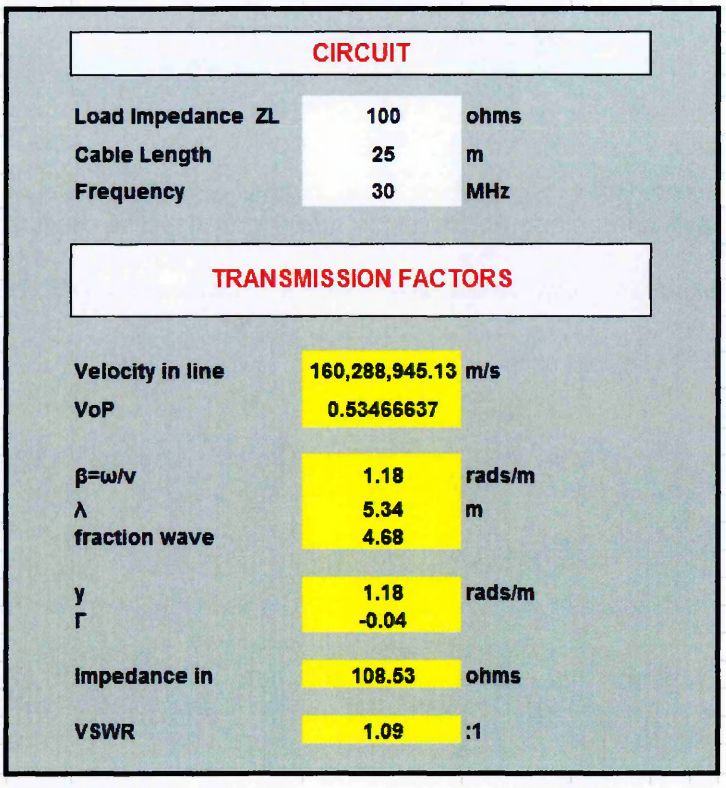

CIRCUIT		
Load Impedance ZL	100	ohms
Cable Length	25	m
Frequency	30	MHz
TRANSMISSION FACTORS		
Velocity in line	160,288,945.13	m/s
VoP	0.53466637	
β=ω/v	1.18	rads/m
λ	5.34	m
fraction wave	4.68	
γ	1.18	rads/m
Γ	-0.04	
Impedance in	108.53	ohms
VSWR	1.09	:1

Figure 3.8.2 Calculation of Transmission Factors for 2.5mm^2 'twin and earth'

Such range of impedance, as confirmed by measurement (Haq, 2012) indicates that the variation in impedance on a 'live' LVDN is dominated by the combination of connected loads and that the fixed impedance of the circuitry is less influential.

Whilst the LVDN differential impedance DMZ has been much studied and measured, far less effort has been undertaken to determine a nominal value for the asymmetric or common mode impedance CMZ.

The common mode or asymmetric impedance relates to the circuit shown in Figure 3.8.3, which is formed via the transmission line and associated 'external' earthing conductors. These earthing conductors, forming a common bonding network (CBN) as described above, are made of a limited number of

conductors, which within the domestic context have a defined topology and essentially consist of the LVDN circuitry, the bonding connections to incoming services such as water and gas supplies and the extent of metallic pipework presented by these extraneous conductive parts.

As part of the ETSI programme to define the principal characteristics of the LVDN (ETSI, 2003) measurement of CMZ in several European countries was completed via the division of V_{CM} by the I_{CM}. This indicated an average impedance of 200Ω.

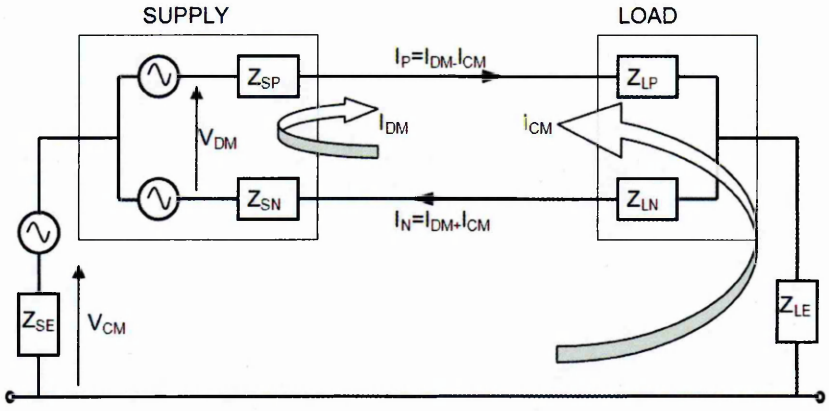

Figure 3.8.3 Sketch identifying the Extent of the Asymmetrical Circuit

Conversely the Japanese PLC Committee, for the purposes of allowing laboratory based simulation of the LVDN via a L-ISN have suggested that CMZ is to be assumed as 25Ω. Whilst this does not appear to be based on an extensive measurement campaign or a desire to replicate the common mode impedance it is more likely selected to represent the considered worst case longitudinal conversion loss (LCL) value of 12dB. As testing of the Japanese building stock (Kitigawa, 2008) demonstrated values of LCL below 12dB were rare and therefore a L-ISN, having a differential impedance of 100 Ω, could

replicate the worst case LVDN, through application of Equation 3.9.1. when having a common mode impedance equal to 25Ω.

Finally testing by Martin (CISPR, 2003), as part of the Federal Communication Commission (FCC) review of the Part 15 rules for assessment of powerline measurement, suggests that the use of HF current probes allows determination of an average common mode impedance (CMZ) of 48Ω across the 1-30MHz spectrum.

From Figure 3.8.3 we can see that CMZ comprises the circuit described by Equation 3.8.4:

$$CMZ = Z_{LE} + \left(\frac{Z_{LP}.Z_{LN}}{Z_{LP} + Z_{LN}} \right)$$

Equation 3.8.4

Having established the impedance of the LVDN consideration of the inherent imbalance on the transmission line allows determination of the common mode voltage V_{CM}. This is generally obtained via measurement of the longitudinal conversion loss (LCL).

3.9 Transverse and Longitudinal Conversion Loss (TCL & LCL)

Transmission and signal cables are often considered in terms of their ability to limit the differential mode signal (DM) from producing a common mode signal (CM). A high quality signal cable of good construction will offer little attenuation or distortion to the wanted (DM signal) that circulates via a pair of

signal conductors. Equally a high quality cable also limits the losses occurring between the signal conductors and the associated common paths, i.e. those paths common to either of the signal conductors that may exist within or external to the cable. Common mode paths are often established where an imbalance occurs between the signal pair due to the presence of stray capacitance, inductance or through radiation coupling. Where such paths do occur an element of the differential mode signal is routed via these common mode paths and creates what is termed as the common mode current (CMC), which has a characteristic feature of having the same direction of current flow on both the signal conductors.

Measurement of the cable performance, i.e. the ability to limit the conversion from differential mode to common mode, is undertaken by comparing the ratio of the DM current to the CM current and this parameter is known as the transverse conversion loss (TCL). However, due the fact that broadcast radio signals received by the LVDN as ingress noise appear as common mode signals they often mask the TCL measurements and it is therefore considered more effective to measure the differential mode signal produced by an injected common mode signal. This measurement is known as the longitudinal conversion loss (LCL).

$$LCL\,(dB) = 20\log\left[\frac{V_{CM}}{V_{DM}}\right]$$

Equation 3.9.1

The International Telecommunications Union (ITU, 1996) in Recommendation G.117 provides a method to derive LCL values of unbalanced transmission lines via the ratio of voltages as Equation 3.9.1.

Equally by employing the impedance values relative to these voltages with *k* to represent the degree of unbalance the extrapolation of Equation 3.9.2 allows a relationship between the cable LCL and circuit impedance to be given.

$$LCL(dB) = 20\log\left[\frac{1}{k}(Z_{SE} + Z_{LE})\left(\frac{1}{Z_{SP} + Z_{SN}} + \frac{1}{Z_{LP} + Z_{LN}}\right)\right]$$

Equation 3.9.2

From this expression we can determine that as common mode impedance increases the resulting LCL will also increase and conversely as the differential mode impedance increases then LCL will decrease. This would suggest that the more extensive the CBN through the provision of more parallel paths then the lower the LCL will result for the installation as a whole.

As stated above, although it is considered more effective to measure LCL the parameter of interest when considering the production of a common mode current is in fact TCL. Many researchers, such as Mahbub ar Rashid et al (2003) have assumed that the LVDN is a passive system and that measurement of the TCL is the reciprocal of LCL. Magesacher (2002) confirmed this to be the case for ADSL cable measurements and as such the terms TCL and LCL are generally used interchangably. However,measurements made (CISPR, 2003) which recorded both TCL and

LCL found the LCL to be consistently 6dB lower than the TCL across the frequency range of 1-30MHz.

It can be seen that this parameter has been much studied and numerous conclusions drawn as to whether there are any benefits in employing LCL measurements within the PLT environment. Opinions vary from complete dismissal (Verpoorte, 2003) to perfect correlation with radiated field (Oka, 2007), Pang (2008) and Miyoshi (2005).

Experimental data presented at a CISPR/I/WG3 meeting also caused serious doubt as to whether the near-end LCL measurements could be of use to predict common LVDN performance. Major concerns expressed were that error in LCL increases with cable length, i.e. the error increases when the LCL at the far end decreases with the inductance having the most dominating influence. This was subsequently supported by Kitigawa (2009) who found that near end LCL measurements to underestimate the common mode current at the unbalanced load.

Finally experiments by Lauder (2005) using various unbalanced transmission lines composed of standard LVDN cabling noted that connection of the neutral conductor to earth, as arranged in a TNC-S installation, degrades significantly the measure of LCL by up to 30dB.

3.10 Reflections & Discontinuities

For reflections at the line end or discontinuities along the line length a reflection coefficient is given as Equation 3.10.1 from page 206 of Paul (2006) by the ratio of impedance 'mis-match', Γ;

$$\Gamma = \frac{Z_L - Z_O}{Z_L + Z_O}$$

Equation 3.10.1

Given a measuring circuit of known impedance we can therefore determine the impedance of the load or circuit under test (CUT) via measurement of the return loss (S_{11}), which indicates the magnitude of the reflected signal with respect to the incident or injected signal.

The reflection coefficient also allows the voltage standing wave ratio (VSWR) to be determined as given by Equation 3.10.2;

$$VSWR = \frac{1+\Gamma}{1-\Gamma}$$

Equation 3.10.2

3.11Skin Depth

Use of the cable characteristics given in Figure 3.4 and application of Equation 3.11.1 from page 273 of Paul (2006) gives the skin depth of a twin and earth cable as;

$$\delta = \frac{1}{\sqrt{\pi f \mu_O \sigma_c}}$$

Equation 3.11.1

where conductivity σ_c for copper conductors is 5.8+E7 Siemens per metre, giving the skin depth δ of 0.017mm at 15MHz. Knowing skin depth is a

function of the square root of the frequency we can expect δ to have reduced at 30MHz to approximately a fifth of the depth from 1MHz.

$$R = \frac{\rho}{\delta p} l$$

Equation 3.11.2

The high frequency resistance of the line is also frequency dependant, being inversely proportional to skin depth, and shows a fivefold increase across the powerline frequency spectrum.

3.12 Common Mode Transfer

Radio frequency emission tests are one of the basic requirements to demonstrate compliance with the electromagnetic compatibility regulations and all electrical products are tested to ensure that other users of the spectrum are protected from the emissions generated when the product is in use.

However, as stated in Chapter 2, the unique arrangement of powerline has meant that neither a defined method to record measurements nor a reliable method to simulate the field environment has been developed. This has resulted in poor understanding of the correlation between the asymmetric currents and radiated fields.

Additionally Schwager (2010) who recorded both the common mode current (CMC) and differential mode current (DMC) at several locations across the LVDN found that the attenuation of the DMC was consistently 16dB greater

than that of the CMC signal and suggests this may be due to mutual inductance from the return conductor.

3.13Field Generation

As indicated in Figure 3.8.1. the DMC circulates via the load and consists of opposing currents of equal magnitude within the phase and neutral conductors. Theory suggests (Paul, 2006) & (Wright, 1990) that the net electrical field produced at a distance of d_m metres parallel to a cable with a differentially injected signal is of limited magnitude, as it comprises the sum of the electrical field components which on the balanced line are equal and opposing.

However, in contrast to the differential mode current the net effect of the electrical field components from the common mode current, shown as the individual currents I_1 and I_2 in Figure 3.13.1 within the balanced line are the same phase and as such add to provide a significantly larger field, as indicated in Figure 3.13.1. Wu et al (2010) suggests that the common mode current resulting from powerline has an influence on the radiated field 95 times greater than the DMC.

As described in Section 3.4 the cable consists of phase and neutral copper conductors with a separation distance of s (metres). The two conductors are insulated and over-sheathed with polyvinylchloride, which is characterised by the permeability $\acute{\varepsilon}$. These conductors form a pair of dipole antennas, of the circuit length L and it can be shown (Donohoe, 2012) that the electrical field at an angle θ is given by Equation 3.13.1.

$$E_\theta = j\eta \frac{e^{-j\beta r}}{2\pi r} I_o \left[\frac{\cos\left(\frac{\beta L}{2}\cos\theta\right) - \cos\left(\frac{\beta L}{2}\right)}{\sin\theta} \right] = j\eta \frac{e^{-j\beta r}}{2\pi r} I_o F(\theta)$$

Equation 3.13.1

where $\beta = \frac{2\pi}{\lambda}$ and $\eta = \sqrt{\frac{\mu}{\varepsilon}}$

Equation 3.13.2

if for simplicity we assume that all conductors are located in air and ignore the complex arrangement of the insulation of the earth conductor then we can show η =120π.

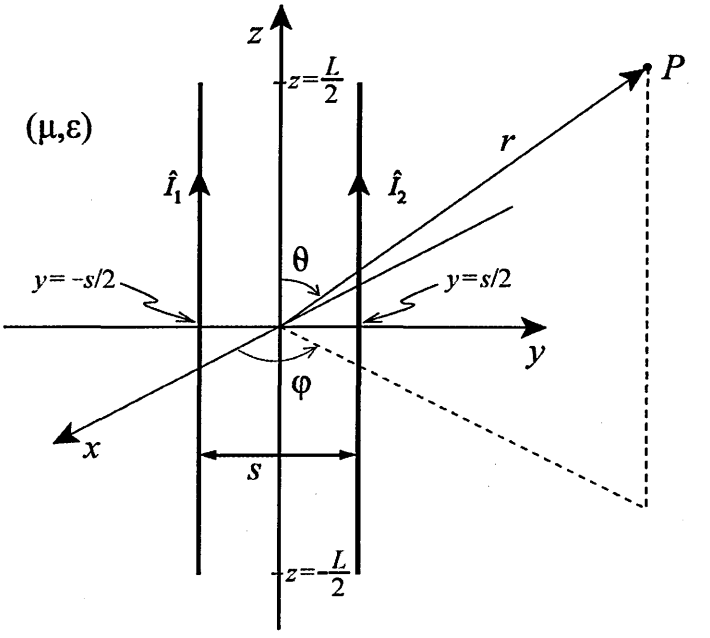

Figure 3.13.1 Geometrical Arrangement for the Common Mode Circuit (Donohoe, 2012)

For dipoles the radiation pattern is shown to be a feature of the dipole length, and where length is less than one wavelength the point of maximum radiation is shown to be at 90° to the conductor. At frequencies greater than this where the cable length becomes several wavelengths long the radiation pattern will vary with the maximum point occurring at an angle other than 90°.

For Hertzian dipoles, which are generally taken to be *L<<1/10* wavelength and the current distribution along the dipole can be assumed as constant, i.e. as a current carrying conductor.

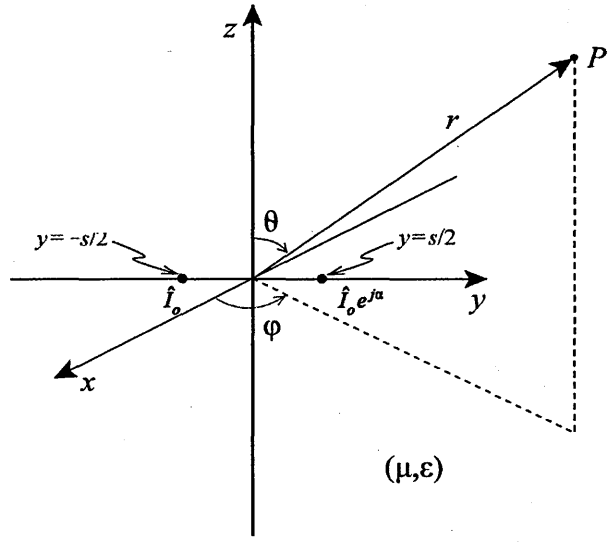

Figure 3.13.2 Image of Array Factor for Common Mode Circuit (Donohoe, 2012)

At a point P, located in the far field and as shown in Figure 3.13.2, from the axis of the dipole the electric field is shown to have a value as given in Equation 3.13.3 from Donohoe (2012).

$$E_\theta = j\eta \frac{e^{-j\beta r}}{4\pi r} I_o \beta L \sin(\theta)$$

Equation 3.13.3

However as the field generated is actually the combination of fields from the pair of dipoles the phase difference of the currents must be considered and as stated above for common mode currents the currents are in phase and as such we can simply the field generation via the array factor as Equation 3.13.4 for the two conductors.

$$ARRAY_{CM} = e^{-j\frac{\beta s}{2}\sin\theta\sin\varphi} + e^{j0}e^{j\frac{\beta s}{2}\sin\theta\sin\varphi} = 2\cos\left(\frac{\beta s}{2}\sin\theta\sin\varphi\right)$$

Equation 3.13.4

The spacing between conductors is in the order of 5mm compared to the measuring distance of 10 metres. We can therefore assume that $\theta=90°$ and neglect the sine of the angle to reduce the array for common mode radiation to that given as Equation 3.13.5.

$$ARRAY_{CM} = 2\cos\left(\frac{\beta s}{2}\sin\varphi\right)$$

Equation 3.13.5

It can be shown that the directional radiation of the common mode current is distinct from that of the differential mode current for all values of φ and this is shown in Figure 3.13.3 below, which indicates that at all angles around the conductors the resulting electric field is constant for the CMC. This contrasts to the differential mode radiation pattern, shown on the right of Figure 3.13.3 which clearly exhibits the points of maximum radiation occurring at 90° only.

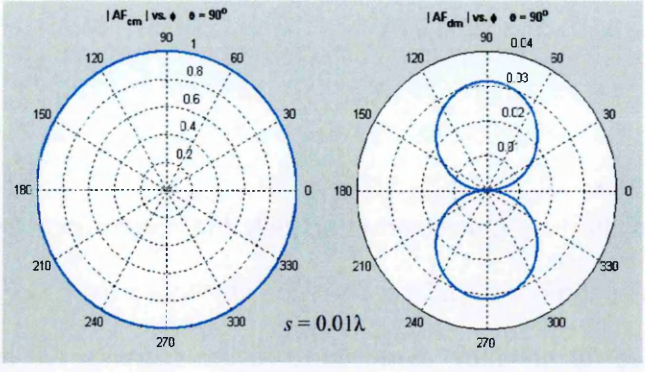

Figure 3.13.3 Image of Field Generation from CMC and DMC (Donohoe, 2012)

Use of the array factor as Equation 3.13.5 with the previously developed radiated field expression in Equation 3.13.3 provides Equation 3.13.6.

$$E_{\theta CM} = j\frac{2\pi}{5}\frac{e^{-j\beta r}}{d_m} f I_C L \sin(\theta)\cos\left(\frac{\beta s}{2}\sin\theta\sin\varphi\right)$$

Equation 3.13.6

Knowing the radiation at all angles from the conductors is equal we can simplify the calculation to give the field strength at a distant point *d* within the plane of maximum radiation as Equation 3.13.7.

$$E_{CM} = j\frac{2\pi}{5}\frac{e^{-j\beta r}}{d_m} f I_C L \cos\left(\frac{\beta s}{2}\right)$$

Equation 3.13.7

And finally this is resolved as Equation 3.13.8. where f is the frequency in hertz, d_m is measurement distance in metres and L the cable length in metres.

$$E_{CM} = \frac{2}{5}\pi f \frac{L}{d_m} I_C = 1.257x10^{-6} f \frac{L}{d_m} I_{CM} \text{ (μV/m)}$$

Equation 3.13.8

It is clear that the radiated field is both length and frequency dependant and not influenced by spacing between conductors. Therefore direct comparison of the field generated from circuits of various cable sizes can be made.

$$E_{CM} = 1.257x10^{-6} \frac{I_{CM} fL}{d_m} \text{ (μV/m)}$$

Equation 3.13.9

Derivation of the radiated emission resulting from the differential mode current (I_{DM}) is shown via the same method and we note from Equation 3.13.10 that the field strength is several orders of magnitude smaller than that of the common mode emission.

$$E_{DM} = 1.316\times10^{-14} \frac{I_{DM} f^2 Ls}{d_m}$$

Equation 3.13.10

Whilst this seems intuitively correct given the proximity of the return conductor and therefore the limited loop area for a typical domestic cable, the impact of placing the earth conductor between the phase and neutral conductors has not been considered. It is therefore to be noted that application of Equation 3.13.9 to calculate the radiated field from the LVDN may incorporate error as a proportion of the common mode current may circulate via the earth conductor, offering both current phase and field cancellation effects, as observed for the differential mode current.

Whilst the above equations relate to free space only, Ishigami (2007) states that building structures also have a large effect on suppressing the radiated field from the common mode current. Whilst this study was conducted solely for Japanese buildings, which included wooden and reinforced concrete walled type structures the following results, as Table 3.13.1 were proposed.

Frequency	Attenuation from Wooden Structures	Attenuation from Concrete Structures
2-10MHz	17dB	27dB
10-30MHz	10dB	27dB

Table 3.13.1 Attenuation of HF signals within structures (Ishigami, 2007)

It is therefore necessary to relate the radiated field with the common mode current in context of the building structure, as this will determine the level of attenuation and form part of the overall transfer function. This parameter includes also the form of electrical earthing, as described earlier, as extensive metallic-work to the building perimeter is likely to increase the CMC generated field emissions.

Ishigami (2007) defined the shielding effectiveness as the ratio of maximum field strength at 10 metres from powerlines not enclosed by a structure to that with powerlines enclosed. The results showed considerable variation with structure type, powerline layout and frequency. The values proposed were not however verified by measurements and this is reflected in Chapter 4.

The ITU also found (ITU, 2010) that the radiated emission from the supply cable outside the property may be 20-47dB stronger than the emissions from the internal LVDN due to the shielding effects from the structure.

3.14 Basis for Measurement

In order to obtain test data from powerline modems there are essentially two methods available;

1. Energisation of the modem via a Line Impedance Stabilisation Network (L-ISN), i.e. providing a defined and stable mains supply and record conducted emissions whilst within the known parameters of a test cell.

2. Inject known signals, via the modem or signal generator into the LVDN and record values of conducted and radiated fields whilst affecting the LVDN performance.

The testing described in Chapter 4 comprises both these methods with the initial arrangement employing a test cable for both modem and injected signal tests within a test cell and then subsequently utilising various circuits comprising the LVDN.

The typical arrangement for the measurement of conducted emissions via a test cell is shown in Figure 3.14.1 below and is described in EN 55011 and EN 55016. Ideally the test cell is required to provide a ground plane of minimum dimensions to ensure all test equipment is provided with a common low impedance connection.

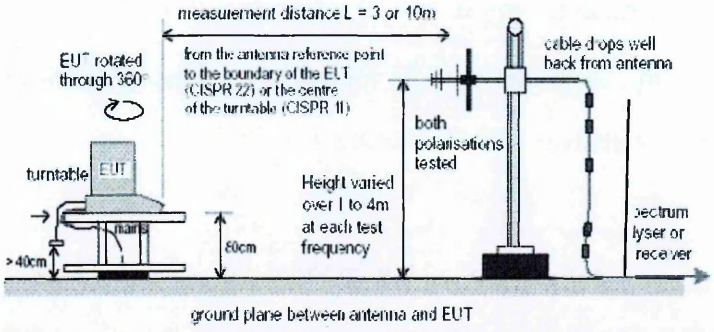

Figure 3.14.1 Indicative Arrangement for Test Cell 'setup' (EN 55016)

In order to achieve this all test cell measurements were undertaken within the OU anechoic chamber which consists of a cladded structure with an open steel mesh flooring, allowing all equipment to be strapped to the ground plane and the 'cable under test' to be placed at a known height above the ground plane.

Whilst radiated RF measurements pertaining to product emissions are generally completed according to EN 55011 and EN 55016 standards and are usually performed on an open area test site (OATS) this is impractical to apply when testing on LVDNs within homes, buildings. As a known ground plane is not available nor a defined reflection of the radiated wave the received signal is therefore liable to variation.

Defining the measurement distance from the source to receiver is also unclear as the convention of placing the receiving antenna at a known distance from the building does not allow for a known distance from the source to the antenna.

It is equally unclear as to which frequencies should be measured when obtaining conducted measurements from the LVDN. Given that both the PLT signal and intentional radio broadcast signals are both present on the LVDN the creation of intermodulation frequencies is possible given the non-linearity of the connected loads. Such intermodulation products may coincide with the frequency of measurement to provide significant errors and therefore historically the OUPLCRG used intermodulation software to compute a number of spot frequencies for measurement. The test setup described below however, benefits from the ability to provide conducted sweep measurements and we shall see that measurements are recorded at 100kHz intervals and include the defined intermodulation frequencies.

Having established which frequencies to measure the convention, i.e. that established by CISPR, is to require measurements to be made as quasi peak (QP) which introduces a 160ms dwell time to ensure transient signal effects are removed. The limitations on much of the recording equipment, including the Signal Hound spectrum analyser, provide for average or peak measurement only and therefore Table 1 of EN 55016 allows for the adjustment of measurements within Band B (0.15-30MHz) from QP to peak via the addition of 6.6dB.

This value was verified on initial OUPLCRG measurements via the Rhode and Schwartz receiver which is configured to make sweep measurements of average and peak values only. However, on completion of the sweep the software will perform QP measurements on the higher signal strength values, which when averaged indicate a 6dB reduction.

3.15Ingress & Conducted Noise Floor

Ingress relates to the RF level residing on the LVDN, as measured between phase to neutral, which is received by the LVDN components from the incident broadcast signals. Within Technical Specification 102578, ETSI (2008) also qualify ingress signals as being those 14dB above the conducted noise floor with a minimum threshold of -95dBm.

Figure 3.15.1 indicates such a signal, which corresponds to the centre of a short-wave radio band. We can see that ingress signals are more prevalent in the lower frequencies ($1<f<16$MHz) with the conducted noise floor in the upper frequencies ($16<f<40$MHz) stable at a base -120dBm.

Whilst the sensitivity of radio receiving equipment is governed by the creation of internal noise from the components, the operating temperature, most modern receivers have suitable dynamic range to allow the recording of noise floor levels in excess of that shown in Figure 3.15.1.

Accordingly the measurement of the noise floor requires considerable care to determine a 9kHz free band and generally sweeping the spectrum using an spectrum analyser does not provide an accurate measurement.

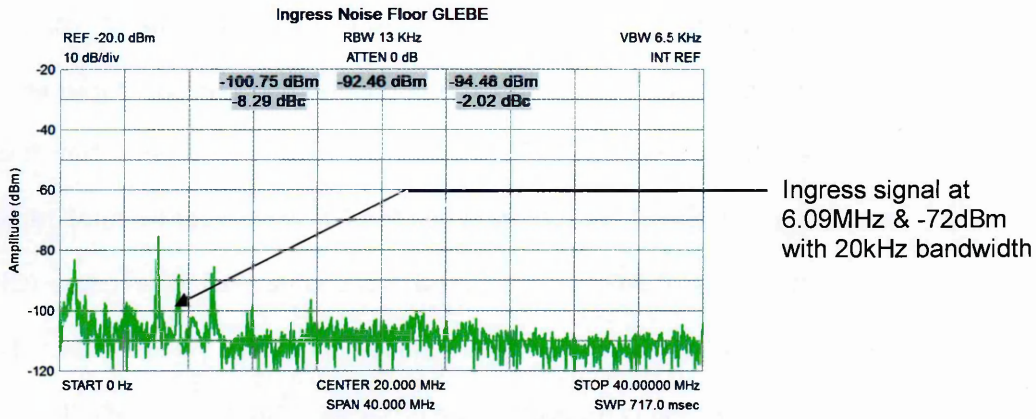

Figure 3.15.1 Typical ingress noise floor at GLEBE, 2010

One method to overcome the limitation of using such equipment is to use a narrower bandwidth and then convert values to a 9kHz bandwidth for direct comparison with other measurements. However, in order to identify the ingress signals the sweep was conducted with the resolution bandwidth (RBW) set to 25kHz and therefore an adjustment of -4.5dB, to normalise to 9kHz, would indicate that the conducted noise floor is in the order of -125dBm.

3.16 RF Noise floor

Ultimately all radiated and conducted emissions resulting from PLT signal propagation can create electromagnetic interference (EMI) and it is under the auspices of the ITU-R to manage and protect the radio communication spectrum from such interference.

Within the HF bands the threshold for signal reception is determined by the ambient noise level or RF noise floor. The RF noise floor is made up of both natural ambient noise such as radiation discharge from lightning activity and the incidental man-made noise from electrical apparatus.

The impact of 'leaked' manmade emissions is of particular concern as EMI can propagate by sky-wave and thus increase the noise floor at remote locations, as concluded by OFCOM (2010) who suggested that the widespread deployment of PLT will increase the RF noise floor to 'rural' regions of the UK in excess of 5dB. Conversely the Japanese PLT Committee (Oka, 2007) has concluded that PLT systems should not raise the RF noise floor when the radiated field is measured at a distance of 3m from the LVDN.

Calculation of the noise floor is given via ITU-R P.372-10 (ITU, 2009) which allows calculation of the field strength *E* for a half-wave dipole in free space, where *B* is the measurement bandwidth.

$$E = F_a + 20\log f + B - 98.9$$

Equation 3.16.1

F_a, the median noise figure, is given by the following Equation 3.16.2.

$$F_a = c - d\log f$$

Equation 3.16.2

Where factors *c* and *d* are the application of constants appropriate for the level of urbanisation corresponding to the measurement location and are shown below in Table 3.16.1.

Environmental Category	c	d
City	76.8	27.7
Residential	72.5	27.7
Rural	67.2	27.7
Quiet Rural	53.6	28.6
Galactic Noise	52.0	23.0

Table 3.16.1 Value of constants c & d

Substituting these values gives the equation for rural noise floor field strength as Equation 3.16.3 below.

$$E = 67.2 - 27.7 \log f + 20 \log f + 39.54 - 98.9$$

$$= 7.84 - 27.7 \log f + 20 \log f$$

Equation 3.16.3

At nominal values of 5, 15 and 25MHz this equates to a field strength of 2.8, -0.63 and -2.2dBµV/m respectively. Comparison of these values with the measured sweep of a 'rural' noise floor, as shown in Figure 3.16.1 demonstrates, after adjustment for RBW and antenna factor, that generally far higher field strengths are recorded at 10, 7 and -3dBµV/m. Such readings suggest that, from an RF perspective, that the accepted residential curve may now be more appropriate for the environment found at a UK rural location.

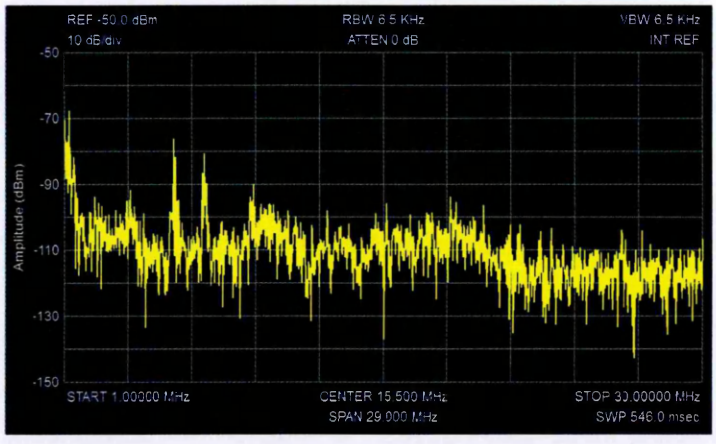

Figure 3.16.1 Typical 'rural' noise floor, 2010

3.17 k Factor, Antenna Factor & Emission Factor

The *k* factor defines the relationship between the power injected into the LVDN and the resulting radiated electric field measured at a given distance of 3 metres from the installation. This was proposed by Wirth (2003) via a CISPR submission as;

$$k[dB\mu V/m] = E[dB\mu V/m] - P[dBm]$$

Equation 3.17.1

However, in order to relate the injected power directly to field strength the *k* factor incorporates all assumptions regards the LVDN impedance, LCL, common mode transfer and measuring distance from the LVDN.

If we were to assume that the LVDN is not a passive system then the term antenna factor is applied to the relationship between the ingress voltage measured and the field strength of the incident broadcast signal. Antenna factor is therefore given as;

$$AF[dB] = E[dB\mu V/m] - e[dB\mu V]$$

Equation 3.17.2

Further to his review on the implementation of these factors, Brannon (2005) proposed an improved correlation of field measurements via an Emission Factor, which allowed for more accurate analysis, as shown in Equation 3.17.3.

$$EF[dB\mu V/m] = LCL - 10\log B_w[kbps] - 10\log D[km]$$

Equation 3.17.3

Whilst this improvement overcame some of the errors relating to the assumptions stated earlier and allowed direct comparison of test sites, as Table 3.17.1 indicates, it did not provide a means to determine those features of the LVDN having a significant contribution to the radiated emission.

measurement point	system	sub-band (MHz)	LCL (dB)	distance (km)	capacity (kbps)	measured emission (dBuV/m)	emission factor (dBuV/m)
Elgin master	Ascom	1 - 4	21.2	0.15	570	33.15	35
		4 - 7	15.8	0.15	570	38.86	35
		7 - 10	12	0.15	570	50.94	44
Lotland Road slave (cleansing depot)	Ascom	1 - 4	39.5	0.021	570	31.1	60
		4 - 7	41.8	0.021	570	20.02	51
		7 - 10	36.4	0.021	570	22.55	48
Woolley Hall	Ascom	1 - 4	only one carrier in use				
		4 - 7					
		7 - 10	24.9	0.05	570	60.55	71
Woolley Hall	Main.net	1 - 4	39.8	0.05	173.5	35.6	66
		4 - 7	28.5	0.05	173.5	40.46	60
		7 - 10	24.9	0.05	173.5	48.43	64

Table 3.17.1 Emission Factors for several OUPLCRG Test Sites (Brannon, 2005)

Also, the principal benefit realised is allowing comparison of access PLT systems where measuring distances vary considerably.

Notwithstanding the above definitions we note from Chapter 2 that the gain of an LVDN, relative to an isotropic antenna (dBi), and relating the PLT modem power to the radiated emission is generally referenced as the antenna factor of the installation. This empirically derived value has become the assumed default factor for the RF performance of the LVDN.

3.18 Near Field/Far Field Transition & Regression

Derivation of the above factors requires measurement of the radiated field strength at given distances from the source and whilst EN 55016 indicates that this should be done at a distance of 3m or 10m the United States give limits at a distance of 30m from the source. There is clearly a need to be able to relate and compare measurements taken at different distances from the source.

Ideally all measurements would be taken in the far field, where the radiating waves are perpendicular to the measurement antenna and are related via the impedance of free space. However, the distance for the transition from near field to far field for structures whose physical dimension is an appreciative ratio of the propagated wavelength (Barclay, 2012) is normally quoted as the Raleigh distance (d). This distance is found as $d>2D^2/\lambda$, where D represents the dimension of the radiating structure, and shows that measurements for 30MHz would require a measuring distance to be in excess of 20m from the source, assuming that the structure had a dimension (D) of 10 metres.

If we maintain measurements within the far field, the regression in field strength should reflect the variation in distance as $1/d$, equating to a 20dB decrease per decade. Whilst this is a recognised and desirable condition it is often not practical to achieve and so measurements made in the near field are

expected to decay as $1/d^2$ equating to 40dB decrease per decade. However, Salehian (2011) undertaking regression measurements from PLT systems found the actual attenuation with distance in the near field to be 18.3dB per decade and therefore regression (r) has been calculated as a linear function for all frequencies as Equation 3.18.1.

$$r = 20\log\left(\frac{d}{3}\right)$$

Equation 3.18.1

3.19 Isotropic Equivalent Field

To provide a measure for comparison of antenna or inadvertent radiating structures the equivalent field strength produced from an isotropic antenna is often used and given as gain (dBi). From Semtech (2007) the following equations allow calculation of the power density and consequential electric field at a distance d from an isotropic radiating source. The isotropic antenna radiates energy equally in all directions; hence the radiation pattern in any plane is circular.

Power density (P_D) from a given source of power (P), allows derivation of the electric field (E) at a measurement distance (d) as Equation 3.19.1.

$$P_D = \frac{P}{4\pi r^2} = \frac{E^2}{120\pi}$$

where $E = \sqrt{\frac{30P}{d}}$

Equation 3.19.1

3.20Summary

Having reviewed the theory applicable to the powerline environment and considered those parameters pertaining to the RF performance of the system we can utilise the equations given above to allow a theoretical determination of the conducted and radiated values to be calculated.

MODEM		
Modem power	-55	dBm/Hz
CONDUCTED		
Measuring bandwidth	9	kHz
Earth Connection Type	1	(Factor 1-3)
LVDN Dimension	22	m
Cct Conductor Separation	5	mm
Diff Impedance	100	ohms
CM Impedance	50	ohms
LCL for circuit	40	dB
Diff Signal Voltage	95	dBµV
Diff Signal Current	55	dBµA
CM Voltage	50	dBµV (TCL used)
CM Current	16	dBµA
RADIATED		
Frequency	10	MHz
Measuring Distance *D*	10	m
Efield from DMC at *D*	18	dBµV/m
Efield from CMC at *D*	44	dBµV/m

Figure 3.20.1 Predicted Performance of a PLT system

This is shown in Figure 3.20.1 below, via an excel spreadsheet, and provides the predicted field strength for a given frequency and measuring distance. Utilisation of the derived parameter values for impedance, LCL, as described above indicates a common mode current (CMC) of 16dBµA and a radiated field from this common mode current of 44dBµV/m.

Whilst the above spreadsheet allows manipulation of the predicted field values, the following chapter reviews the practical testing undertaken to verify the system performance and describe salient features influencing the production of EMI.

4.1 Introduction

Previous chapters have considered the progress made in developing a standardised measuring methodology for PLT installations and considered those mechanisms involved in the propagation of the injected signal relative to radiated EMI. This chapter describes the methodology and the extent of the measurements undertaken as part of this thesis. Prior to discussion on the testing itself we shall review the testing procedures and the equipment used for each of the tests described.

The initial measurements described below are conducted on LVDN circuits which are not energised and rely on an injected signal to derive a measurement. On completion of these tests and having defined the RF characteristics of the CUT further 'live' circuit measurements are undertaken employing the Comtrend 902 modem operating in polling mode.

The full sequence of measurements undertaken to underpin the overall model is therefore as follows:

1. Define the characteristic impedance for the standard twin and earth cable in order to establish the measurement setup, i.e. the BALUN ratio.

2. Record the electrical parameters for the test cable and individual circuits comprising the LVDN of a typical UK property, a detached bungalow subsequently referred to as BRAMBLE.

3. Apply the developed model to the 'live' situation with Comtrend units operating to the same LVDN.

4. Finally further measurements are undertaken of particular features such as TCL variation to all measuring points on a single circuit and earth current at the PME connection.

4.2 Test Methodology

As stated in Section 2.10 the complexity and variability of the circuits comprising the LVDN results in a need to assess their RF performance due to their unique wiring arrangements and not describe their unique physical arrangement within each property. This is best observed by analysing the CUT as a two port network and applying S parameters to describe the performance.

S parameters are a mathematical concept that provides a method to describe the magnitude of RF energy propagating through a network having multiple ports. Use of S parameters allows us to describe such a network as a "black box" across which we measure the input and output voltages.

Injection of an RF signal to the network results through impedance mis-match in a level of signal reflection from the input port. In addition, some of the signal is also 'scattered' and appears on the remaining ports as output signals demonstrating a level of gain or attenuation.

Although S-parameters are complex, providing both magnitude and angle their use within this thesis is based on magnitude only, as it was only possible to record this value and thus the S_{11} measurements refer to the ratio of signal

magnitude reflected from the input for a given signal and the S_{21} measurement refers to the voltage response at the output for a given signal.

In addition several characteristics of the CUT, as described in Chapter 3, are also recorded to assist in the correlation of measurements and construction of an overall model or transfer function. This arrangement is shown in Figure 4.2.1 below.

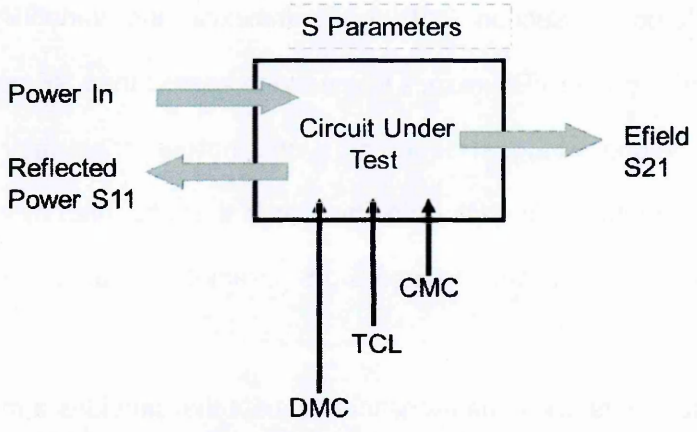

Figure 4.2.1 S Parameters

In order to define the RF characteristics of the CUT we first inject a swept signal, of known magnitude, and determine the magnitude of the reflected power, due to impedance mismatch. This parameter is often defined as Γ, the input voltage reflection coefficient, and allows a scalar comparison of the impedance of the CUT relative to the nominal input impedance to provide the return loss S_{11}.

$$S_{11} = -20\log|\Gamma|$$

Equation 4.2.1

The 'standard' input impedance for unbalanced measurement equipment is generally taken as 50Ω, however, as the excitation of the CUT consists of both the phase and neutral conductors, which are electrically balanced with respect to the earth plane, the injected signal needs to be applied via an unbalanced to balanced transformer or BALUN. The provision of a BALUN also provides an opportunity to therefore match the impedance of the test equipment to that of the CUT in order to minimise the reflected signal due to mismatch.

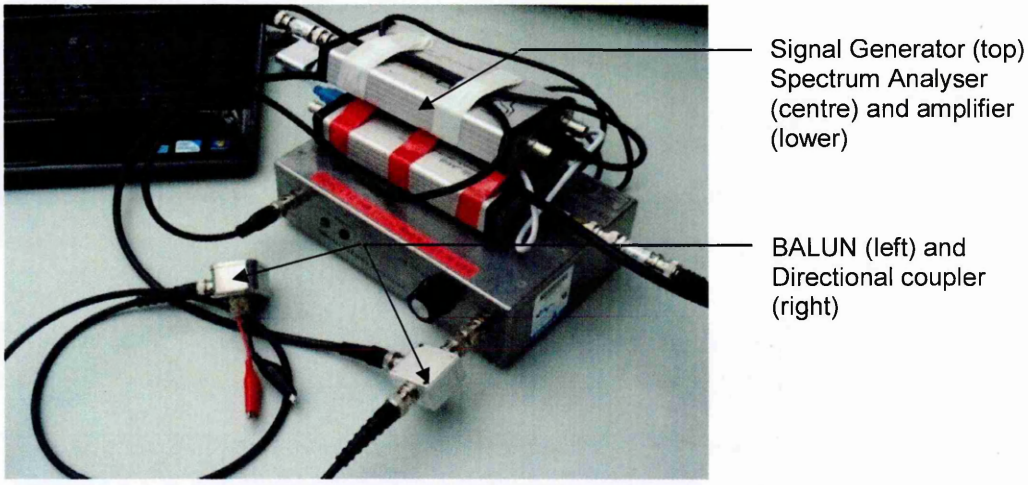

Figure 4.2.2 Measurement Setup

As described in Chapter 3 circuits forming part of the LVDN have considerable impedance variation across the 1-30MHz range and generally the value of 100Ω is accepted as the nominal impedance. In order to validate this assumption and to determine the ideal ratio of the BALUN a measurement of the characteristic impedance of the test cable, i.e. standard UK domestic 2.5mm^2 twin and earth cabling, was made.

4.3 Characteristic Impedance (Twin & Earth Cabling)

When using a 3m length of cable it is impractical to try and separate the capacitive and inductive reactances to allow the discrete measurement of each parameter and therefore we employ the formula, as Equation 4.3.1 below from Butler (1989) to determine the characteristic impedance Z_O through the open and short circuit impedances.

$$Z_o = \sqrt{(Z_{open} * Z_{short})}$$

Equation 4.3.1

Testing was conducted using a Hewlett Packard 4192A Impedance Analyser which allowed measurement of the impedances shown in Table 4.3.1 up to 13MHz.

f(MHz)	Z_{open}	Z_{short}	Calculated Z_o
1MHz	38.1-j1031Ω	0.48+j11.89Ω	110-j0.2Ω
2MHz	16.8-j516.7Ω	0.68+j23.72Ω	110+j0.2Ω
5MHz	5.3-j192.4Ω	1.16+j62.64Ω	110+j0.5Ω
10MHz	2.95-j61.1Ω	0.6+j173.7Ω	103+j2.3Ω
13MHz	3.22-j20.4Ω	11.7+j414.6Ω	92+j5.9Ω

Table 4.3.1 Characteristic Impedance Measurements

We can see that the characteristic impedance Z_O is a complex impedance although the imaginary component is almost negligible, allowing us to quote domestic twin and earth cabling as having a nominal characteristic impedance that is constant and real at 110Ω.

It is to be noted that all testing described within this thesis has been conducted on twin and earth cabling and it is likely, although not considered here, that

older cabling having increased spatial separation between the phase and neutral conductors and using other forms of insulation will have distinctly unique impedance and RF properties.

4.4 BALUN

In order to carry out transmission line tests on LVDNs, comprising the above cable and operating as a balanced pair a BALUN providing a 1:2 ratio (50Ω unbalanced to 100Ω balanced) was selected providing wideband transmission in excess of the required 30MHz. The wideband transformer from North Hills, model NH14023, achieves this providing both high return loss, high common mode rejection, i.e. greater than 20dB and with an insertion loss of less than 1dB.

This BALUN was utilised for all conducted measurements, as detailed below, except for the TCL tests.

4.5 Directional Coupler

Having connected the test equipment to the CUT we need to arrange for the simultaneous operation of the tracking generator and swept measurement of the reflected signal via the spectrum analyser. In order to achieve this, a directional coupler is required, which provides a means to separate the injected and reflected signals.

A Mini Circuits ZFDC-10-5 coupler was selected having a suitable wideband frequency response, which again provided high return loss in excess of 30dB, a coupling loss from the input port of 11dB and a maximum insertion loss of 1.2dB.

The ZFDC coupler was utilised for all return loss and TCL measurements, in conjunction with the spectrum analyser and tracking generator described below, and all losses were accounted for in the subsequent evaluation of measurements.

4.6 Spectrum Analyser & Tracking Generator

Whilst EMC receivers complying to EN 55016 are generally employed for the testing undertaken below, the extended timescale and limited budget of this thesis required careful selection of an appropriate device that was more cost effective. It was also apparent that the majority of radiated emission tests and measurements on the LVDN require a high degree of portability, including the ability to operate without mains power being available.

A review of the available equipment concluded that the scalar network analyser offered by Signal Hound, when utilising the TG44 signal generator and SA44B spectrum analyser from Test Equipment Plus, California would provide the best compromise. In addition to meeting the above criteria, by virtue of being USB powered, the devices also provide a wide dynamic range: -151dBm to +10dBm with an extended RF frequency range up to 4.4GHz.

Although measurement accuracy is given as 0.25dB it was found that significant improvement resulted when 10dB pads were placed on both the generator and analyser ports, as this increased the return loss created by the spectrum analyser input. The combined tracking generator (TG) and spectrum analyser (SA) are used for all swept measurements on both conducted and radiated emissions.

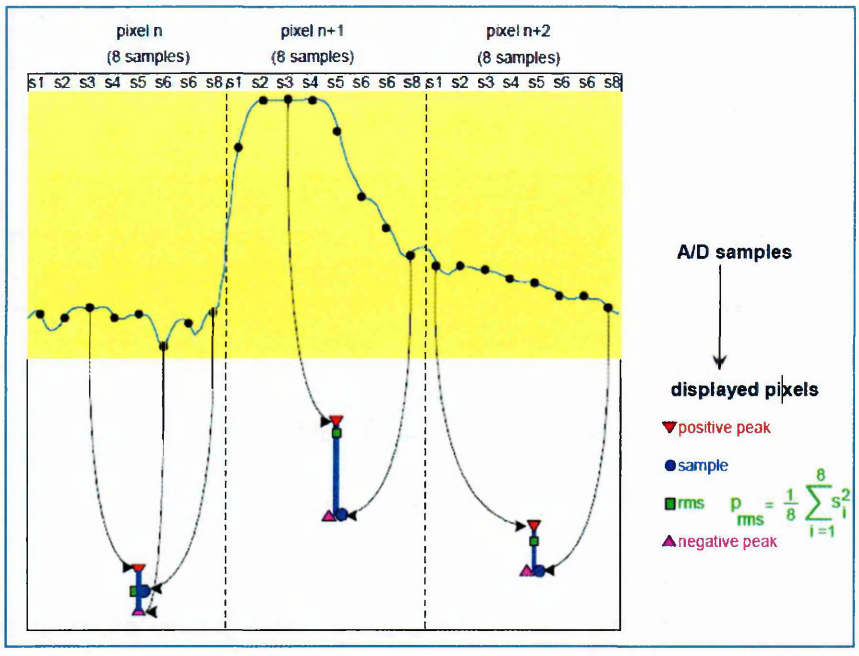

Figure 4.6.1 Image of spectrum analyser sample processing (RS, 2008)

Measurements are made using the 'maximum hold' function, which as indicated in Figure 4.6.1, displays the greatest value sampled. As the frequency span and RBW determine the number of data points in a sweep (given by Test Equipment Plus as 2.5 x SPAN/RBW) and assuming the graticule is composed of 300 pixels the displayed maximum relates to the highest value of the 25 samples. It is reasonable therefore to assume this equates to a peak value and we can convert to both average detection (AV) and quasi peak (QP) where required, from this figure.

As stated in Chapter 3 the conversion from peak to QP equates to a reduction of 6.6dB, and knowing that the Comtrend 902 PLT modems utilise orthogonal OFDM modulation comprising 1536 carriers, we can relate peak to average power ratio *(PAPR)* which is determined via Equation 4.6.1.

$$PAPR = 10\log|S_n|$$

Equation 4.6.1

Where the Sn is the number of sinusoidal and is dependent on the sinusoidals having frequency separation, where each sinusoidal is modulated to provide independent information. Whilst it is unlikely that all subcarriers are modulated simultaneously the Sn equates to unity and the conversion from peak to AV results in a reduction of 10dB.

Generally all images produced within this thesis are captured as maximum hold and a 10dB reduction has been made to allow calculations, where required, to be given as AV figures.

4.7 Current Probe

In order to make conducted current measurements on the LVDN a HF current probe is required and again these are commercially available with those used for EMC testing constructed in accordance with the requirements of EN 55016.

However, as they are relatively simple they can be constructed. The probe used for the testing described herein essentially comprises a ferrite core which is wound with a number of close turns of copper wire terminated in a 50Ω resistance. The ferrite aperture was sized to allow insertion on most standard domestic cables, i.e. providing a 10mm internal diameter and selected as a split unit allowing simple insertion around live conductors and cables.

In order to calibrate the probe we determine the transducer factor which is found by applying a known RF current to the line and recording the resultant flow through the resistor. Therefore the transducer factor is:

$$F_T = I_{PRIMARY}(dB\mu A) - I_{MEAS}(dB\mu A) = 26dB$$

Equation 4.7.1

However, as the spectrum analyser readings are given as dBm it is more convenient to convert the measured dBm to the RF current flow in the conductor (dBμA) by applying an overall correction as Equation 4.7.1.

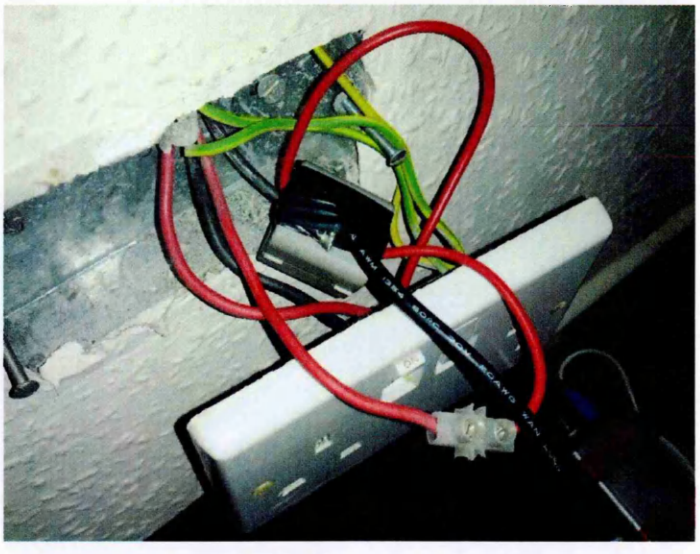

Figure 4.7.1 HF Current probe on ring main recording Comtrend DMC

It is also to be noted that insertion of the probe around the cable will record the 'net' current in the cable, however by exposing the conductors within the cable and placing the probe around both the phase and neutral conductors, as Figure 4.7.1 indicates, we can record the common mode current (CMC), as the differential signal is cancelled out and provides a resultant reading of $2I_C$.

Equally by reversing either the phase or neutral conductor through the ferrite we can arrange the probe to read the differential mode current (DMC), as this arrangement effectively negates the CMC field and provides a reading of $2I_D$.

Total corrections to be applied to the measurements made with the probe are;

- the addition of 10dB for the inserted pad to the SA results, as detailed in Section 4.6
- conversion of dBm to dBμA (as for 50Ω systems) requires 73dB addition, as described in Section 3.2
- transfer function of the current probe, as detailed in Section 4.7, requires addition of 26dB
- reduction in reading for probe on 2No conductors, as detailed in Section 4.7, results in reduction of 6dB
- reduction to normalise 13kHz measurement to 9kHz requires reduction of 1.6dB, as described in Section 3.2

All measurements are corrected in the following graphs as Equation 4.7.2.

$$DMC = probe + 10dB + 26dB - 6dB + 73dB - 1.6dB$$

$$= probe + 101.4dB$$

Equation 4.7.2

4.8 TCL Probe

As described in Chapter 3, a probe allowing the measurement of TCL as suggested by MacFarlane (1999) has been constructed by the Open University (version OU J2330LCL), and modified to allow connection to a 230V supply, via the addition of isolating capacitors and diode limiter to provide mains isolation and transient suppression.

The probe consists of multiple high permeability toroidal ferrite cores which offer either high impedance to the common mode signal, allowing presentation of the differential signal to the output port, or a low impedance such that the output port presents the asymmetric signal. All TCL measurements were made using the tracking generator (via the common mode port) and spectrum analyser (via the differential port) to record swept measurements across the 1-30MHz range.

As the differential output port is arranged to measure the average phase and neutral voltage with respect to earth, the full differential signal is twice that measured and when calculating the TCL we subtract 6dB from the measured differential value to provide the full V_{DM}. This equates as Equation 4.8.1.

$$TCL(dB) = V_{CM}(dB\mu V) - V_{DM}(dB\mu V) - 6dB$$

Equation 4.8.1

The probe design incorporates a calibration mechanism, consisting of a 470Ω 'unbalancing' resistor as which introduces a TCL of 26dB. Calibration of the probe is therefore simple and easily performed before each measurement to prevent error in connection.

4.9 Signal Level

Given both the power limitation of the tracking generator, having a maximum amplitude of -10dBm and the enhanced accuracy provided by operating with 10dB attenuators on both the generator and analyser ports, an external amplifier is utilised to allow a 20dB increase in the injected signal. The amplifier is used for all measurements and consists of an Open University constructed and calibrated model, as IFEC J2330.

Measurement of the injected signal, as seen at the input port of the directional coupler, i.e. the CUT was recorded as -3dBm and therefore allowing for the additional loss on the BALUN the CUT injected signal (P_{IN}) is taken as -5dBm.

4.10 S_{21} Radiated Field

Having determined the CUT return loss and consequently calculated the absorbed power we also record the radiated field, whilst maintaining the known injected signal level. A Wellbrook active antenna, as model ALA1530, is placed orthogonally at a single location 10 metres from the CUT and records both the E field generated by the EMI and the ambient noise floor at the time of measurement.

As described in Chapter 3 the ideal arrangement is to locate the antenna in the far field allowing the application of regression as *1/r* and facilitating the simple conversion of the E field measurement to an equivalent H field via the characteristic impedance (Z_o) of free space, as given in Equation 4.10.1. However, as the practicality of achieving this arrangement in terms of both the distances and residual signal levels are considerable the compromise of

locating the antenna at 10m from the source results in far field conditions being achieved for all frequencies less than 15MHz.

$$Z_O = 120\pi = 377\,\Omega$$

$$Z_O = 20\log(377\,\Omega) = 51.5 dB\Omega$$

Equation 4.10.1

In order to relate these measurements to those provided by other researchers at distances other than 10m, i.e. the nominal 3m distance applied by the PLT standards described in Chapter 2, the Efield values are adjusted for regression (r) as described in Section 3.17 and Equation 4.10.3. The addition of a regression adjustment of 10.54dB to the 10m measurement allows presentation as an Efield at 3m from the source. This adjustment is further utilized to allow calculation of the k factor, which as described in Section 3.17 is defined as a product of the Efield measurement at a 3m distance (dBμV/m) less the injected power (dBm).

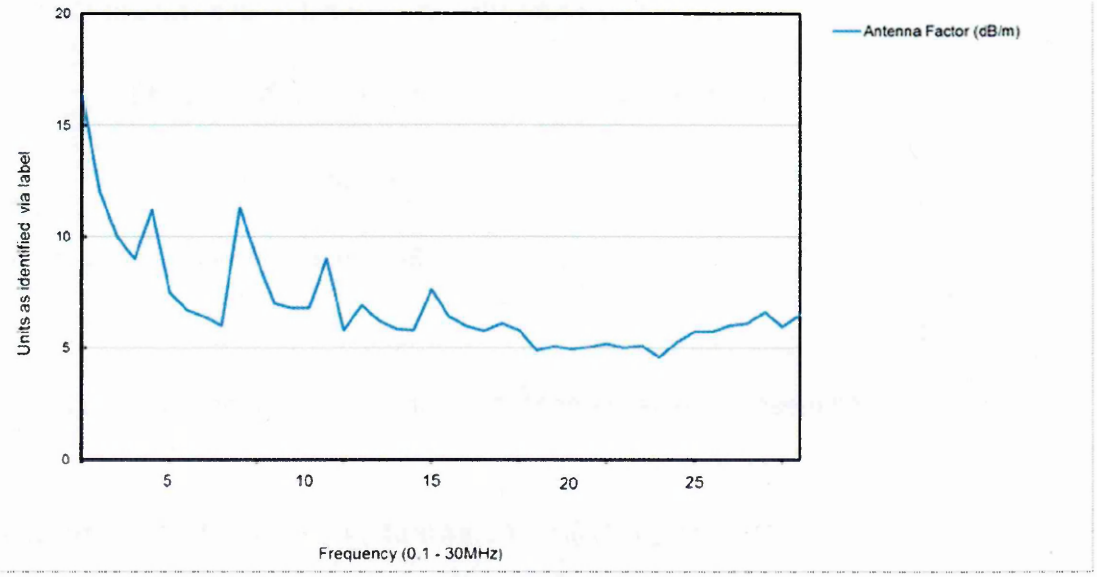

Figure 4.10.1 Antenna Factor for Wellbrook Loop

Determination of the Efield value also requires addition of the antenna factor (AF) and as an active antenna the antenna factor is an essential consideration of the design to prevent overload of the antenna or receiver.

The above AF has been applied to the S_{21} and noise floor swept measurements.

The ALA 1530 has an AF of approximately 0.1 at 150kHz and tends to unity at 30MHz, as demonstrated via the UKAS Laboratory Calibration Report (Wellbrook, 2011) and measurements performed at the Open University, using both an antenna of known performance and through calculation of known transmitter powers/distances.

Total corrections applied to the measurements made with the loop antenna are therefore;

- correction for 10dB pad to SA results +10dB
- correction for 30m length of RG58 co-axial results +2dB
- dBm to dBμV (as 50Ω system) requires +107dB
- antenna factor (as curve in Figure 4.10.1)
- reduction to normalise 13kHz measurement to 9kHz as -1.6dB

All measurements are corrected in the following graphs as Equation 4.10.2.

$$Efield\,(dB\mu V/m) = Loop(dB\mu V) + AF + 10dB + 2dB + 107dB - 1.6dB + r$$

$$= probe + 117.4dB + AF + r$$

Equation 4.10.2

$$\text{where regression } (r) = 20\log\left(\frac{d}{3}\right)$$

Equation 4.10.3

4.11 Mains Coupler

In order to allow the connection of RF receivers to the LVDN a mains coupler was developed by the OUPLTRG, as Figure 4.11.1, to isolate the receiver from mains voltages.

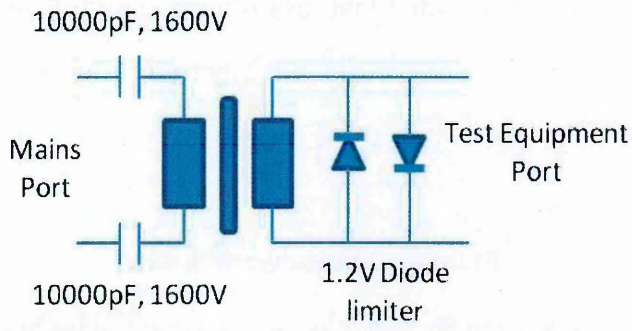

Figure 4.11.1Circuit Diagram for mains coupler

Isolation from the mains voltage is provided by the two 10000pF, 1600V rated capacitors and a miniature wideband transformer with a 1:1 ratio, which additionally matches the modem source and load impedances to the power line impedance to ensure maximum signal power transfer

Test equipment signal port protection is provided by the diode limiter, which prevents signals greater than 1.2V peak to peak being applied to the test equipment, by means of the short circuit which is applied to the test port in such conditions. The operation of the limiter is assisted by the high saturation

impedance of the transformer. This arrangement is sufficient to protect the test gear ports from short-duration high-voltage transients.

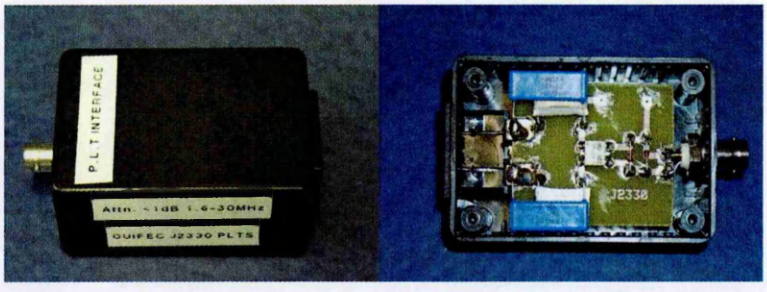

Figure 4.11.2 Image of completed coupler

Calibration of the coupler was completed using a signal generator and receiver and demonstrated that loss of less than 1dB resulted across the 1-30MHz range. No correction has therefore been taken for all DMV measurements utilising the mains coupler.

4.12 Line Impedance Stabilisation Network (L-ISN)

As described in Chapter 2, and given the complexities in undertaking radiated field measurements both CISPR and some nations have decided to implement EMI controls on powerline installations via the employment of an Impedance Stabilisation Network (ISN), providing a known and stable artificial mains network to allow pre-defined LVDN conditions to be presented to the test modem during measurement of the conducted disturbance voltages.

Artificial mains network (AMN), L-ISN, T-ISN or V-network are terms often used to describe such equipment which provide the following RF functionality.

- Provides a defined RF impedance equivalent to (50μH+5Ω ‖50Ω) between the point of measurement and the ground reference plane across the 9kHz to 30MHz range.
- Couples the RF interference, i.e. conducted disturbance from the phase and neutral conductors to the receiver, while isolating the LF mains voltage.
- Attenuates external interference present on the incoming mains supply.

Whilst CISPR/I257 (CISPR, 2008) anticipates that a T-ISN appropriately calibrated to represent the worst case situation within the domestic LDVN comprises an LCL of 16dB, differential impedance of 100Ω and a common mode impedance of 25Ω, the Rohde & Schwarz V-network L- ISN used in the measurements described below demonstrates a TCL of 12.5dB, as shown below in Figure 4.12.1, and has given impedances of 100Ω and 25Ω respectively for the differential and common mode paths.

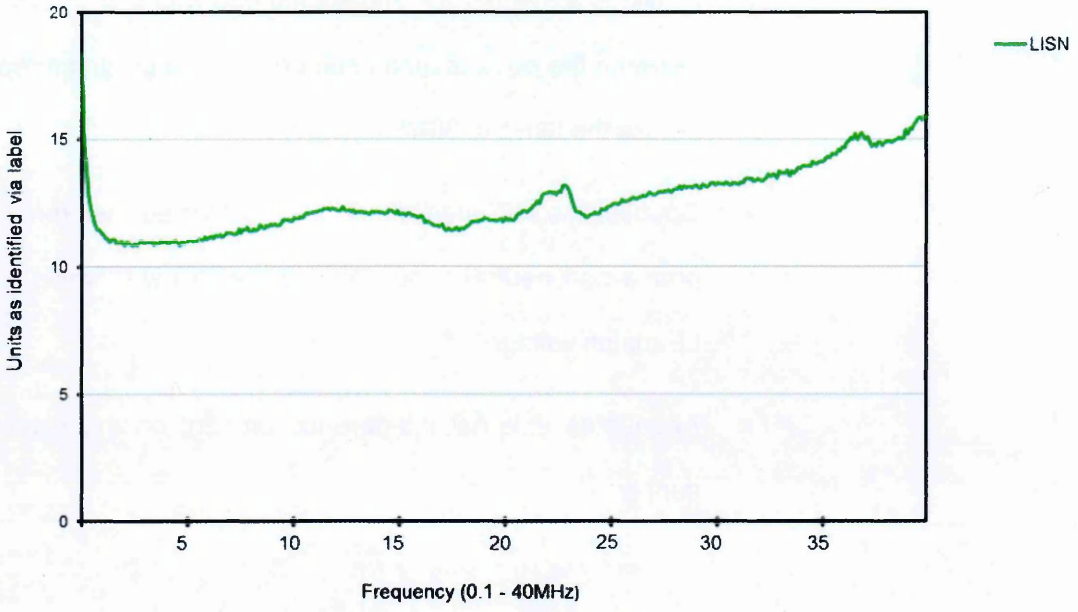

Figure 4.12.1 TCL Measured for the Rohde & Schwarz L-ISN

4.13 Measurements

All measurements below are displayed using the spectrum analyser traces, as shown via the graticule screen capture and given as dBm. Following the application of the above correction factors the equivalent graphs are provided on which several traces may be shown simultaneously and the respective units associated with each trace are included within the legend.

Where reference to 'average value' is given within the text below this refers to the arithmetic mean of the non-logarithmic values, i.e. the base data in units of volts, amps as recorded by the spectrum analyser over the 1-30MHz range. As such this mean value when presented as the logarithmic average value is several dB greater than the range observed on the trace.

4.14Test Cable – Unterminated

To gain an understanding of the transmission line properties for twin and earth cabling measurements are first undertaken on a 3metre length of 2.5mm^2 cable arranged as follows.

The test cable is left unterminated, i.e. as an open circuit and with the conductors aligned within the cable sheath. The cable is located at one metre above ground level on a bench towards the centre of the property Bramble, as detailed below, allowing direct comparison of cable radiated measurements to the LVDN circuitry. In line with the description above the test setup was arranged to provide a -5dBm injected signal to the phase and neutral conductors.

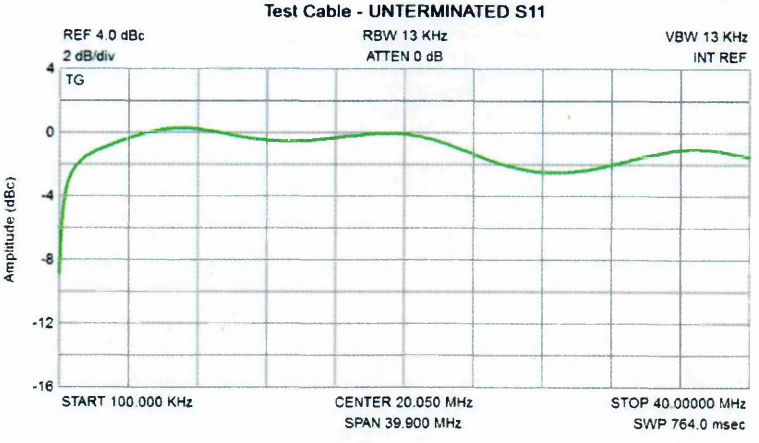

Figure 4.14.1 S_{11} for Unterminated Test Cable

As anticipated the S_{11} measurement, as Figure 4.14.1, shows a significant return loss, tending to 0dB at the lower frequencies. The reflection coefficient Γ and absorbed power (PA) are derived from this return loss, as given in Equation 4.14.1, and the average absorbed power is calculated as -12.7dBm.

$$P_A = P_{IN} + (1 - \Gamma^2) \quad \text{where} \quad \Gamma = 10^{\left(\frac{S11}{20}\right)}$$

Equation 4.14.1

Given the high impedance mis-match of the open circuit impedance relative to the BALUN impedance the differential mode current, as shown in Figure 4.14.2, is not insignificant with a corrected average value across the 1-30MHz range of 67.3dBμA. It is noted from the differential mode current (DMC) trace that a prominent reduction in current at 32MHz occurs and this same profile, albeit at a reduced magnitude, also applies to the common mode current (CMC) trace, shown in Figure 4.14.3 and we note a 9MHz shift in the frequency at which this occurs.

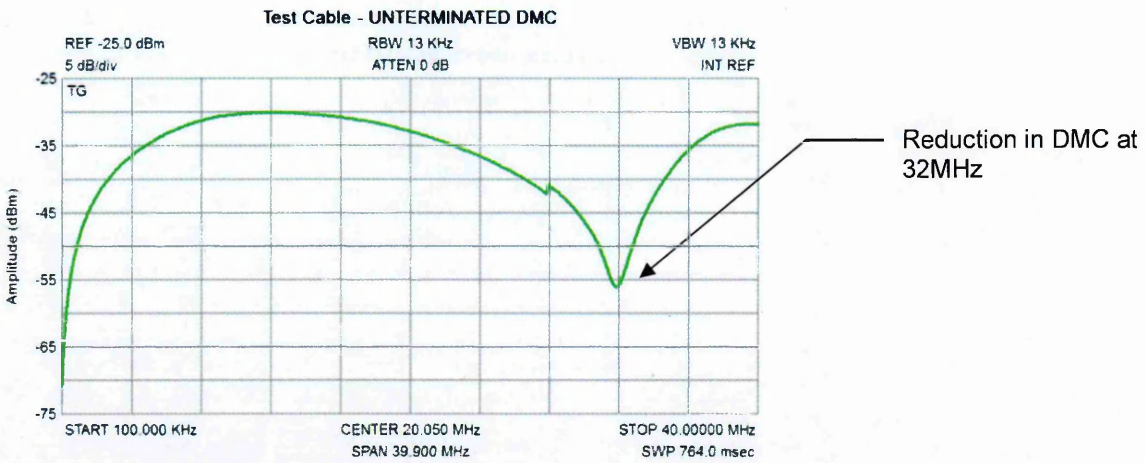

Figure 4.14.2 DMC for Unterminated Test Cable

Application of the velocity of propagation (VoP), as derived in Equation 3.18.3, in conjunction with the cable construction, Figure 3.4.2, indicates that as the earth conductor is constructed from a bare copper conductor without PVC insulation a reduction in the permittivity per meter length results and we can determine that the electrical length for the differential and common mode

paths, at the frequencies identified in Figures 4.14.2 and 4.14.3, is therefore coincidental with the signal wavelength due to the increased VoP to the common mode circuit.

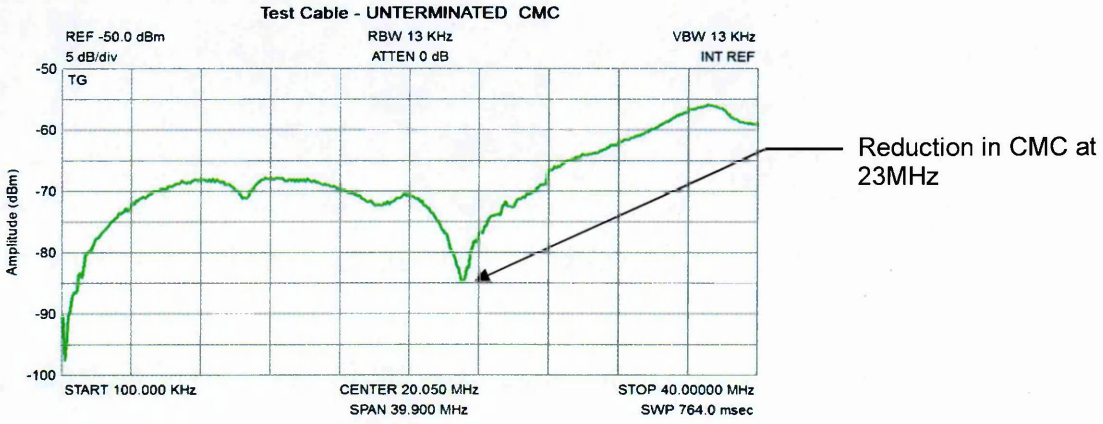

Figure 4.14.3 CMC for Unterminated Test Cable

The calculations in Figure 4.14.4 are based on the assumption that the permittivity of the common mode path is half that of the differential path, i.e. due to the combination of the insulated phase and bare earth conductors. The combined length of the two conductors is therefore acting as a dipole antenna whose length of 6metres physically matches the signal wavelength resulting in a high impedance.

CABLE TYPE		
ε Permitivity	8.85E-12	
εr Rel Permitivity	1.25	polyvinylchloride
Frequency	23	MHz
μ Permeability	1.26E-06	
μr Permeability	0.999	copper conductors
Conductivity	5.80E+07	Seimens/m
Resistivity	1.68E-08	ohms/m
Distance betw'n cond	2	mm
Conductor radius	0.89	mm
Cable Length	3	m
Capacitance C	7.06E-11	Farads/m
Inductance L	1.97E-07	Henrys/m
Char Impedance Zo	52.78	ohms
Skin Depth δ	0.014	mm
Impedance in	1.55	ohms
VoP	0.895111	
VSWR	2.10	:1
λ	11.67	m

CABLE TYPE		
ε Permitivity	8.85E-12	
εr Rel Permitivity	2.5	polyvinylchloride
Frequency	32	MHz
μ Permeability	1.26E-06	
μr Permeability	0.999	copper conductors
Conductivity	5.80E+07	Seimens/m
Resistivity	1.68E-08	ohms/m
Distance betw'n cond	5	mm
Conductor radius	0.89	mm
Cable Length	3	m
Capacitance C	4.11E-11	Farads/m
Inductance L	6.76E-07	Henrys/m
Char Impedance Zo	128.35	ohms
Skin Depth δ	0.012	mm
Impedance in	1.40	ohms
VoP	0.632939	
VSWR	1.16	:1
λ	5.93	m

Figure 4.14.4 Reduction in Electrical Length to Differential Mode Path

Manipulation of the traces above allows generation of the current graph shown in Figure 4.14.5. This clearly indicates that no direct correlation between TCL and CMC is provided, and conversely that the TCL lowest value of 27dB corresponds with the lower values of CMC at 23MHz.

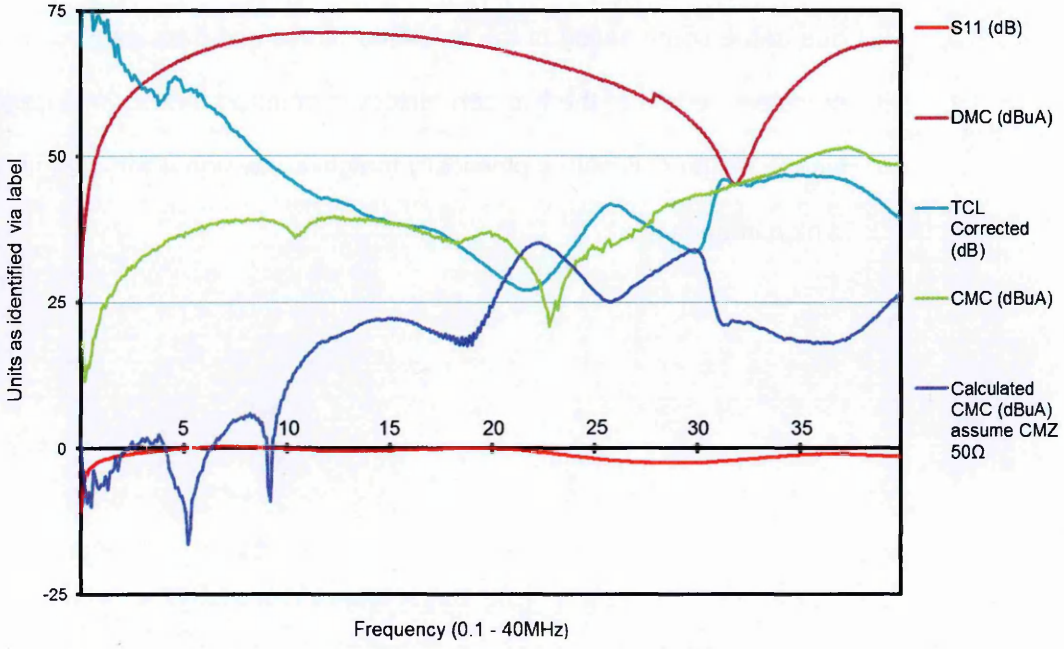

Figure 4.14.5 Current Graph for Unterminated Test Cable

This is further demonstrated by the purple trace, identified as Calculated CMC, which for comparative purposes demonstrates the anticipated CMC that would be generated from the measurement of the return loss and TCL only. This calculation assumes a constant impedance on the differential mode circuit (DMZ) of 100Ω and the common mode impedance (CMZ) of 50Ω.

Calculated CMC is therefore applied via the following correction directly to the absorbed power value, as Equation 4.14.2.

$$CMC = power(dBm) + 110dB - TCL - 34dB$$
$$= power(dBm) + 76dB - TCL$$

Equation 4.14.2

This approximation is used on all following circuit tests to allow direct correlation of the results and, as described later, provides a reflection of the magnitude of currents generated on the L-ISN.

The unterminated cable is seen to radiate liberally, as the trace of the S_{21} in Figure 4.14.6 identifies, with the measurement at 10metres from the cable. Once again no direct correlation can be seen between the radiated field and the current profiles shown above. We note also that the distinct reductions in current at 23 & 32MHz described earlier are not features of the radiated field, however, between 20-40MHz the field strength indicates a 4MHz cyclic profile.

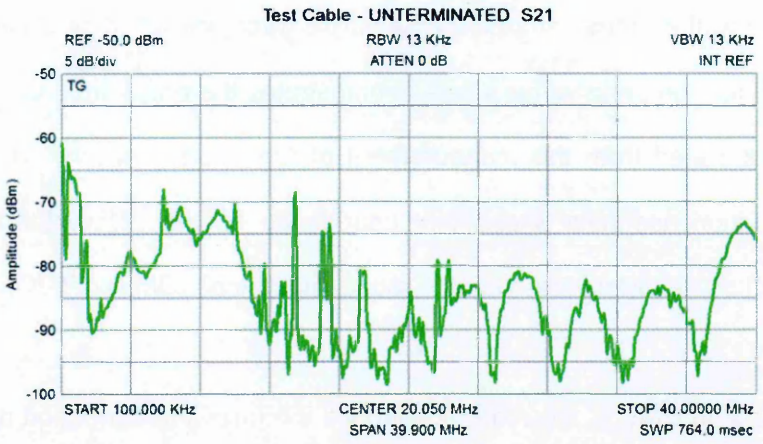

Figure 4.14.6 S_{21} for Unterminated Test Cable

Use of the S_{21} measurement allows production of the radiated graph, as Figure 4.14.7 which identifies both the measured Efield and Calculated Efield. The Calculated Efield is formulated from the CMC measurement and the maximum radiated emission equation, as Equation 3.13.9.

It is clear that no direct correlation can be derived from the Calculated Efield and the measured field strength and beyond 10MHz the calculated values are typically 17dB greater than that measured. This would suggest that below 10MHz the cable radiates according to the theory, given in Equation 3.13.9 as applied to a hertzian dipole and then becomes an increasing less efficient radiator as the frequency increases. It is also to be noted that the Calculated Efield represents the maximum field produced within the free space conditions of the far field and that no attenuation for the cable or the building structure, through which the signal propagates, has been included.

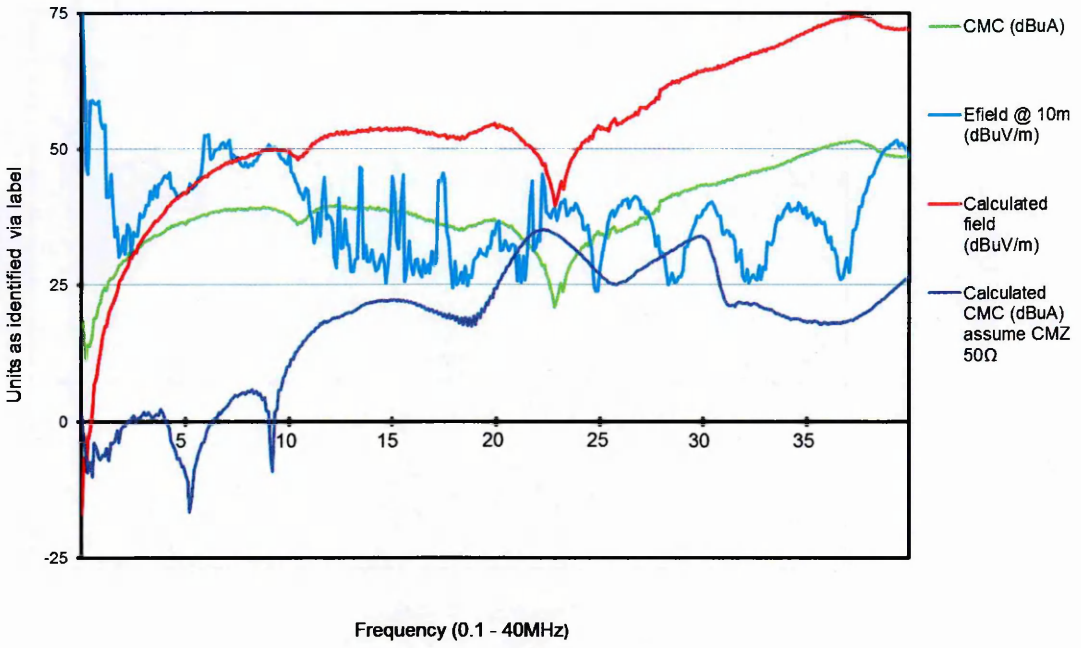

Figure 4.14.7 Radiated Graph for Unterminated Test Cable

Finally we can utilise the combined data from the above graphs to indicate an overall transfer function for the test cable as provided in Figure 4.14.8. This allows construction of performance factors for the cable and the average value of both the k factor and gain (dBi) are calculated as 63.6dBμv/m-dBm and -31.6dBi respectively.

This indicates that the unterminated cable, whilst having a significant return loss, is an effective radiator of EMI. It is also noticeable that a large variation in k factor across the frequencies is produced, i.e. from 45-100dBμv/m-dBm. As k factor is a unique parameter a comparative value is required to make use of this value and the following tests have confirmed that a k factor of 50+ indicates reasonable transfer of power to radiated field whilst 70+ indicates a good transfer and 90+ resembles matched antenna performance.

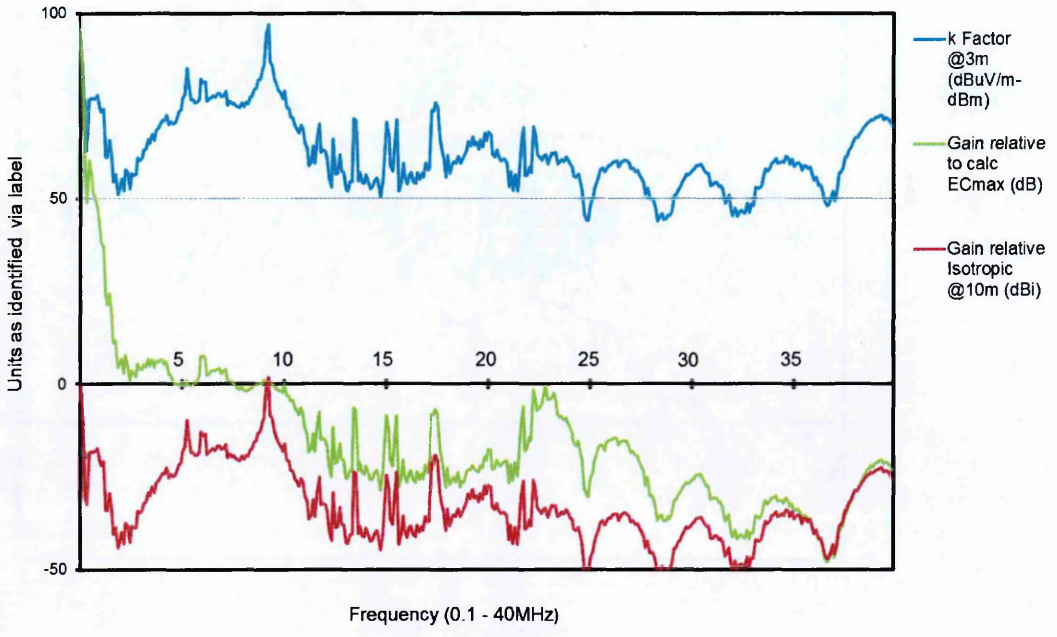

Figure 4.14.8 Transfer Factor Graph for Unterminated Test Cable

4.15Test Cable – Terminated 100Ω

The test cable is now terminated with a 100Ω load across phase and neutral and a 50Ω load between phase and earth. In contrast to the unterminated cable the return loss as Figure 4.15.1 shows minimal reflection and the calculated power absorbed by the cable has now increased to -5.15dBm.

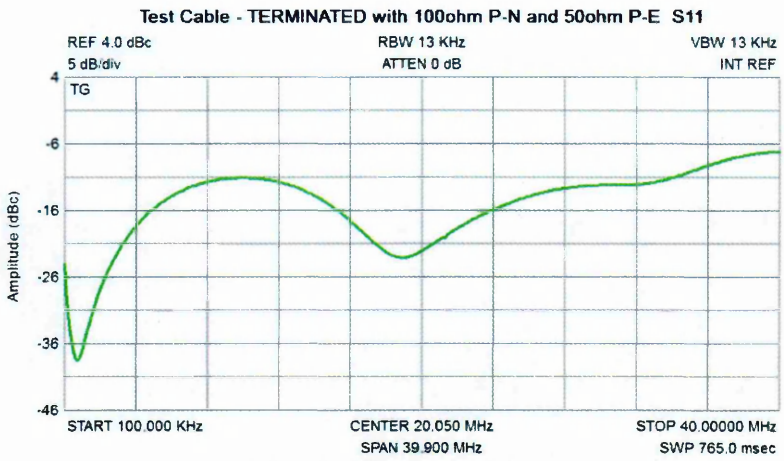

Figure 4.15.1 S_{11} on Terminated Test Cable

Measurement of the DMC, as Figure 4.13.8, now provides an almost constant current profile across the spectrum up to 40MHz, with a corrected average differential current of 65.3dBµA. The generated CMC, as in Figure 4.15.2 has a magnitude approximately 25-45dB less than the measured DMC with a corrected average value of 31dBµA.

As the test cable is isolated from all further circuitry we are assured that none of the CMC measured has been created elsewhere, nor is the result of coupling from other sources. The CMC therefore indicated in Figure 4.15.2 is the product of the differential current and transverse conversion loss (TCL) only, resulting from the cable's construction and RF performance.

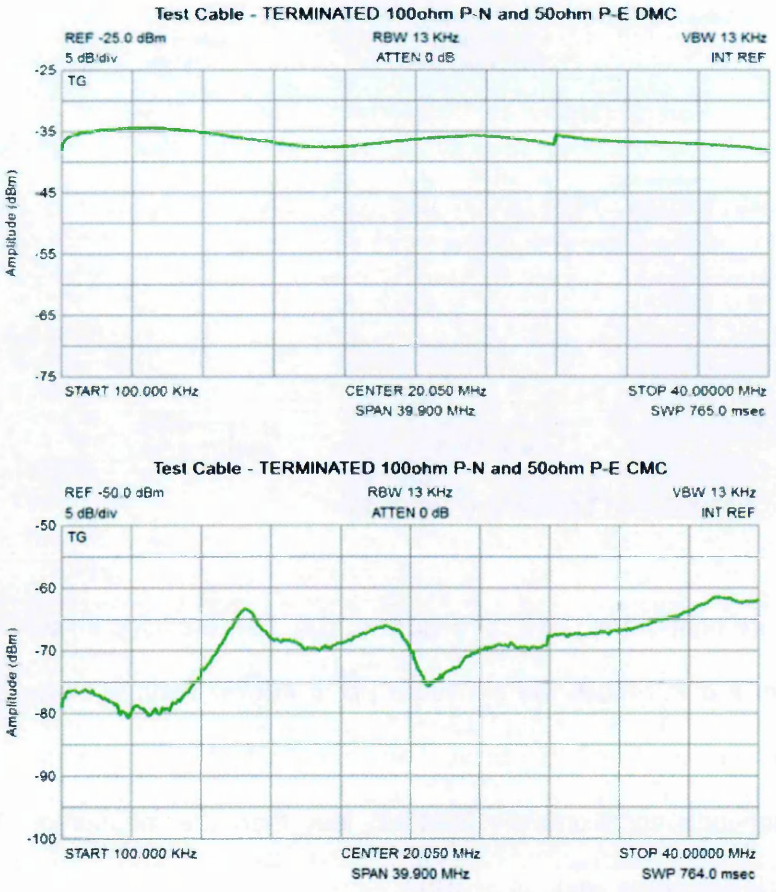

Figure 4.15.2 DMC(Left) and CMC(Right) on Terminated Test Cable

We can therefore calculate the voltage and impedance of the differential mode circuit through utilisation of the power absorbed figure and the measurement of the current. The differential voltage and differential impedance profiles (DMV) and (DMZ) are calculated and it is noted that as the test setup was unable to record phase angle these impedances are not complex and all voltages and currents are assumed in phase.

It is shown in Figure 4.15.3 that the measured TCL as recorded with a symmetrical load of 100Ω, i.e. with a termination impedance as recommended by ITU (2011), indicates values in excess of 60dB to the lower frequencies and gradually falls to provide a near constant value of 50dB from 10MHz to

40MHz. Under this situation we note that the TCL now approximates the reciprocal variation in CMC which conversely increases with a similar magnitude.

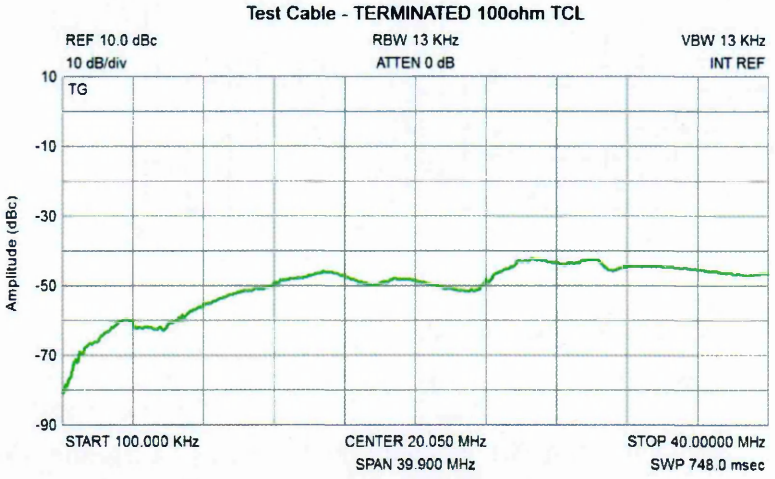

Figure 4.15.3 TCL for Terminated Test Cable

The TCL reading indicates that the HF performance of a generally considered lossy 'non-communications' based cable is surprisingly good, given that such performance is a fortuitous by-product of a construction method providing conductor insulation rated to 600V peak although intended to carry signals with a frequency of 50Hz only.

The corrected average TCL is calculated as 50.9dB and reference to Rohde and Schwarz cable testing (Rohde & Schwarz, 2008) as Figure 4.15.4 shows that the LCL performance of a Category 3 communications cable, as employed in standard local area networks (LAN) is comparable to the values recorded on the twin and earth test cable.

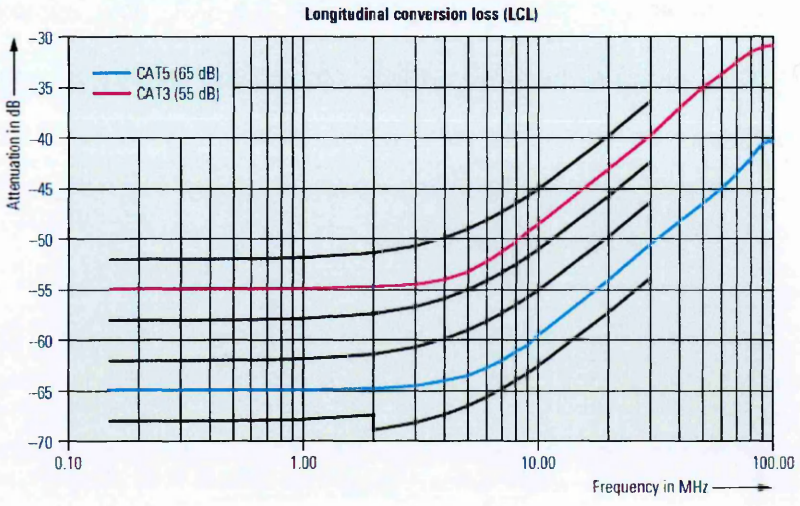

Figure 4.15.4 LCL for Cat 3 Cabling

Further utilisation of the TCL measurement when applied to the DMV provides the common mode voltage (CMV) which, when applied with the common mode current measurement allows calculation of values for both the common mode impedance (CMZ) and common mode power (CMP).

The differential and common mode impedances are indicated in the graphs below as Figure 4.15.5 and shown as dBΩ in order to allow their inclusion with other traces on a common scale. Equation 4.15.1 indicates the manner in which impedances are given as dBΩ.

$$dB\Omega = 20 * \log(impedance\ \Omega)$$

Equation 4.15.1

The differential impedance is calculated at a nominal 40dBΩ across the frequency range, equating to 100Ω with a ±30Ω variation. In contrast the common mode impedance is seen to vary considerably over the frequency

range with a far greater variation, i.e. from 4-85Ω and a less defined nominal average of approximately 35Ω or 30dBΩ. Whilst this verifies the characteristic impedance of the differential mode circuit it also demonstrates the more complex nature of the common mode impedance.

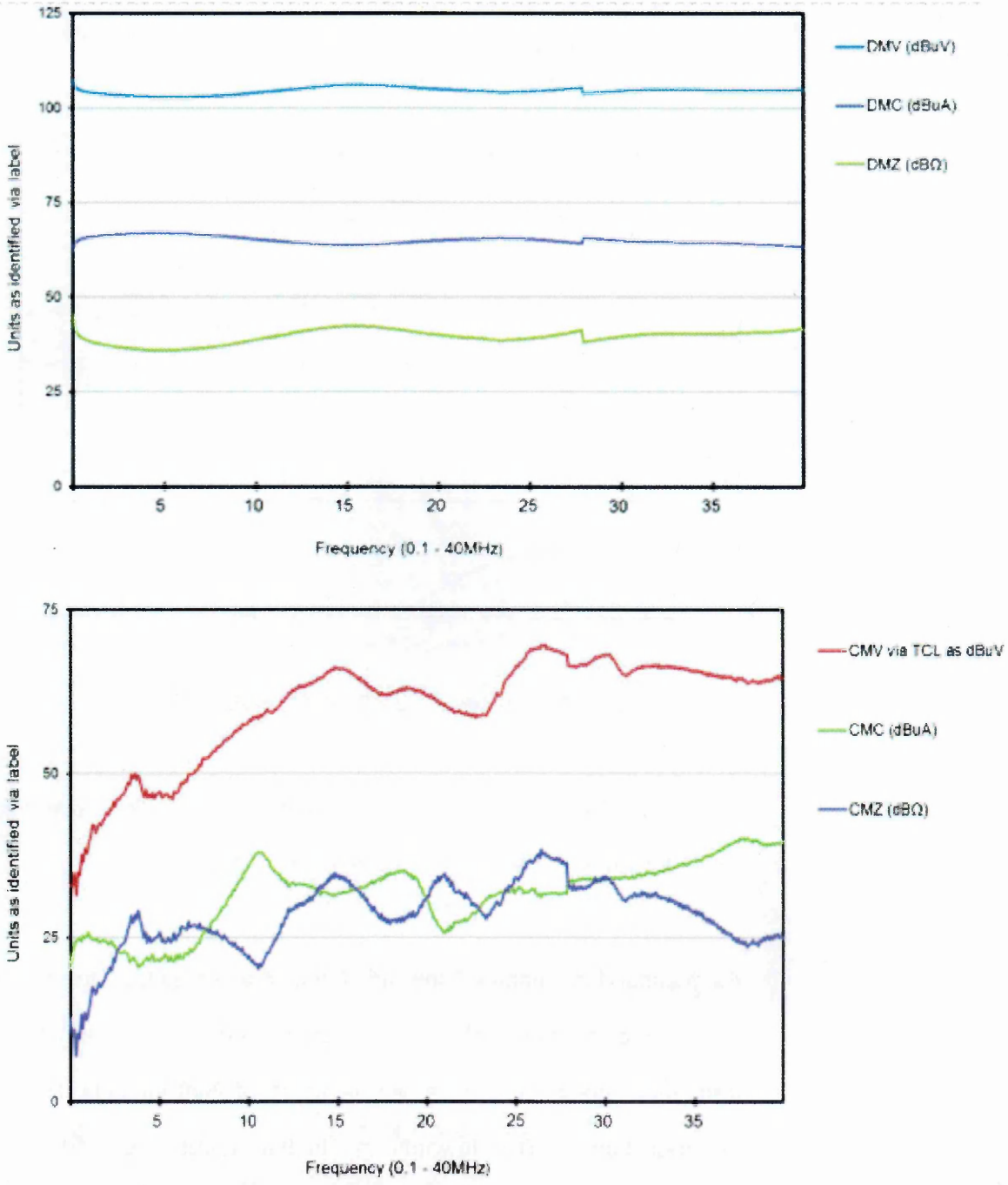

Figure 4.15.5 Impedance Graphs for Terminated Test Cable

The Current Graph, as Figure 4.15.6, now demonstrates the direct inverse relationship between TCL and CMC when a stable differential impedance exists. The Calculated CMC indicates that despite the steady differential impedance the calculation of common mode current remains some 10dB in error and suggests that even under perfectly defined conditions the calculation of CMC is not viable.

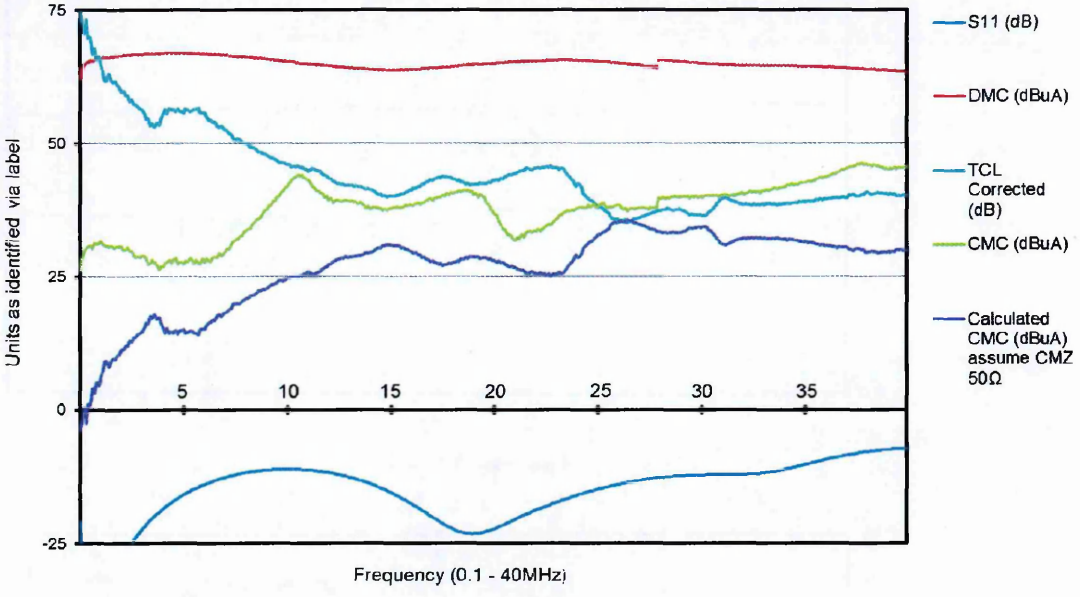

Figure 4.15.6 Current Graph for Terminated Test Cable

Correction of the S_{21} measurement, as Figure 4.15.7 allows direct comparison of the traces on the Radiated Graph, Figure 4.15.8.

As described in Chapter 3 the radiated field resulting from the common mode current is directly proportional to frequency and as such a tenfold increase in frequency should result in a field increase of 20dB/decade. However, given the reduction of TCL towards the higher frequencies and the reciprocal

increase in CMC we note that the Calculated Efield has a 30dB/decade increase.

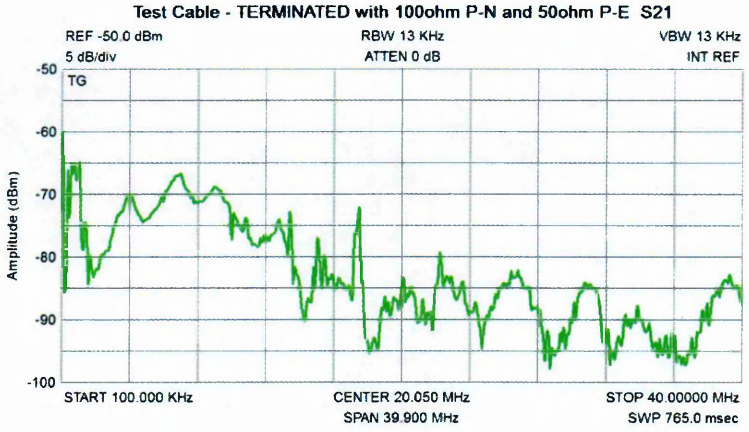

Figure 4.15.7 S_{21} for Terminated Test Cable

In contrast to the Calculated Efield we note a distinct decrease in the measured Efield with frequency and with correlation between the measured and calculated values at 10-13MHz only. This suggests that the radiated field is not a direct result of the circulation of common mode current within the test cable.

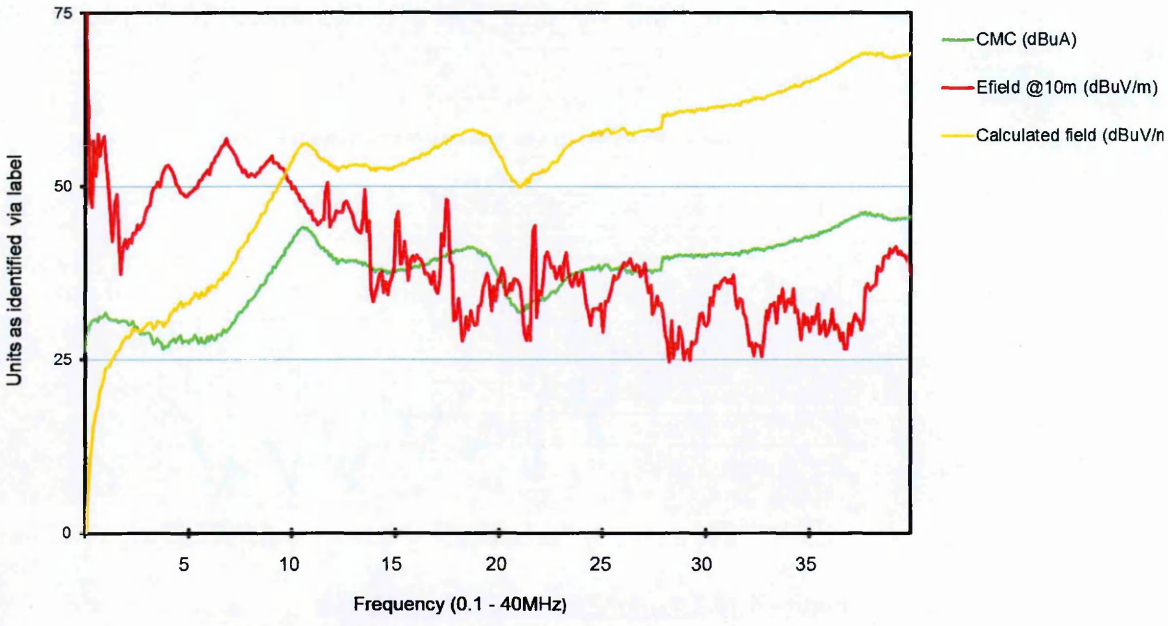

Figure 4.15.8 Radiated Graph for Terminated Test Cable

The transfer graph as Figure 4.15.9 and Table 4.15.1 below indicate that the power absorbed by the terminated cable with respect to the un-terminated case has increased by 7.6dBm. This increase in power does relate to a small increase in radiated field, i.e. 1.9dBμV/m but both k factor and gain (dBi) have decreased with respect to the un-terminated case.

This confirms that use of these parameters to compare the RF performance of different cables and circuits can lead to confusion and that neither k factor nor gain (dBi) inform directly on the ability of a circuit to radiate energy.

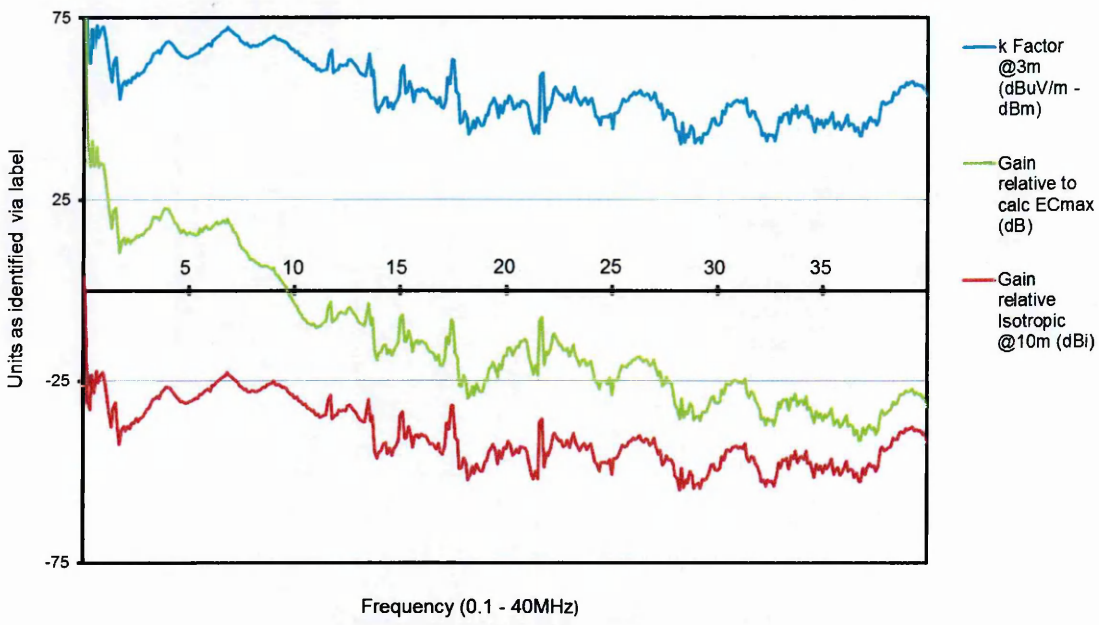

Figure 4.15.9 Transfer Factor Graph for Terminated Test Cable

Table 4.15.1 records the average values computed for all parameters and forms the basis for general performance analysis. Comparison of the energy flow through the test cable under each condition reveals that whilst the absorbed power increases by 7.6dB, on the application of the load, the power increase to the common mode circuit is 3.7dB and the resulting Efield measurement increases by 1.9dB.

	UNTERMINATED	TERMINATED CABLE
S11	-0.8	-14.7
Power Absorbed PA (dBm)	-12.7	-5.1
DMC (dBuA)	67.3	65.3
DMV (dBuV)	102.3	104.5
DMZ Mismatch (Ω)	2951.4	141.7
DMZ (dBΩ)	69.4	39.4
TCL (dB)	55.3	50.9
CMC (dBuA)	30.5	31.0
CMV (dBuV)	53.9	61.4
CMZ(dBΩ)	27.4	30.0
Common Mode Power (dBm)	-46.8	-43.1
Calculated CMC (dBuA)	23.7	27.5
S21 EFIELD @ 10m (dBuV/m)	44.1	46.0
k Factor (dBuV/m-dBm)	63.6	57.4
Gain(dBi)	-31.6	-37.9
Calculated EFIELD via CMC (dBuV/m)	46.1	47.1
Gain relative to calculated field (dB)	-3.6	-0.5

Table 4.15.1 Average Values for Test Cable

Having gained appreciation of the measurements derived from the test cable the following measurements represent those undertaken on a standard property of the UK building stock, namely a three bedroom bungalow of circa 1980 brick and tiled roof construction. All measurements relating to this property are identified below as Bramble.

4.16Bramble – LVDN Measurements

The test setup, as arranged for the test cable, is now used to measure the same parameters on a low voltage distribution network, comprising several ring circuits & radials, in which the incoming supply is via an underground cable and utilises PME earthing. All cabling is PVC twin and earth based and generally installed at high level throughout the roof space with drops to low level sockets via the cavity walls, to serve the outlets as shown in Figure 4.16.1. The inclusion of luminaires and other electrical loads, such as domestic appliances, were left connected, although generally switched off,

during the tests and as such the LVDN represents the situation during normal PLT operation.

It is immediately noticeable that the return loss in Figure 4.16.2, when measured at the mains 'consumer unit', across all the circuits comprising the LVDN is significantly more constant than that observed previously on the test cable.

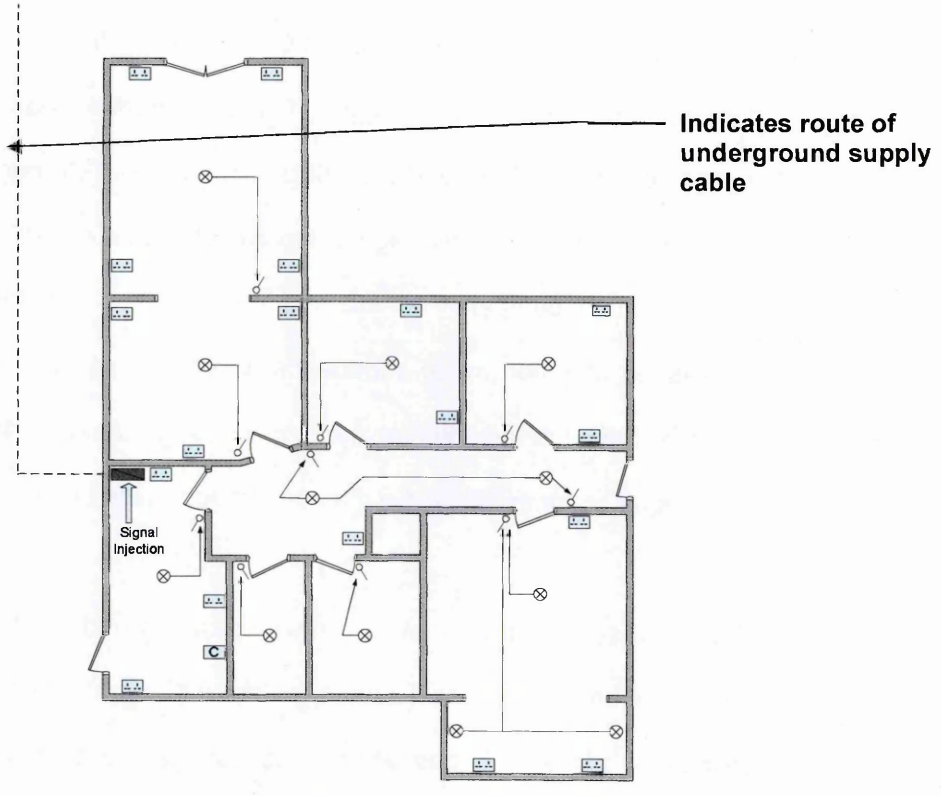

Figure 4.16.1 Bramble Layout and Outlet Positions

The impedance mis-match, referenced to the BALUN, creates a significant reflection coefficient at all frequencies and the average absorbed power is calculated as -11.2dBm.

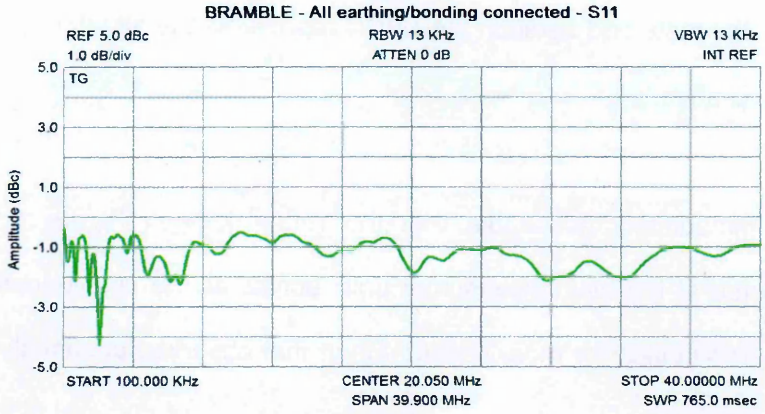

Figure 4.16.2 S_{11} for Bramble

The TCL measurement maintains much of the profile of the test cable and demonstrates, as shown in Figure 4.16.3, a gradual reduction towards the higher frequencies from 60dB to 30dB. The overall TCL performance is seen to remain high with an average value calculated at 44.3dB. This indicates a 6dB reduction compared to the test cable which is reflected by the 6dB increase in common mode impedance as suggested by Equation 3.9.2. This indicates that the addition of the considerably larger earthing system with extraneous bonding has had a marked impact on the comparative impedance.

In comparison we note that LCL measurements undertaken by ETSI (2003) and the Communications Research Centre Canada (2009) within domestic properties agree with this value. They suggest a 60% probability of LCL exceeding 46dB within Europe with an average value of LCL in North America found as 35-40dB.

It is noted that at 31.5MHz a 40dB improvement in TCL is observed in the measurements and this typifies features found by other researchers, who suggest (Vukicevic , 2006) that such prominent variations in TCL are the result

of changes in the boundary conditions creating standing waves created in the circuit. This is considered further, below, where such conditions are altered by varying the measurement location.

When corrected the lowest value of TCL recorded across the LVDN is 25dB and we shall observe this minimum value, i.e. the worst case, as we proceed to measure the individual circuit types.

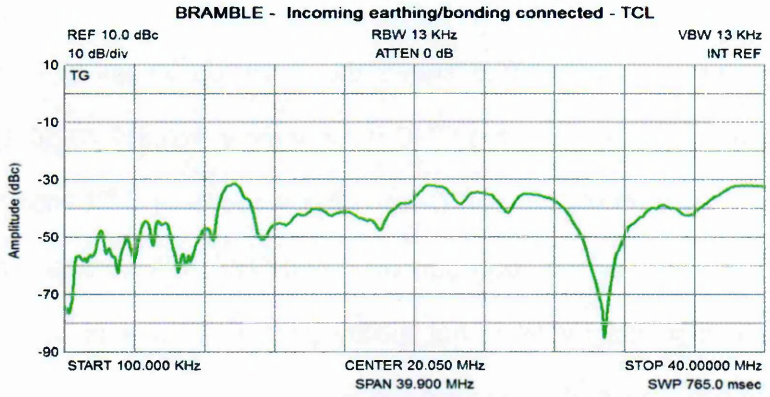

Figure 4.16.3 TCL for Bramble

As noted on the return loss we also see the radiated field, given as S_{21} in Figure 4.16.4, displays a 'flat' emission compared to the test cable, which on removal of the intentional broadcast signals, shows a variation in measured field strength in the order of 15dB.

This suggests (Williams, 2000) that connection to the wider earthing network, or CBN, which provides multiple alternative current paths for the energy dissipation results in a high degree of equipotentiality over a wide frequency range.

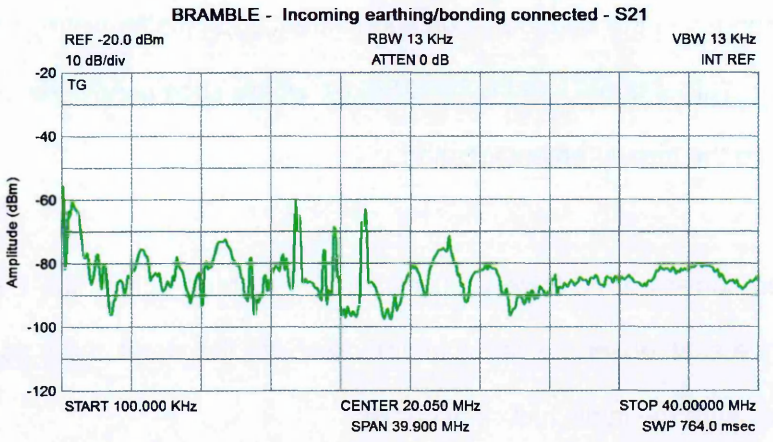

Figure 4.16.4 S_{21} for Bramble

The graph in Figure 4.16.5 shows the corrected values of both DMC and CMC, and identifies that the CMC value is now typically 40-50dB lower than the differential mode current. Despite the reduction in TCL, compared to the test cable, the variation between DMC and CMC has increased and we note that although the LVDN is not electrically live it remains connected to the service cable beyond the service meter.

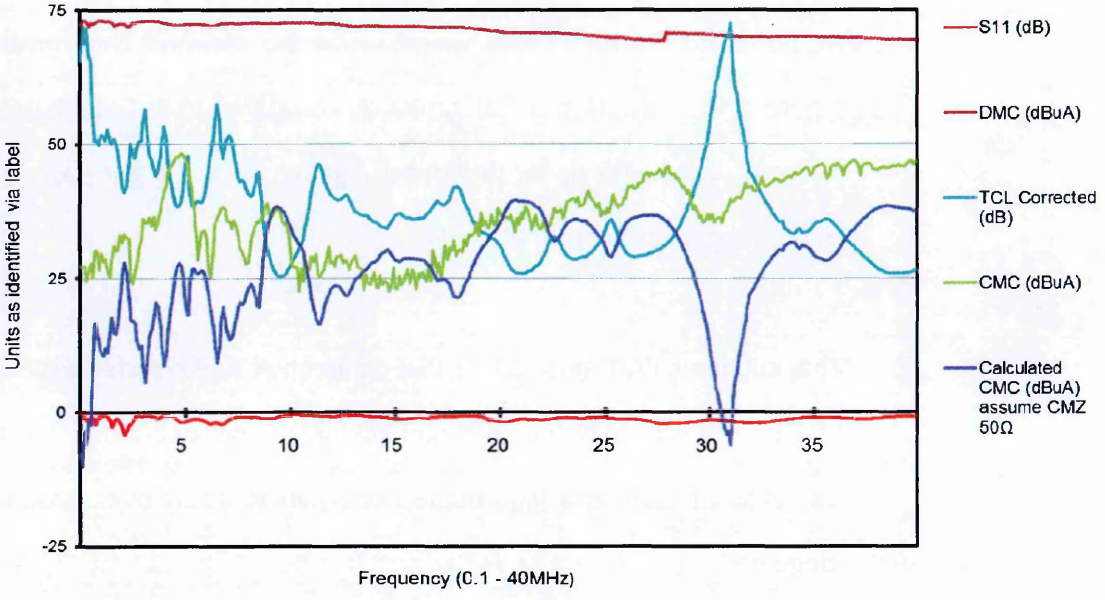

Figure 4.16.5 Current Graph for Bramble

In order to observe the level of CMC on the external PME connection the insertion of the HF probe to the external side of the service head and electrical meter was completed as Figure 4.16.6, with an average value of 24dBμA being recorded.

Whilst this current level appears high the ITU (2011) found that the differential mode current measured on the service outside the property is 0-30dB less than that measured on the LVDN, whilst the common mode current is found to be 10-30dB larger than that on LVDN.

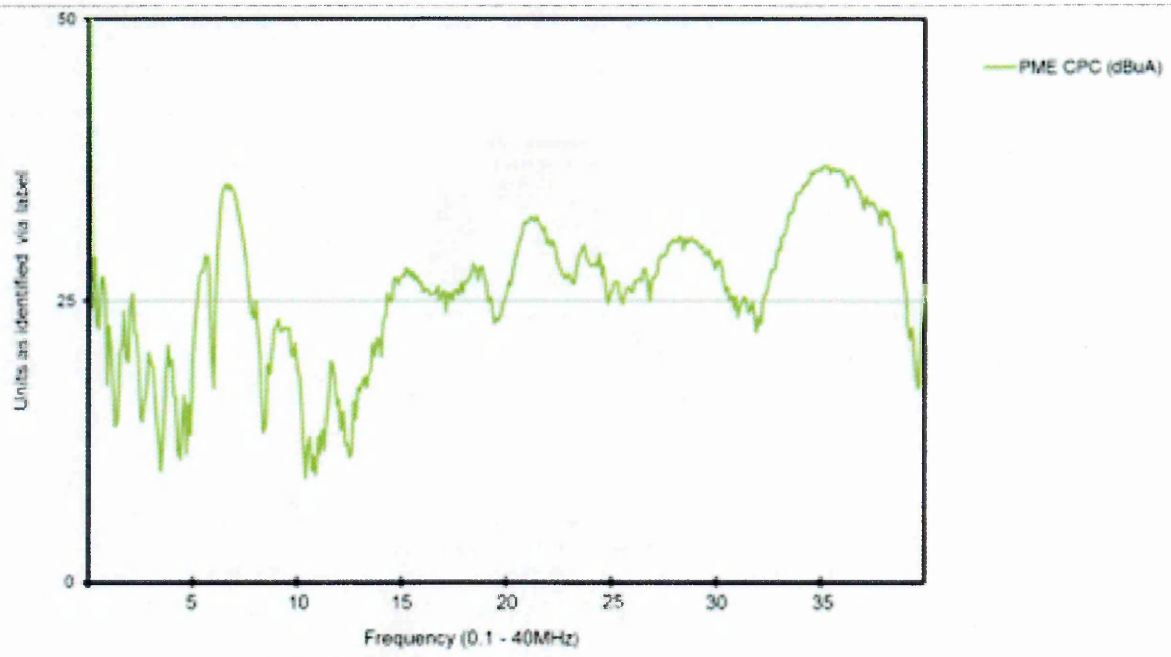

Figure 4.16.6 Current Graph for Bramble

Whilst the magnitude of CMC measured above does not reflect that found by the ITU, as cited previously, but does highlight the fact that under a PME connection the neutral is directly connected to the earth conductor and so ultimately all common mode current circulates via the combined conductive

and extraneous earthed network to the external supply conductors, as indicated in Figure 5.5.3.

In order to determine whether this would impact the radiated field we record the S_{21} whilst both the principal PME conductors are connected and disconnected, as illustrated in Figure 4.16.7, below. It is seen that no appreciable overall increase in field strength is recorded whilst the PME connection is removed, although the complete isolation of the LVDN from earth via this disconnection was not assured. Luo (2005) also modelled the effect of radiation from supply cables and found that when the cables were routed within the ground there was no effect to the radiated fields.

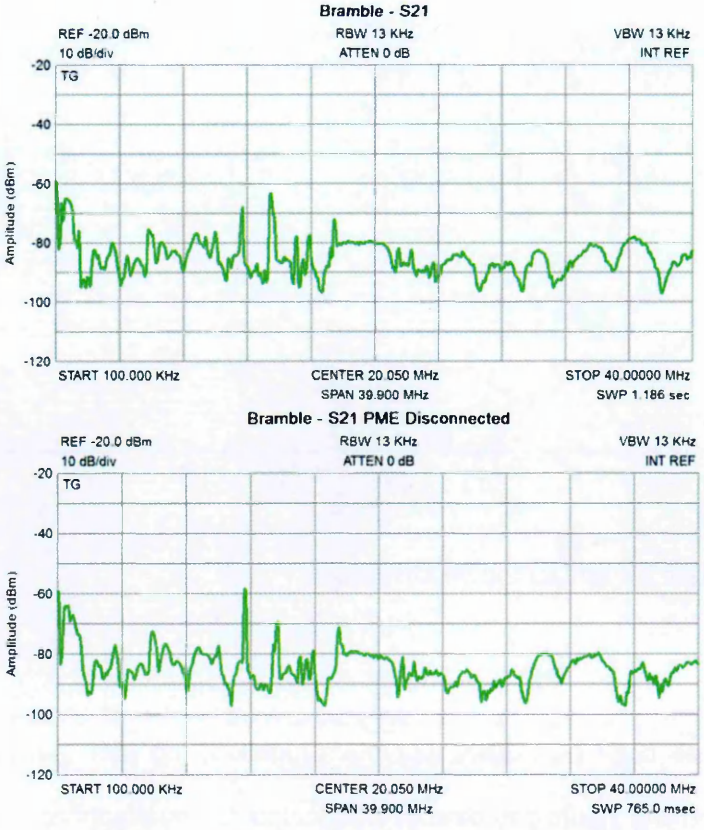

Figure 4.16.7 S_{21} for Bramble with PME Disconnected

This suggests that whilst TCL has reduced a corresponding rise in CMC is not observed, due to signal propagation beyond the LVDN and demonstrates that on larger more complex circuitry the accurate measurement of common mode current to allow calculation of radiated field strength is not simple.

Figure 4.16.8 below shows the differential and common mode impedances and we note that both remain typically in the tens of ohms across the frequency range. The common mode impedance is calculated to have a higher average value than that of the differential circuit (DMZ), which is in direct contrast to the test cable and demonstrates that the parallel arrangement of the multiple circuits of the LVDN offer lower impedance than the overall CBN.

The radiated Efield has increased, compared to the test cable, by an average of 6dB, despite the reduction in absorbed power and common mode current.

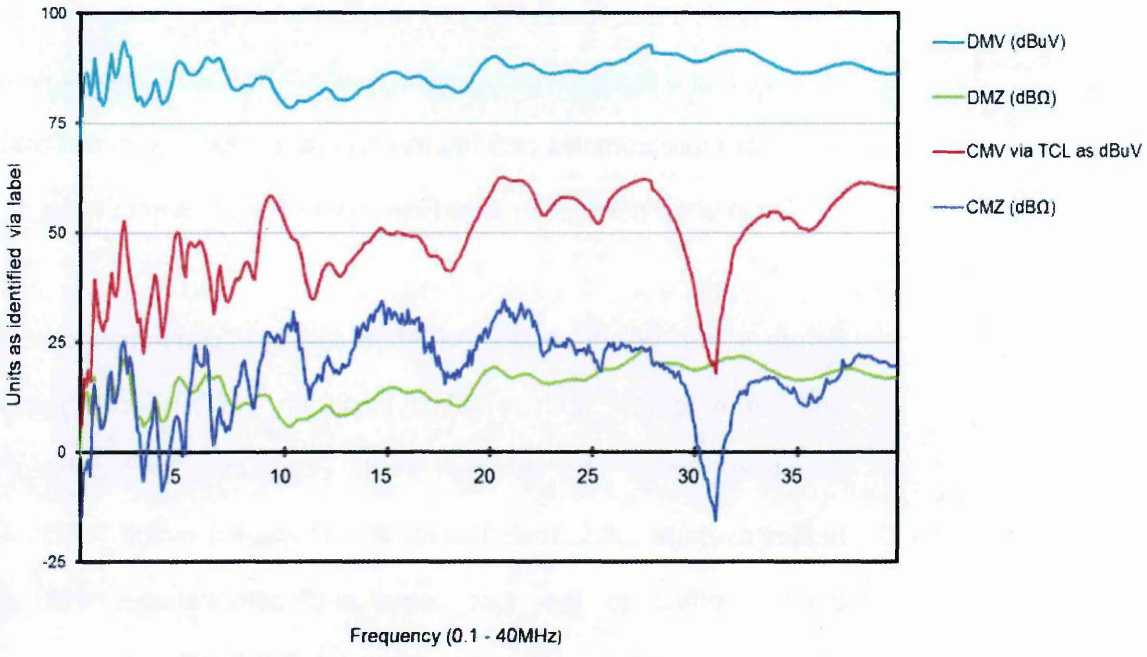

Figure 4.16.8 Impedance Graph for Bramble

However, given the relevant increase in circuit size as indicated by the Calculated Efield, which is based on the considerably longer circuit length of Bramble taken as 75 metres, we note that correlation now exists between the measured and calculated values of Efield for the lower frequencies only. Beyond this the disparity between calculated and measured values increases to a maximum of 56dB.

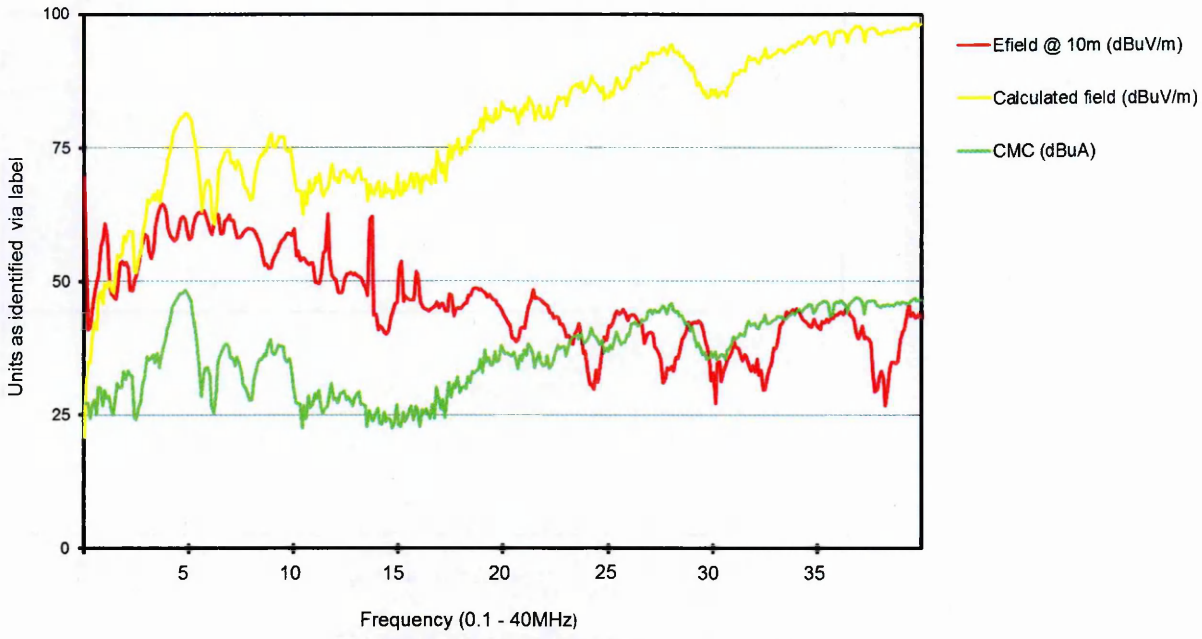

Figure 4.16.9 Radiated Graph for Bramble

Therefore notwithstanding the previous commentary regards under-estimation of the CMC we note that the increased cable length and the variation in boundary conditions as a result allow accurate calculation of the radiated field below 5MHz.

The Transfer Graph of Figure 4.16.10 indicates the increase of k factor to provide an average value exceeding 70.4dBμV/m-dBm. This would suggest that Bramble is a far more effective radiator of energy, thus producing more EMI when compared to the test cable in either of the test conditions, i.e. when provided with a matched load or unterminated.

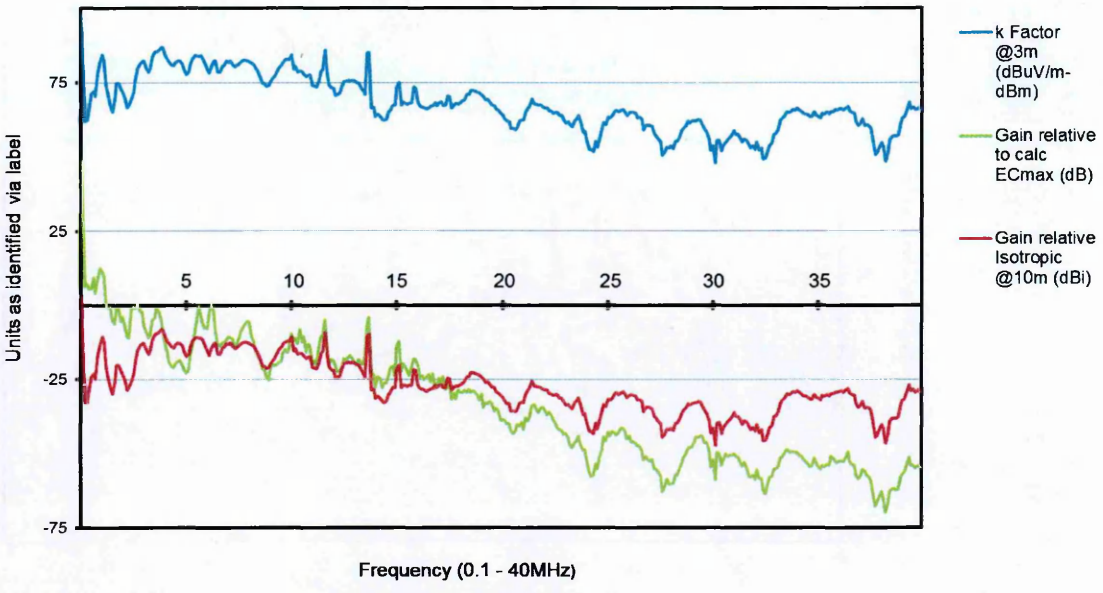

Figure 4.16.10 Transfer Graph for Bramble

The overall performance of Bramble is also given as gain relative to an isotropic antenna and this is a key measurement to be noted. In Chapter 2 it was stated that despite little formal documentation the PLT regulatory bodies had generally adopted -30dBi to represent the typical domestic property. However from Figure 4.16.10 we see that at the lower frequencies, i.e. up to 15MHz the gain is recorded is as high as -10dBi before falling to -40dBi at 23-30MHz.The average value calculated over the 1-30MHz range is -24.8dBi at 10 metres from the source.

Whilst this initial result validates the magnitude of the previously quoted figure we must also consider that in addition to the previous observations that this figure is derived from the injection, at the mains position, of a sinusoidal waveform.

Further tests below, as live tests, will confirm whether introduction of the HF source within the LVDN and the use of orthogonal frequency division multiplexing (OFDM), as employed by powerline modems will affect the LVDN RF performance.

4.17Summary of Initial Measurements

The observed change in RF performance from the test cable to the LVDN is as a result of the change in physical and electrical properties and the above measurements have shown that we can determine each of the electrical parameters to measure the power transfer through the circuit and this is shown as the Power Diagram in Figure 4.17.1.

The power absorbed within the differential mode circuit is calculated via the return loss, whilst the power delivered to the common mode circuit is derived as the product of the common mode voltage and current. Finally the power radiated, i.e. the power density (S) of the radiated signal can be calculated from the Efield measurement, which is assumed as being in the far field.

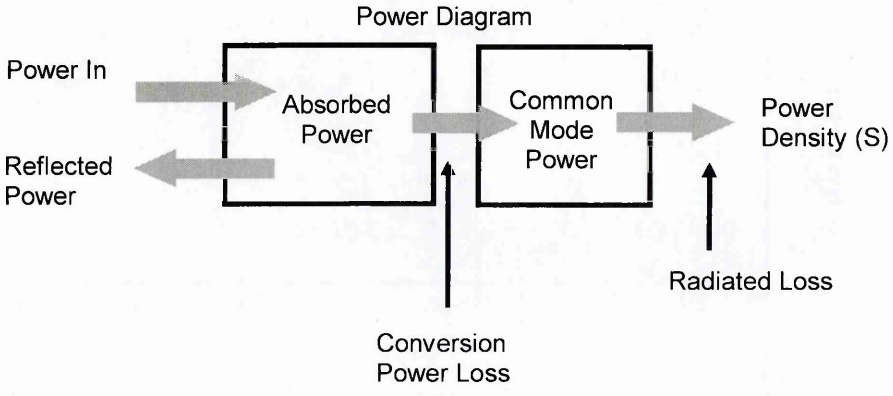

Figure 4.17.1 Power Diagram

The mechanism of power transfer shown above indicates that there are two factors of interest, namely the Conversion Loss given by the Absorbed Power (dBm) less Common Mode Power (dBm) and the Radiated Loss which is found as the Common Mode Power (dBm) less the signal Power Density (dBm/m^2). With reference to the transfer factors for the subsequent individual circuit tests we shall develop a model to determine the radiated power as predicted from knowledge of the electrical and physical properties of the circuitry alone.

Figure 4.17.2 below shows the transfer factors for Bramble and we note that the conversion loss has a calculated average value of 46dB and the radiated loss a calculated average value of 30.3dB. Observations to be noted are that below 13.5MHz we appear to see negative gain on the radiated loss, implying that the power density of the calculated radiated signal is greater than the measured common mode power.

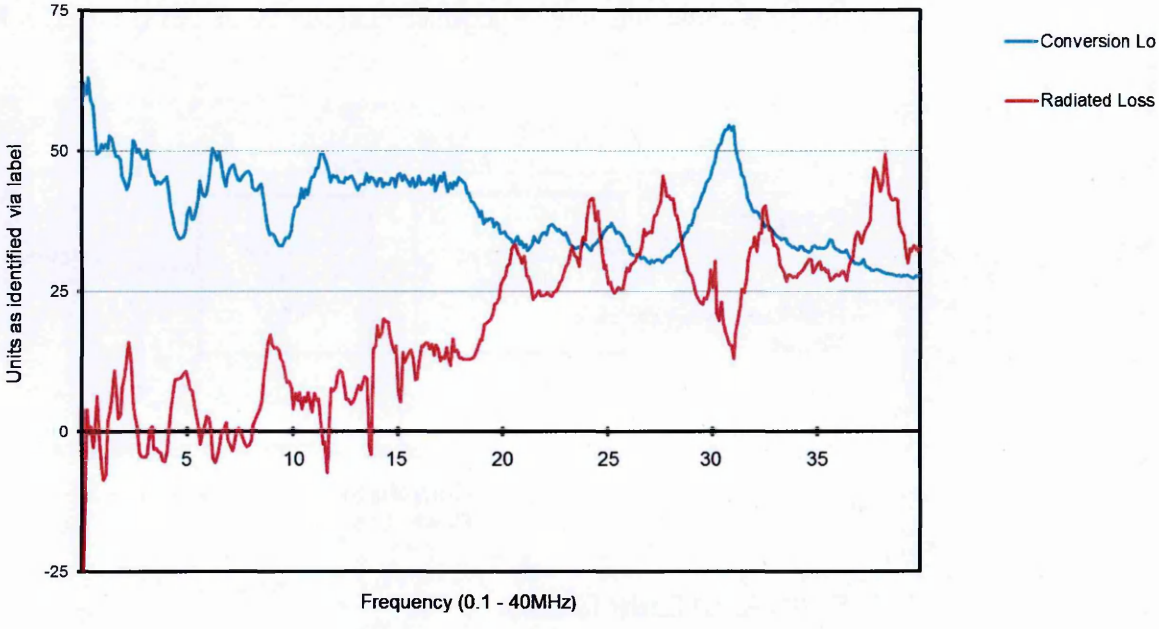

Figure 4.17.2 Factor Graph for Bramble

As the calculation for power density takes the dimension of Bramble (*D)* as the façade facing towards the antenna, shown in Figure 4.17.3, which equates to 10 metres the Raleigh distance (d_{NF}) for a frequency of 13.5MHz is therefore shown via the Fraunhofer equation as;

$$d_{NF} = \frac{2(D^2)}{\lambda} = \frac{2(10^2)}{22.2} = 9m$$

Equation 4.17.1

This indicates that for structures of this physical dimension the antenna located at 10m is in the far field for all measurements up to 13MHz and that the application of the impedance of free space to the power density calculation at frequencies beyond this will introduce an error.

This may explain the significant variation in radiated loss across the 1-40MHz with the radiated loss at 20MHz increasing to some 25dB. As both the radiated field measurement extends into the near field, for signals over 13MHz, and the circuit radiation pattern is seen to depart from that of a dipole for the higher frequencies the radiated loss falls.

Reference to Section 3.18 above allows us to re-consider the accuracy of the radiated field measurements

Reducing the size of the radiating structure will overcome this and provide far field conditions beyond 30MHz. This was a factor of the next series of tests, which examined the behaviour of the LVDN in more detail by considering individual circuit tests.

Figure 4.17.3 Image of Wellbrook Antenna at 10m range

4.18Bramble – Individual Circuits

In order to relate the above measurements of a complete LVDN the same measurements were performed sequentially on the separate circuits.

Each of the following circuits was individually isolated and tested in the manner as described above. Generally the neutral and earth conductors were disconnected from the common bars to ensure that the radiated field measured was applicable to the injected power and circulating currents within the individual circuit only.

In order to encompass the features described in Chapter 3 the following circuits were selected;

- A short, 20 metre long, lighting radial comprising downlights to the kitchen and two fittings to the hall. All luminaires fitted with energy saving lamps and in total the circuit contained four light switch

locations. This circuit therefore comprises several branches with switch-wires varying between 1.5 and 4 metres in length.

- A simple cooker radial circuit with a 10m cable run without any branches. However, this circuit is connected via cable of the same construction but with conductors of $10mm^2$. The circuit is terminated into a single switch, whereby both poles are broken when off. Turned on the cooker unit forms part of a more complex load given the multiple connections within the appliance for ovens and fans.

- A standard UK ring main circuit, of around 30 metres total length serving four socket outlets. All appliances were removed or switched off during the measurements.

4.19Lighting Radial –All luminaires off

With all lights switched off we note a return loss of average value -3.6dB, as shown in Figure 4.19.1 below. A reasonable impedance match is achieved at all frequencies, with exception of 25MHz where the reflection coefficient is less than 5%.

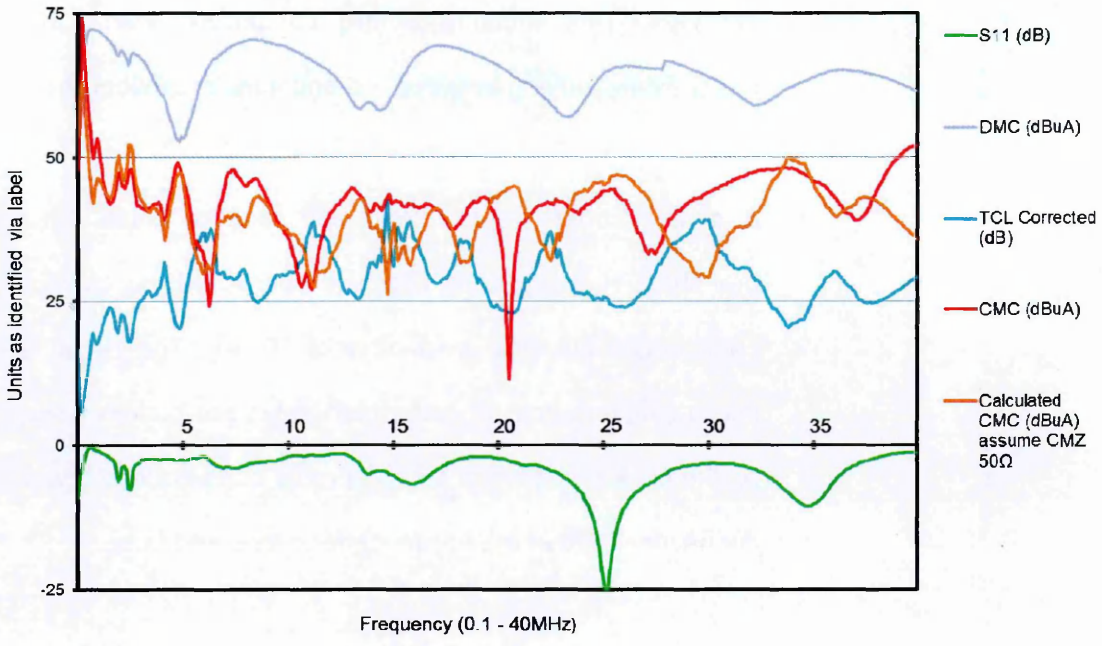

Figure 4.19.1 Current Graph for Lighting Circuit – OFF

As described earlier the lighting circuit is relatively short at 20 metres in length and as it consists of four light switches we can conclude that nearly half the circuit cabling is made up via the switchwires. With the lights turned off, i.e. switches open there are eight individual lengths of switchwire varying between 1.5 and 5 metres in length and the opportunity for resonant branches to occur is therefore significant. In addition, testing undertaken (Chandna, 2010) on complex circuits with multiple branches found that powerline signal to be highly attenuated at 500 metres with significant bit error rate due to the numerous reflections and standing waves.

We also note a significant reduction in the TCL, compared to the previous measurements, i.e. 14dB less than Bramble as a whole and 20dB less than the test cable, with the TCL measurement providing a distinctly more constant value, yet demonstrating sharp peaks across the full frequency range.

The lowest value of TCL recorded is now 20dB and this may be explained by the unique physical arrangement of the circuit or the increased number of electrical loads, i.e. luminaires which are connected in parallel along the circuit length. We noted earlier within Section 4.15.1 with test cable that even the introduction of a balanced load to the far end of the cable related to a 5dB reduction in the TCL. Given the number of parallel branches, of various lengths there is the opportunity for standing waves to be present across the branch and create a resulting accentuation of the reduction or increase of the transverse conversion ratio. The voltage standing wave ratio (VSWR) as determined from the reflection coefficient and Equation 3.10.2 is shown in Figure 4.19.2, however, no direct relationship with TCL is noted.

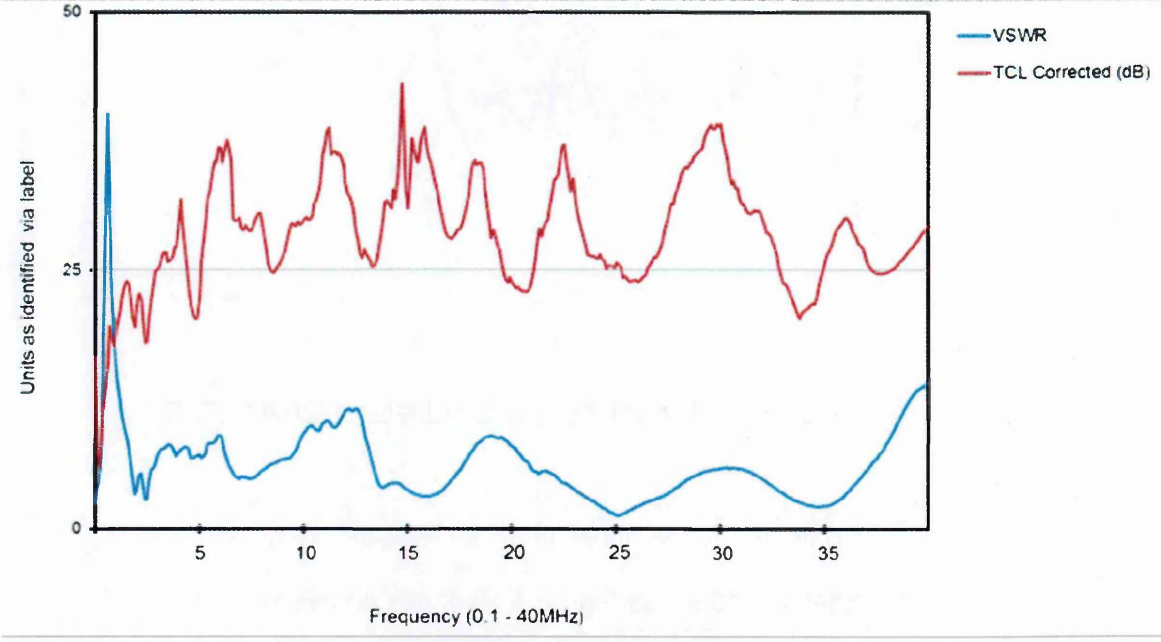

Figure 4.19.2 VSWR Graph for Lighting Circuit – OFF

Further works should consider the standing waves to the common mode circuit also and whether the combination of the two waves is seen to create the more pronounced and sharper profile of TCL to circuits such as this.

With the exception of 20.5MHz we see that the lighting circuit has a stable common mode impedance across the frequency range and shows an average value of 103Ω, which is towards the higher values previously noted and described in Chapter 3. The reduction in CMC at 20.5MHz again suggests that the circuit is coincidental with the half wavelength and we note that the more complex arrangement of combined switchlines provides further possibilities for this.

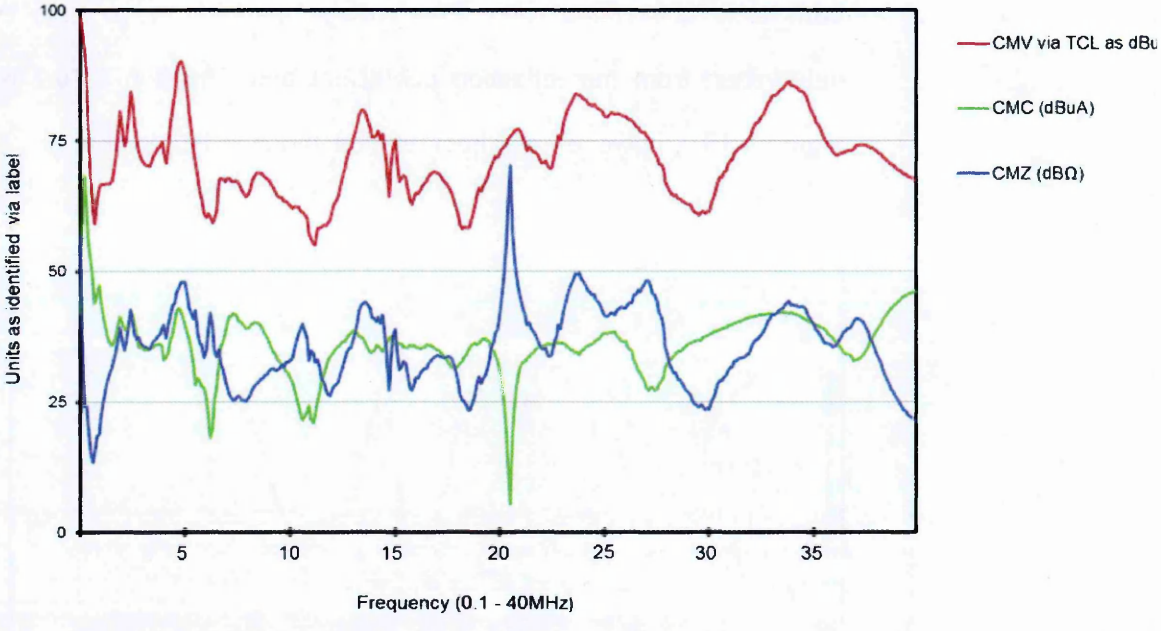

Figure 4.19.3 Impedance Graph for Lighting Circuit – OFF

Compared to the previous measurements we note an increase in the radiated Efield by 10dB, as Figure 4.19.4 with an average value of 60.4dBμV/m. With respect to the variation between calculated and measured Efield the error noted previously is seen to have reduced at the lower frequencies suggesting that the radiated field can be calculated directly from the common mode current, however beyond 12MHz we note a severe variation in values.

Given the significant reduction in CMC noted at 20.5MHz we also note that a similar reduction to the Efield reading occurs at 21.2MHz. This is likely to be the same event and the introduction of the HF probe in order to undertake the CMC reading has introduced inductance and through extending the circuit electrical length shows the profile shifted slightly towards the lower frequencies.

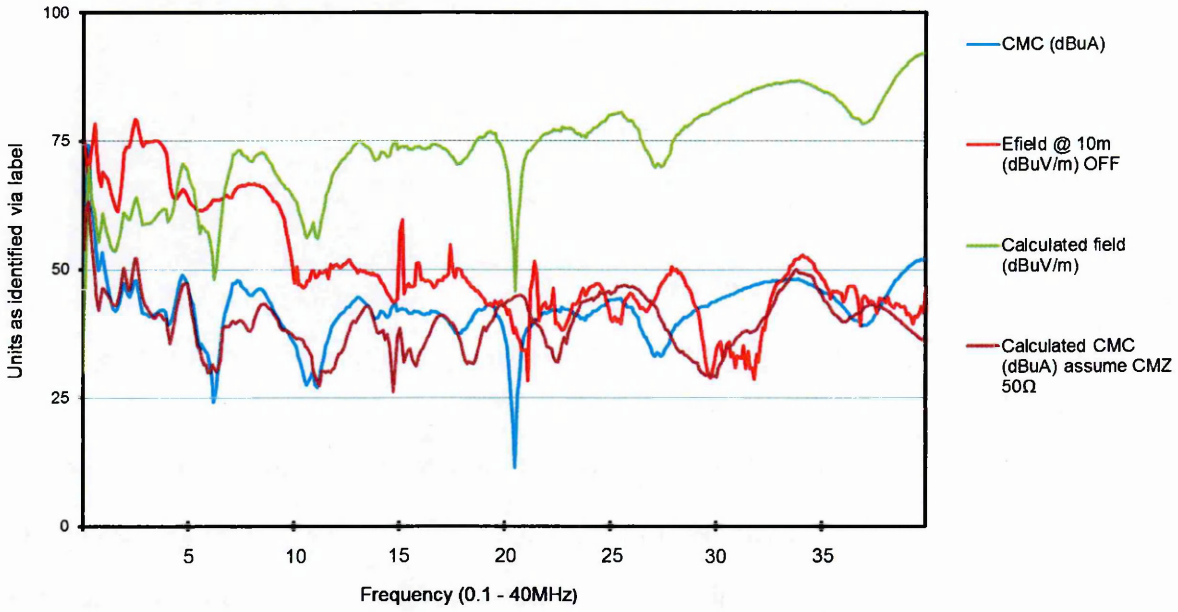

Figure 4.19.4 Radiated Graph for Lighting Circuit – OFF

The average k factor value is shown to be equal to the full Bramble LVDN at 70dB and suggest that both are able radiators of energy, however if we consider the power transfer factors, as Table 4.19.1 we note several key points.

The conversion loss, i.e. the reduction in power from absorbed power in the differential circuit to the common mode power is seen to reflect, within a few decibels the transverse conversion loss and suggests therefore that

knowledge of the currents and impedances is not required. It is noticeable that the radiated loss, i.e. the conversion of common mode power to the power density of the radiated field shows that the lighting circuit has nearly twice the losses to that of the LVDN.

	LIGHT OFF	BRAMBLE
Power Absorbed $P_{A\ (dBm)}$	-7.5	-11.2
TCL (dB)	30.7	44.3
Conversion Loss (dB)	29.5	40.9
Common Mode Power (dBm)	-30.3	-47.6
S_{21} EFIELD @ 10m (dBuV/m)	60.4	52.4
Power Density via Efield (dBuV/m2)	-50.0	-60.4
Radiated Loss (dB)	26.1	14.9
Power Density via CM power (dBuV/m2)	-61.3	-78.6
Gain (dBi CM)	5.0	16.1
Gain 0-20MHz (dBi CM)	10.5	24.2

Table 4.19.1 Power Values for Lighting Circuit – OFF & Bramble

Finally in order to assess the effects of applying an earth connection to the circuit we record the CMC and radiated fields whilst the lighting circuit remains off but with the circuit protective conductor (cpc) terminated within the earth bar of the fuseboard.

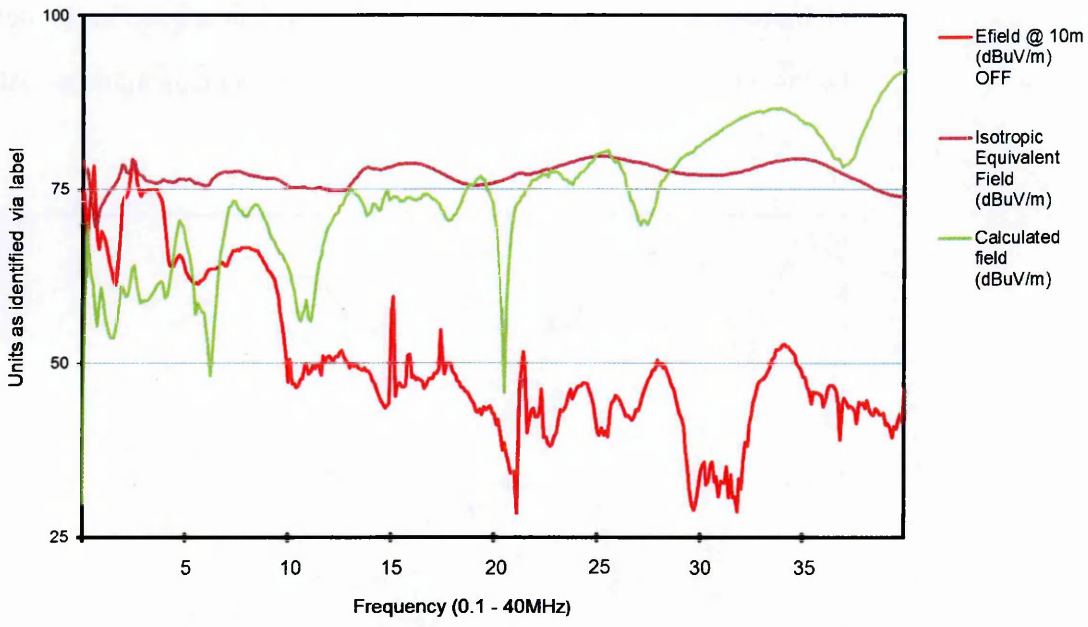

Figure 4.19.5 Radiated Graph for Lighting OFF and Earthed

This is shown above in Figure 4.19.5 and we observe very little modification to either parameter is noted, therefore indicating that no CMC within the CPC circulates towards the switchboard anti-phase to that in the phase and neutral conductors.

4.20Lighting Radial – All luminaires on

The introduction of the luminaires to the lighting circuit is shown to have little effect on the return loss and consequently the power absorbed increases marginally to -7.1dBm.

Degauque et al (2010) suggests that the application of electrical loads to the circuit results in a direct variation to the differential mode signal without any variation being observed to the CMC. The current graph below, as Figure 4.20.1 however contradicts this and shows slight variation to both currents at

all frequencies. The common mode current in fact is seen to be more affected by the introduction of the loads at the lower frequencies than the DMC.

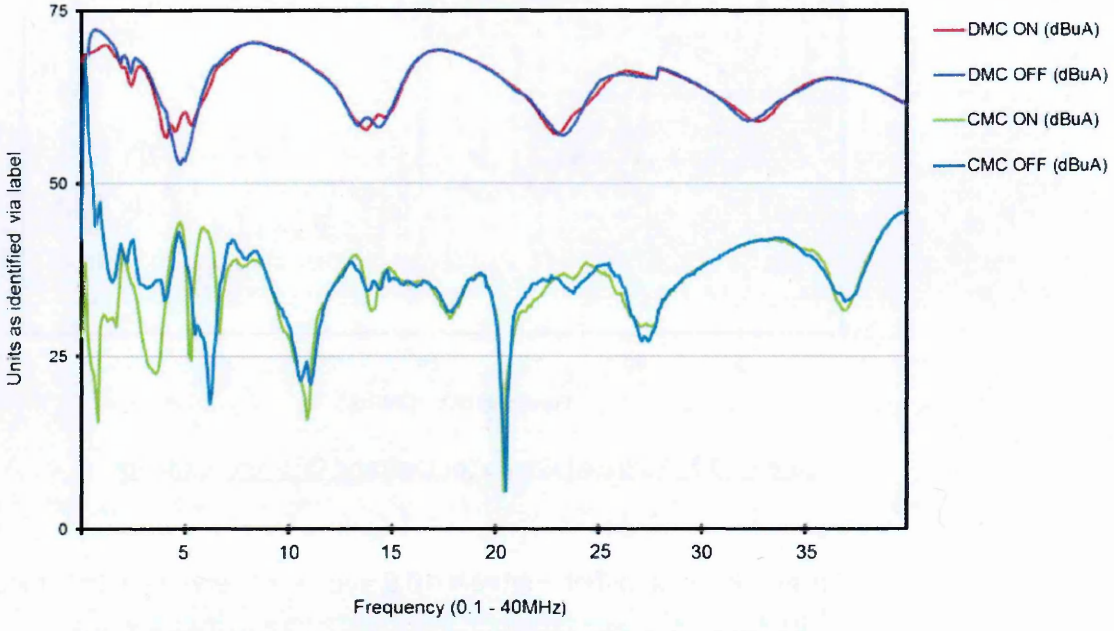

Figure 4.20.1 Current Graph for Lighting Circuit – ON & OFF

Favre (2007) also conducted measurements on typical lighting circuits and found that switching the luminaires on decreased the common mode current by 5-10dB on average.

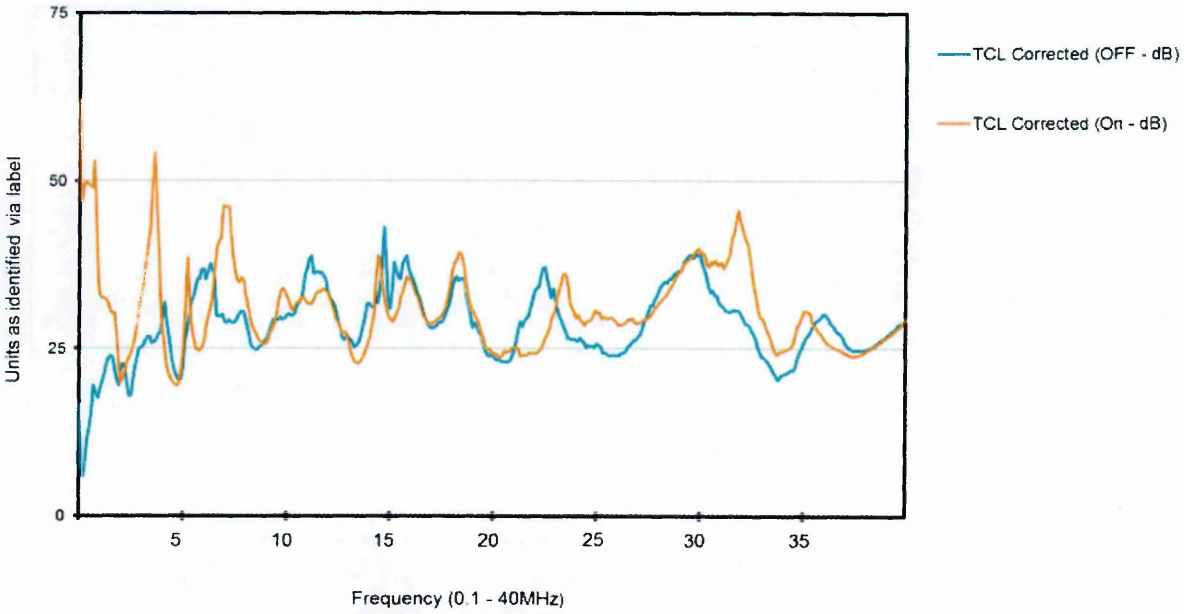

Figure 4.20.2 TCL Variation for Lighting Circuit– ON & OFF

The graph shown in Figure 4.20.3 identifies the variation in Efield when closing the lighting circuitry and this indicates two distinct regions, i.e. the lower frequencies where the field strength increases when turning the circuit on and a region above 20MHz where the field strength appears to decrease.

This is also clearly shown when considering the gain of the circuit relative to the power density of an isotropic signal generated via the common mode power. If we compare the power density of the actual radiated field less the power density of the field generated by the common mode power to determine gain as (dBi CM) Figure 4.20.4 is produced. We note that closing the switchlines, in order to turn the lighting on, results in a markedly improved gain, i.e. an increased level of EMI radiation (dBi CM) below 10MHz whilst a reduction in gain or EMI radiation occurs by a nominal 3dB above 25MHz.

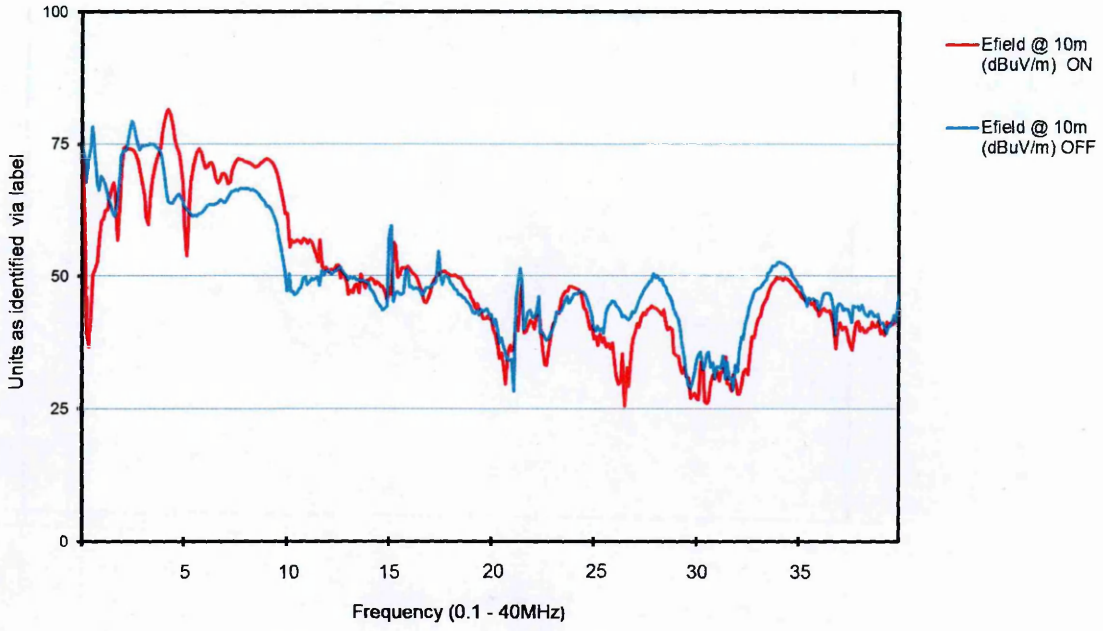

Figure 4.20.3 Radiation Graph for Lighting Circuit– ON & OFF

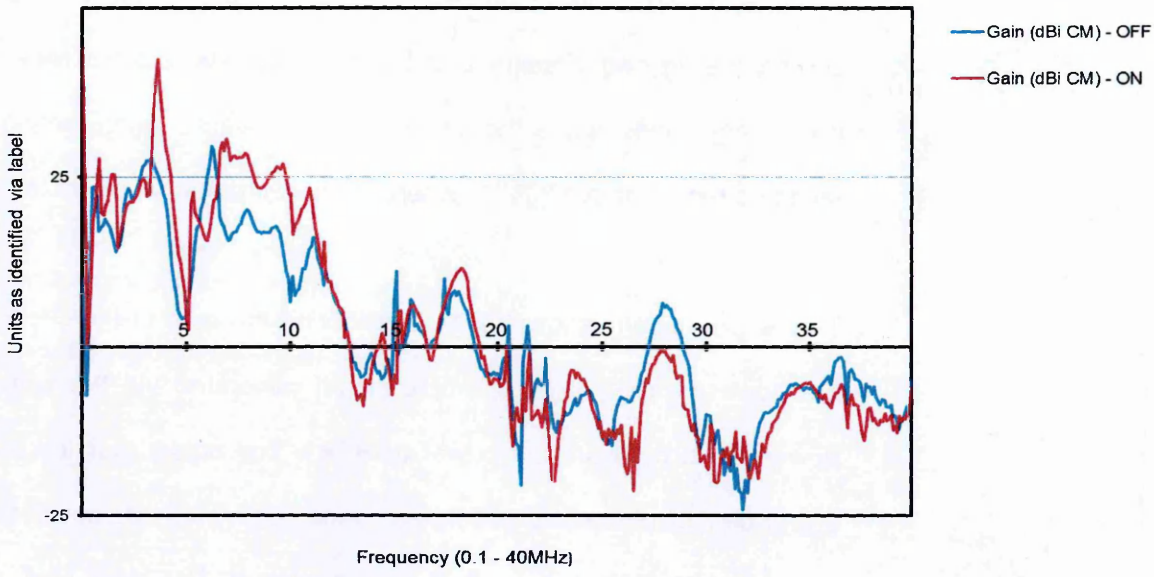

Figure 4.20.4 Gain Graph for Lighting Circuit – ON & OFF

In summary we can conclude that closing the switchlines has the effect of reducing the circuit electrical length and improves the radiation due to circuit length and the wavelength for the frequencies between 1-11MHz. This

reduction in electrical length equally reduces the ability of the circuit to radiate energy at the frequencies above 20MHz.

However, as noted from Table 4.19.1, the radiated loss from the lighting circuit, in either condition, is still significantly higher than that generated from the LVDN measurement as shown for Bramble. We therefore note that despite the alteration of the bounding conditions for the lighting circuit the effects on the radiated field are negligible compared to that generated from the same common mode power on the LVDN as a whole.

Finally we note from Figure 4.20.5 that the measured Efield directly correlates with the calculated value for the frequencies below 11MHz and demonstrates that the insulated conductors are effectively operating as a combined Hertzian dipole array, as described in Chapter 3. However, it is also to be noted that beyond 11MHz the variation between measured and calculated values becomes quite abruptly large and this would appear to be the result of more than the gradual decrease of the ratio between wavelength and circuit length.

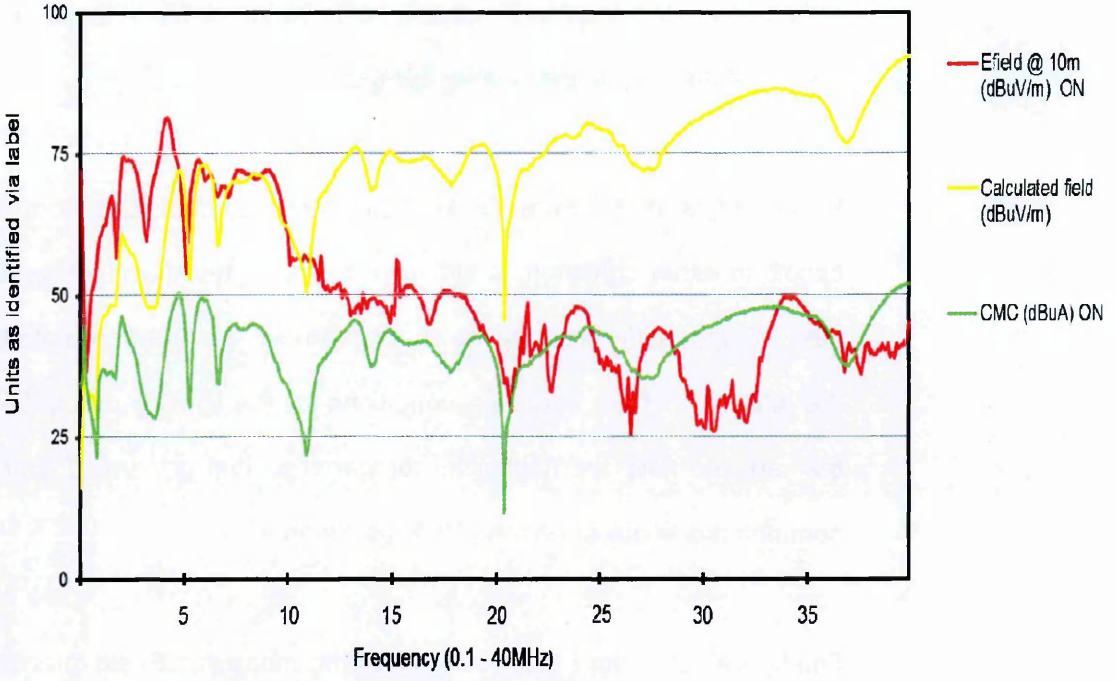

Figure 4.20.5 Measured and Calculated Efield

4.21Cooker Radial – OFF

In contrast to the lighting circuit the cooker radial comprises a linear run of 10metres of 10mm^2 cable and provides a far less complex arrangement.

The increase in cross sectional area of the phase and neutral conductors is also reflected in the earth conductor which is increased to 2.5mm^2. Figure 4.21.1 defines the calculated characteristics for this cable, and shows a characteristic impedance of 98Ω and VoP at 0.63.

CABLE TYPE (10mm2)		
ε Permitivity	8.85E-12	
ε_r Rel Permitivity	2.5	polyvinylchloride
Frequency	37	MHz
μ Permeability	1.26E-06	
μ_r Permeability	0.999	copper conductors
Conductivity	5.80E+07	Seimens/m
Resistivity	1.68E-08	ohms/m
Distance betw'n cond	7	mm
Conductor radius	1.78	mm
Cable Length	10	m
Capacitance C	5.36E-11	Farads/m
Inductance L	5.18E-07	Henrys/m
Char Impedance Zo	98.36	ohms
Skin Depth δ	0.011	mm
Impedance in	1.00	ohms
VoP	0.632939	
VSWR	1.02	:1
λ	5.13	m

Figure 4.21.1 10mm^2 Cable Characteristics

The S_{11} as shown in Figure 4.21.2 now indicates a reduction in reflection coefficient towards the higher frequencies with a return loss of -17dB at 37MHz. Use of the VoP indicated above demonstrates that the 10metre length and the 9MHz cycle observed on the differential mode current (DMC) trace occurs at multiples of the full wavelength.

TCL indicates an improvement from the lighting circuit, with an average value of 40.9dB, but for a less complex circuit we note an increased range of variation in TCL from 25-60dB. If we assume, as stated earlier that the addition of the HF probe moves the current profile slightly to the lower frequencies, and apply this correction to the DMC we note that at the full wavelength frequencies, resulting in high impedances and voltages, the TCL

values also increase. With the large variation in DMC and corresponding voltage fluctuation the overall TCL range is high.

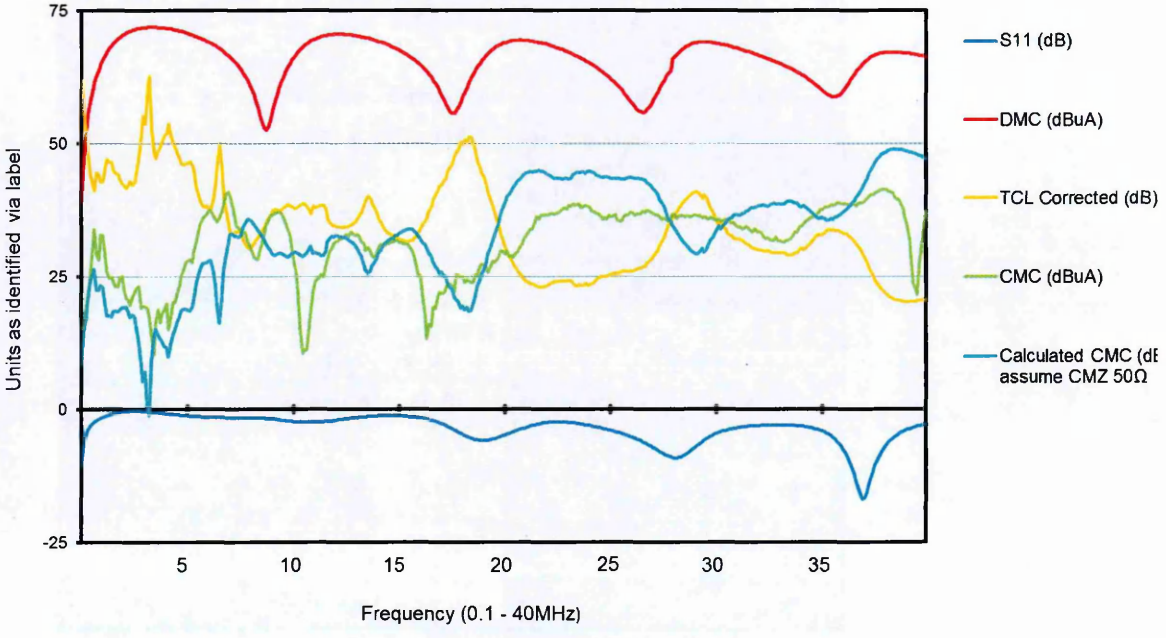

Figure 4.21.2 Current Graph for Cooker OFF

Despite the characteristic impedance of the cable being given as 98Ω, as Figure 4.21.1, the correlation between measured and calculated CMC reduces with increased frequency and we can conclude that despite the simple arrangement of the circuit the variation in common mode impedance is such that calculation of the CMC through the electrical parameters of the circuit is not feasible.

As described earlier the common mode power is the product of the common mode current and voltage, where the voltage is derived from the application of DMV and TCL. It is therefore interesting to note that in lieu of calculating the common mode power via CMV and CMC we can apply TCL directly to the

absorbed power to approximate the common mode power as shown in Figure 4.21.3.

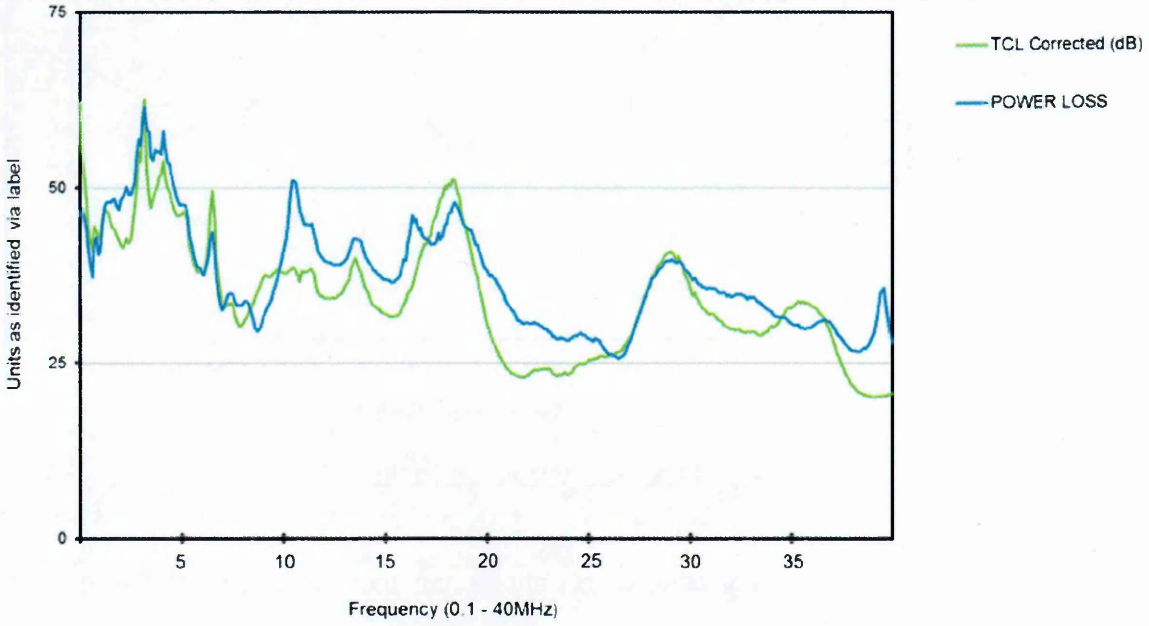

Figure 4.21.3 Power Loss to TCL Comparison for Cooker OFF

This approximation provides a means to indicate the average value of common mode power 3-5dB less than the calculated value.

The most significant property of the cooker circuit is seen when considering the radiated field measurement, as shown in Figure 4.21.4, with an average value of 67.2dBμV/m. In addition we can see the measured field strength when compared to the three calculated values, namely the isotropic field via power absorbed, isotropic field via common mode power and the Calculated Efield via common mode current.

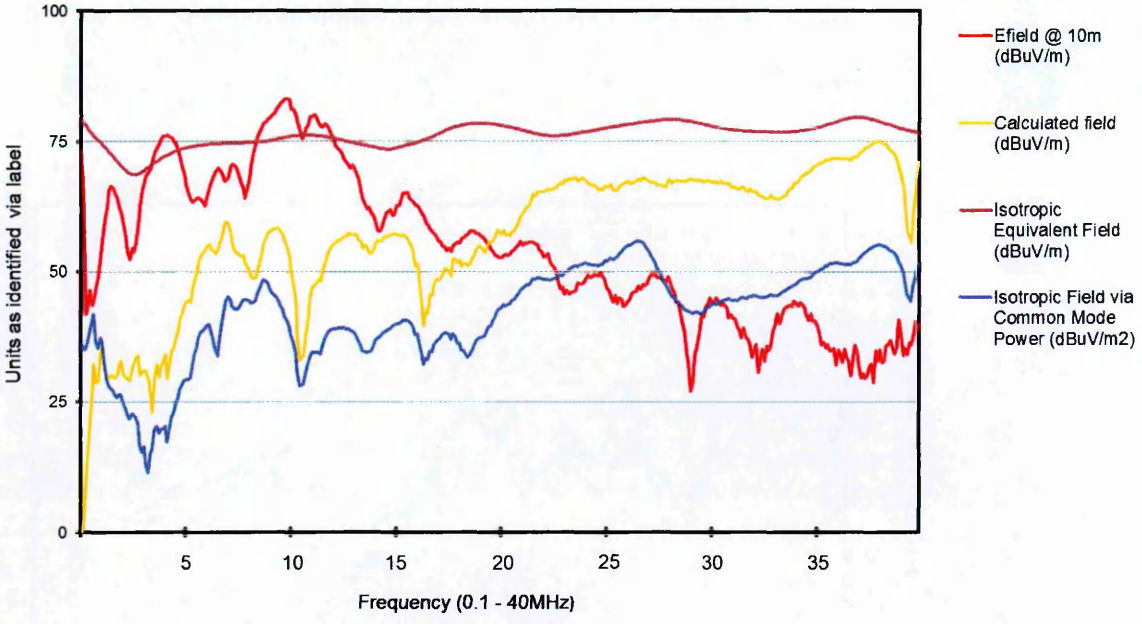

Figure 4.21.4 Radiated Graph for Cooker OFF

The initial observation shows the measured field at the lower frequencies exceeds even that of the isotropic field via power absorbed, clearly indicating the level of gain provided by the cooker circuit. As the frequency increases we see that the measured field more closely relates to the isotropic field via power absorbed.

As the frequency increases the Calculated Efield, which is frequency dependant, also increases to show a variation up to 20dB with the isotropic common mode field and the measured field.

This suggests that the Calculated Efield, which represents the maximum field strength in free space conditions, is not appropriate for estimation of the field generated from the circulation of the common mode current. Jia et al (2012) also confirmed that the phase angle of the common mode current is required

to determine the radiated field and concluded that below 30MHz the use of the common mode current to predict radiated fields was not valid.

For the first time we see the gain (dBi) of the measured field to the isotropic field is positive indicating that the circuit provides directional gain around the 10MHz region. This introduces a further parameter, i.e. that of circuit orientation and the antenna radiation pattern, as the gain may be a result of the cable routing or the unique antenna pattern associated with this circuit.

Although the energy within the common mode circuit is shown to radiate equally in all directions around the conductors, as described in Chapter 3 and not provide a maxima in the plane of the conductors, the cables comprising the common mode circuit have at the lower frequencies a length significantly smaller than the signal wavelength and operate as non-complex dipoles (Schmitt, 2002) radiating liberally at a point 90° to the cable, with the power decreasing in accordance with the reduction in angle to 0°.

As indicated in Figure 4.16.1 both circuits comprise elements of cabling routed parallel (90°) and in line (0°) to the measuring antenna and it is not possible to demonstrate these radiation patterns without taking extensive measurements in all directions. This demonstrates the issues reported by the NSOs in Chapter 2 regarding repeatability of radiated measurements and the difficulty in employing such an approach for legislative purposes.

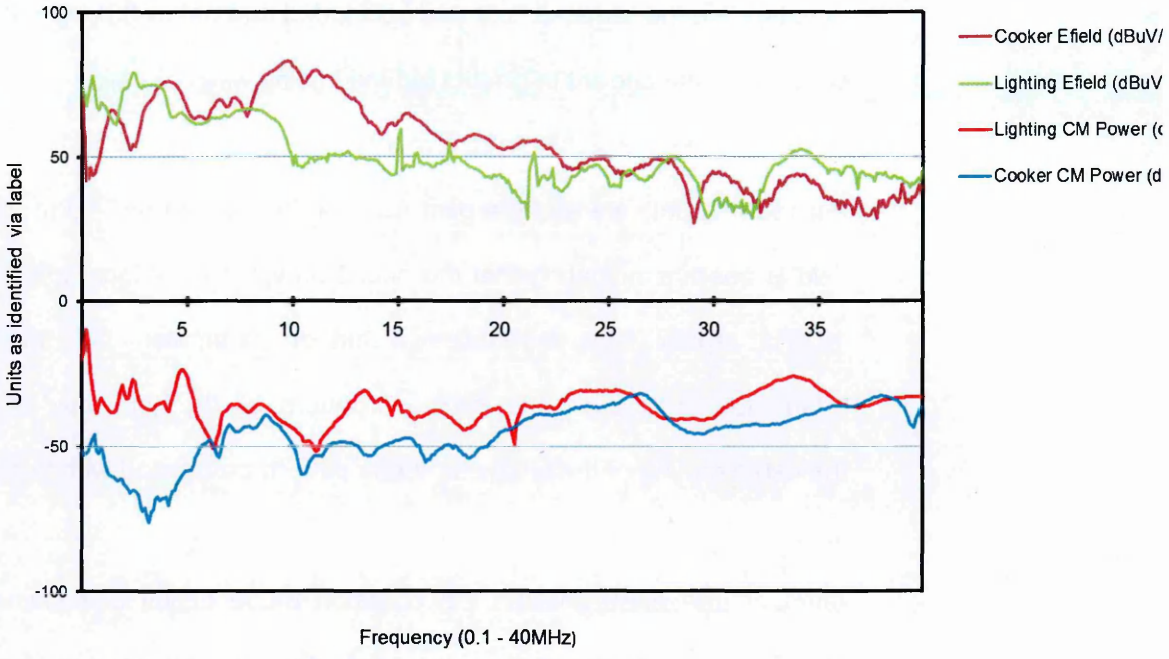

Figure 4.21.5 Graph indicating CM Power & Efield for Lighting & Cooker

We note from Table 4.21.1 that the k factor and gain (dBi) for the cooker radial have increased 8.5dB on the average values compared to the lighting radial and it is difficult to determine from these factors as to what proportion of this increase is due to the changes in the electrical properties of the circuit and which to the physical arrangement of their installation.

Use of this parameter alone does not allow any further judgement. However, if we compare the conversion and radiated losses we can confirm that although the cooker circuit delivers less power to the common mode, as a result of the increased TCL and circuit impedance, is a far more effective in its ability to transfer the common mode power into radiated energy, resulting in increased levels of EMI.

	LIGHT OFF	COOKER OFF
S11	-3.6	-2.6
Power Absorbed PA (dBm)	-7.5	-8.5
DMC (dBuA)	65.8	66.9
DMV (dBuV)	101.5	100.7
DMZ Mismatch (Ω)	5.9	999.6
DMZ (dBΩ)	40.5	47.0
TCL (dB)	30.7	40.9
CMC (dBuA)	37.9	26.2
CMV (dBuV)	74.7	68.0
CMZ(dBΩ)	40.3	41.3
Common Mode Power (dBm)	-30.3	-41.3
Calculated CMC (dBuA)	41.6	35.2
S21 EFIELD @ 10m (dBuV/m)	60.4	67.2
k Factor (dBuV/m-dBm)	70.7	79.2
Gain(dBi)	-24.5	-16.0
Calculated EFIELD via CMC (dBuV/m)	66.4	53.2
Gain relative to calculated field (dB)	-11.3	12.8
Conversion Loss (dB)	29.5	39.0
Radiated Loss (dB)	26.1	8.0

Table 4.21.1 Average Values for Light OFF & Cooker OFF

4.22Cooker Radial - On

Unlike the profile we observed with the Lighting – ON measurements, we note a substantial change to the differential mode current when the cooker load is switched on. The DMC is shown below in Figure 4.22.1 to demonstrate little variation across the spectrum, as the general return loss improves to provide an absorbed power of -5.8dBm and the current maintains a cyclic value around a mean of 66dBμA.

TCL conversely is seen to fall dramatically with the addition of an appliance to the circuit and we note a worst recorded TCL value of 18.5dB, which agrees with See (2005) and verifies the judgement of CISPR/I 257 in proposing that testing carried out via a L-ISN should have an LCL of 16dB. This significant variation is likely due to electric heating elements, which are generally

constructed from coils of nichrome wire mounted within ceramic insulating alumina binder to steel tubes.

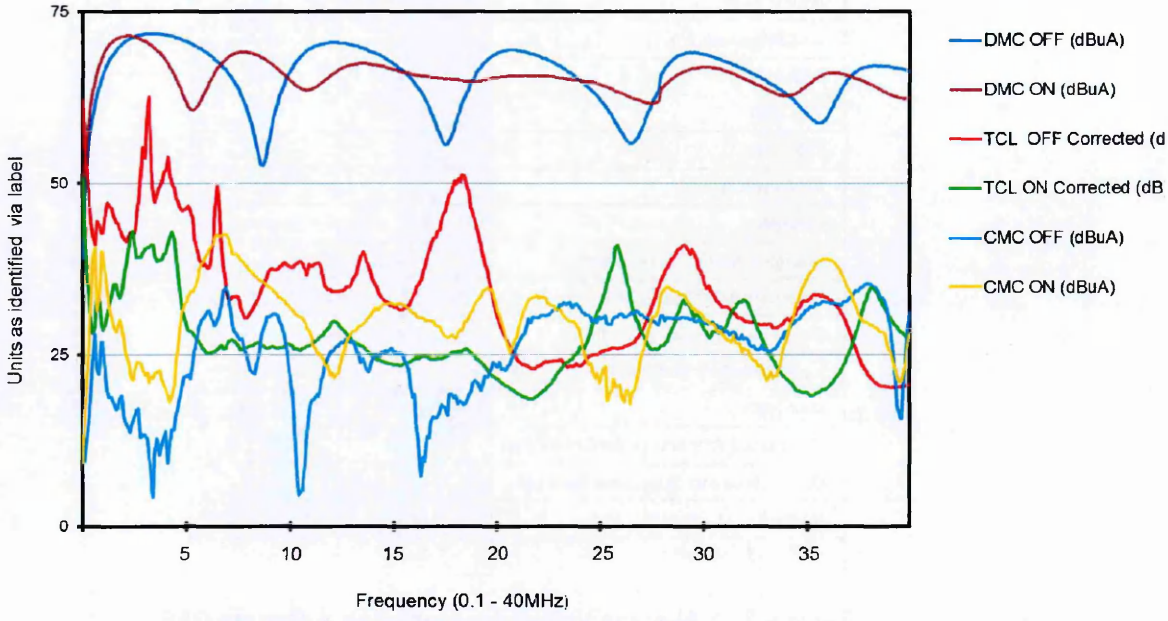

Figure 4.22.1 Current Graph for Cooker - On

The combination of binder having a dielectric constant vastly different from PVC presenting parasitic capacitance at high frequencies and the additional inductance of the windings have been shown to reduce TCL by Yuichiro (2009) at nearly all frequencies.

Comparison of the TCL with the conversion loss again demonstrates that a marginal error exists, i.e. nominally 3-5dB on the assumption that TCL represents the power transfer of absorbed power to power in the common mode circuit. Whilst this clearly reduces the accuracy of the model we are able to relate the common mode power directly to the modem power via return loss and TCL.

The addition of loads to the circuit as stated by Okugawa (2009) was found to increase the radiated field also and this is noted here too, however, clearly the reduction in TCL has resulted in more power created within the common mode and we can compare the circuit's ability to radiate energy by considering the gain as shown in Figure 4.22.2, which compares the actual radiated fields when normalised to the same value of common mode power. It is clear therefore that the addition of an electrical appliance to the circuit actually reduces the radiation properties of the circuit and we note that the average gain reduces from 23 to 14.3dB

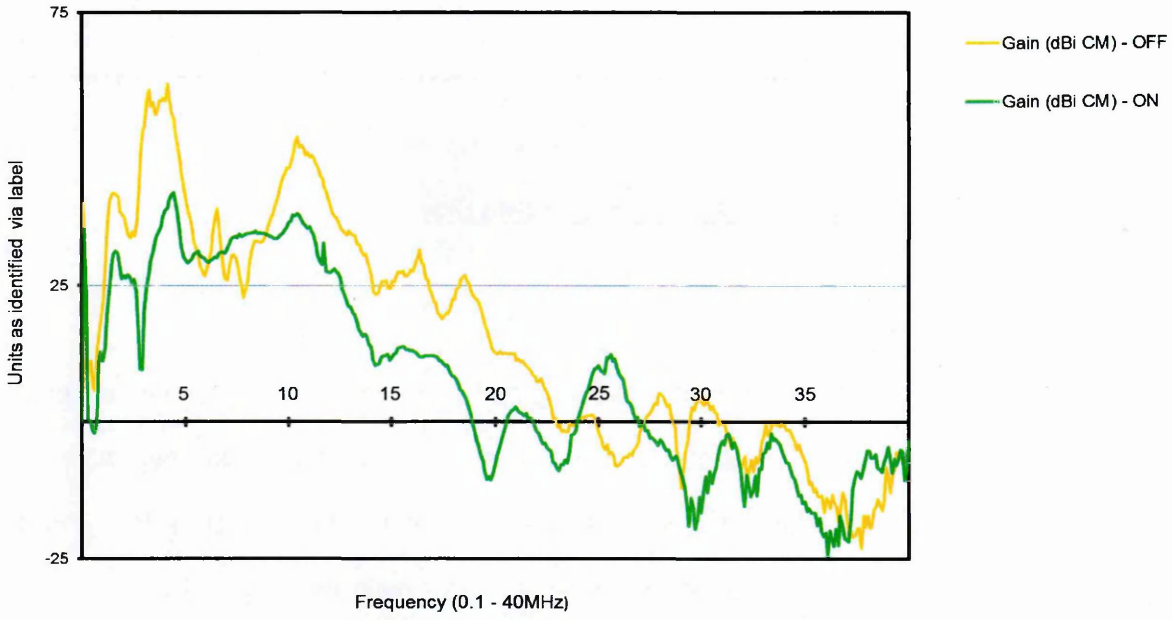

Figure 4.22.2 Gain Graph for Cooker - On

This 8.7dB variation in gain indicates that the application of a single appliance can significantly change the radiation properties of the circuit and that prediction of the radiated field from knowledge of the common mode circuit parameters alone is not viable. This is demonstrated in Figure 4.22.3 where it

is shown that the common mode power increases to nearly all frequencies whilst the Efield variation is limited to particular frequencies.

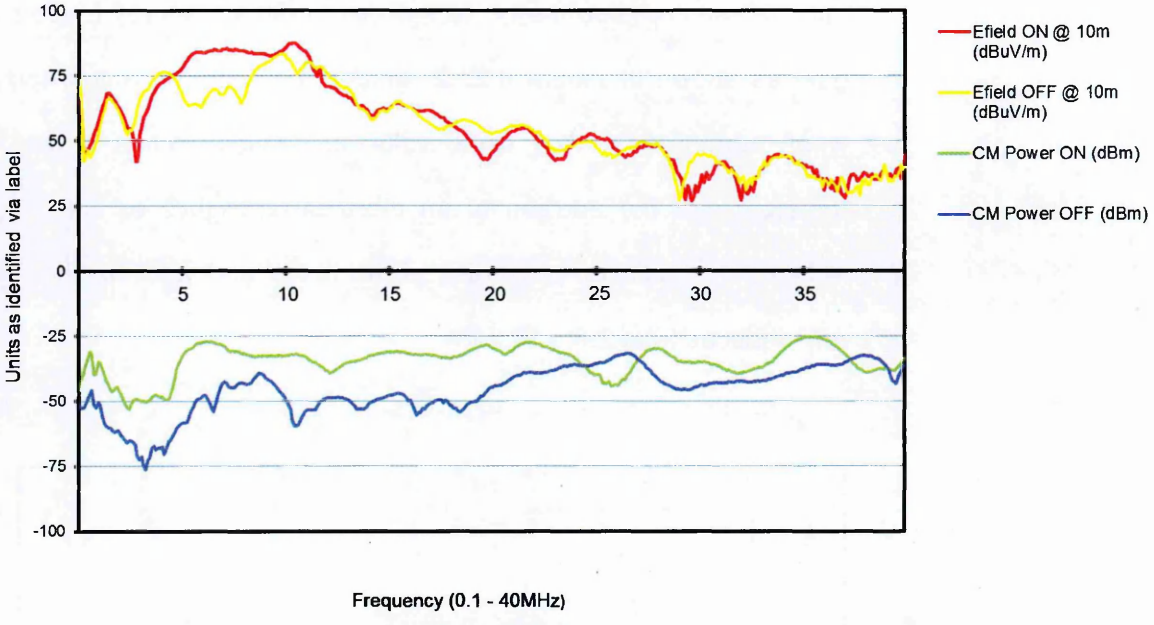

Figure 4.22.3 Power and Efield Graph for Cooker - On

4.23 Ring Main

The ring main as suggested by the name comprises two conductors at each outlet and at the mains position for both the phase, neutral and earth paths. Testing was completed by removing both conductors from the mains board and re-connecting together to maintain the ring and allow connection of the injected signal to both ends of the ring simultaneously.

S_{11} has a very pronounced effect, as Figure 4.23.1, which indicates that the injected signal is returning via the ring to provide a phase or anti-phase contribution to the reflected signal, and as such creates the oscillation on the return loss within the lower frequency range. The effects of this are negated

over the full frequency range and the average power absorbed by the ring main is -6.1dBm.

This same profile is seen to the differential mode current and the average values remains as the other circuits close to 67dBμA.

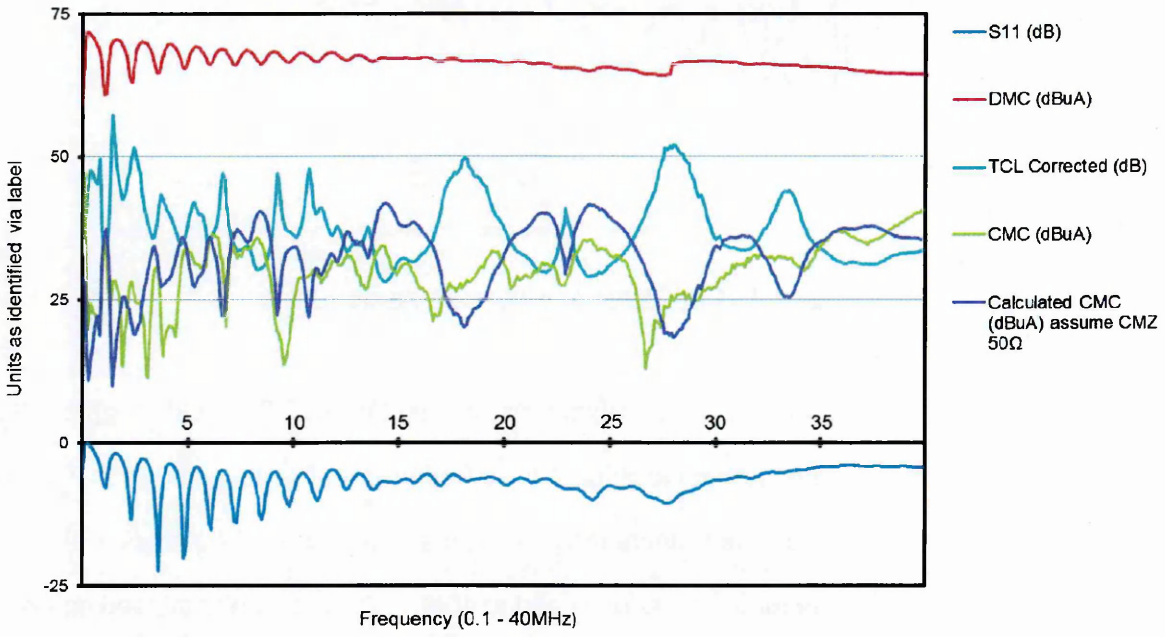

Figure 4.23.1 Power Graph for Ring Main

Given the previously noted feature of TCL measurements, in that significant variation can occur with slight circuit changes, the ring main offers an ability to take several measurements of the same circuit from different measurement locations.

The introduction of the MacFarlane probe at different locations on an otherwise constant circuit is demonstrated in Figure 4.23.2 and we can see the considerable range of TCL values generated as a result of altering the overall circuit impedance by the movement of the probe.

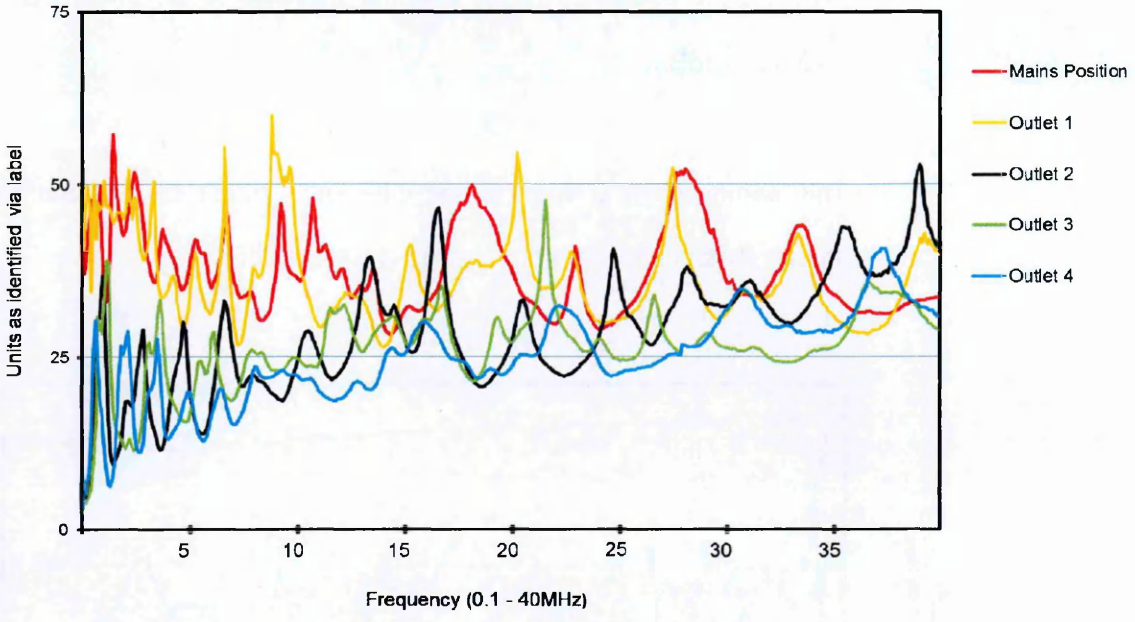

Figure 4.23.2 TCL measurement along Ring Main

Review of the waveforms in Figure 4.23.2 would suggest that as the measurement location moves further from the mains position TCL at the lower frequencies decreases. Towards the higher frequencies the variation in measurement reduces and at 40MHz the average of all readings is 36dB.

Throughout the testing the ring was maintained at all times and we can consider each of the socket outlets as an unbalanced load, i.e. acting as the source current generator for the common mode current in parallel, and we can surmise that moving the probe around the ring locates the probe uniquely between two distinct unbalanced loads which are at unique distances from the probe. The TCL measurement recorded at each socket indicates the combined waveforms residing on the adjacent legs of the ring circuit and this is shown via the measurements of adjacent sockets that demonstrate common features at particular frequencies.

We can further note that TCL values recorded from the above measurements have generally remained above 18dB, however at the location of Outlets 2,3 & 4 values as low as 5dB are indicated for frequencies below 2MHz.

This confirms the view that use of the TCL on complex circuits is not valid and demonstrates that further works are required in this area to define the process for TCL measurement. However, from this initial view it is considered that taking the TCL measurements from the mains position introduces the least error.

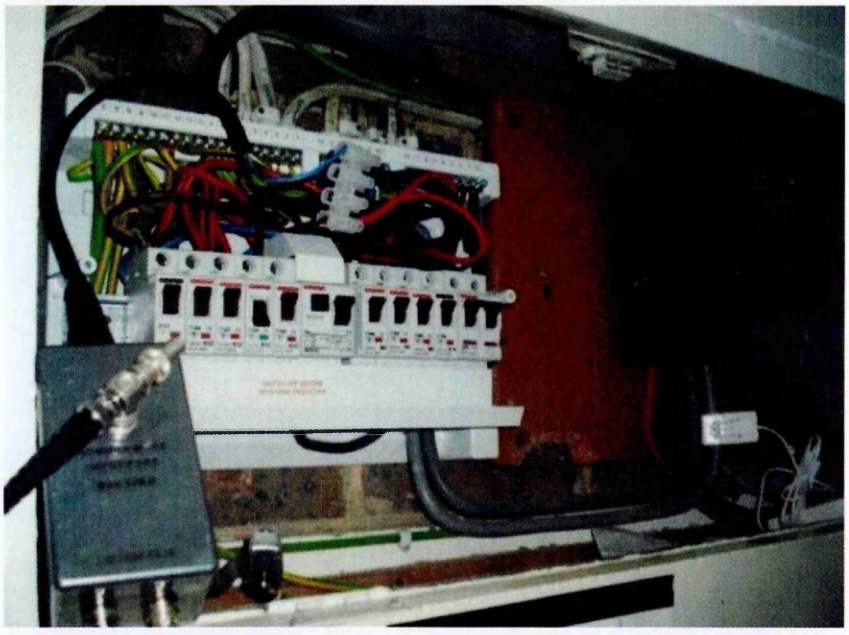

Figure 4.23.3 TCL Measurement on Ring Main at Mains Position

The Efield recorded from the ring main provides an average recorded value of 51.3dBμV/m and by virtue of a ring the circuit is not orientated in any particular direction and so can be expected to provide same gain to all horizontal planes. Carr (2011) proposes that loop antenna whose physical size compares to the

signal wavelength demonstrate a 2dB gain with respect to the equivalent dipole.

The gain for each circuit is shown in Figure 4.23.4, as calculated from the radiated signal power density and the equivalent power density via the common mode power. We note that the gain for all circuit types reduces with frequency until all circuits radiate less than the isotropic equivalent of the common mode power. The frequency at which the gain becomes negative is seen to vary with each circuit and it can be shown that this relates to the circuit length. Knowing the cooker, lighting and ring main are in the order of 10, 20 and 30 metres respectively we can show that the half wavelength of the signal in the common mode circuit is approximately equivalent to the frequencies of high gain with negative gain occurring at the full wavelength frequency.

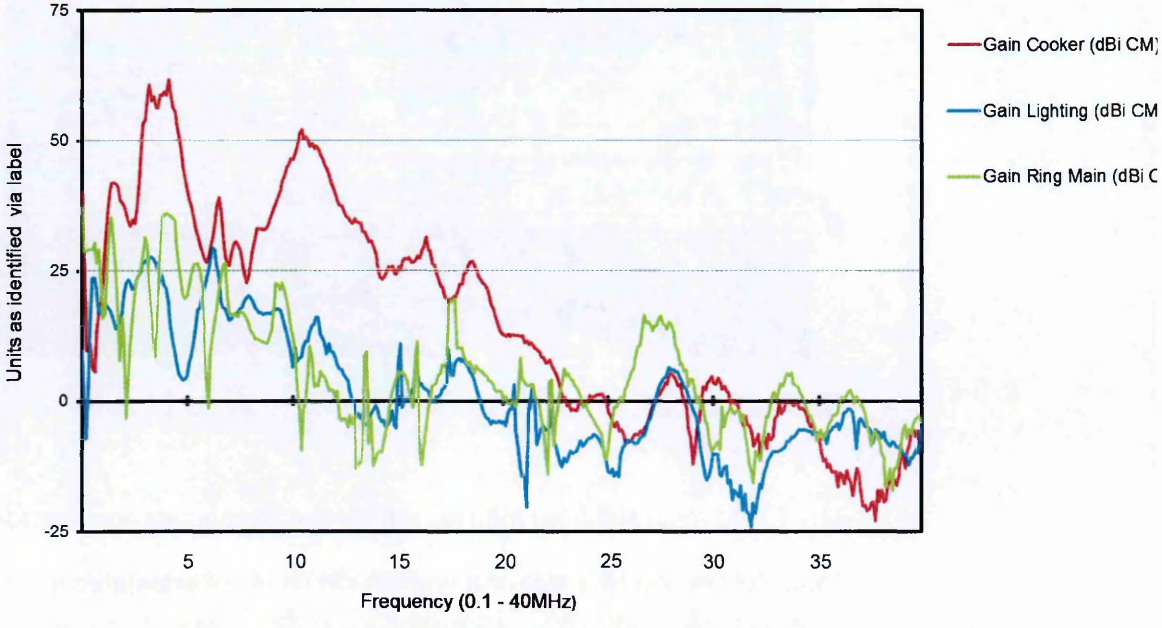

Figure 4.23.4 Gain Graph for Cooker, Lighting and Ring Main

This demonstrates that the energy within the common mode circuit of the ring main radiates in the same manner as a dipole, albeit with 2dB gain and allows direct comparison to the other circuits.

Reference to the average gain, as given in Table 4.24.1 for all circuits shows the ring circuit to provide an average 8dB over the range of 1-30MHz and Figure 4.23.5 clearly shows that beyond the frequency where λ_{CM} = circuit length the radiated field has the equivalent magnitude to that of the isotropic equivalent of the common mode power.

We can therefore suggest that the direct frequency variations, as seen in Figure 4.23.5 between the measured field and calculated isotropic field are due to the environmental conditions of the signal propagation through the structure.

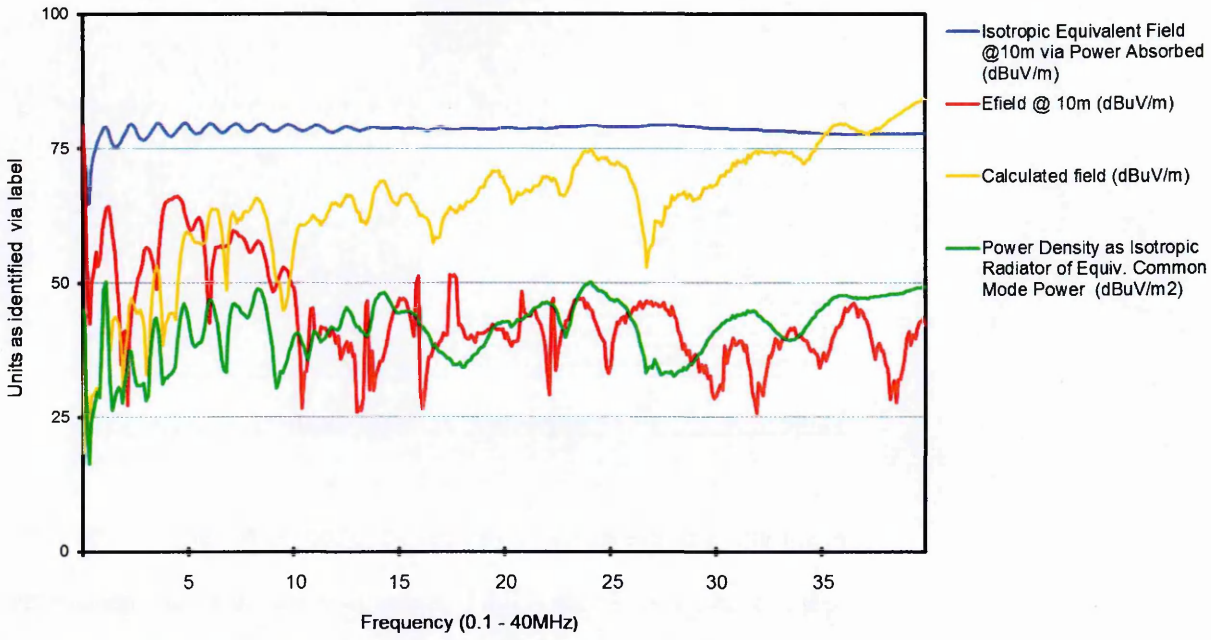

Figure 4.23.5 Transfer Graph for Ring Main

4.24Summary of Circuit Tests

Many researchers such as Ohishi (2008) and Rodriguez-Morcillo et al (2009) have constructed basic models of the LVDN and suggested that correlation exists between the measurement of TCL and common mode current.

However, despite claims of excellent correlation between theory and measurement on simple circuits few have related their influence on the EMI generated from the LVDN. The measurements undertaken above have allowed both the electrical and antenna properties of various circuit types to be described in order to relate the resulting EMI from the injection of the LVDN with a high frequency signal.

	LIGHT OFF	LIGHT ON	COOKER OFF	COOKER ON	RING	BRAMBLE
S11	-3.6	-4.1	-2.6	-7.7	-6.5	-1.2
Power Absorbed PA (dBm)	-7.5	-7.1	-8.5	-5.8	-6.1	-11.2
DMC (dBuA)	65.8	65.6	66.9	66.1	66.9	71.6
DMV (dBuV)	101.5	102.0	100.7	103.5	101.3	86.3
DMZ Mismatch (Ω)	5.9	489.0	999.6	277.1	295.7	1666.0
DMZ (dBΩ)	40.5	40.0	47.0	41.3	35.1	15.1
TCL (dB)	30.7	34.5	40.9	30.4	40.8	44.3
CMC (dBuA)	37.9	35.0	26.2	31.6	23.7	30.2
CMV (dBuV)	74.7	73.5	68.0	77.2	65.4	52.2
CMZ(dBΩ)	40.3	39.9	41.3	47.8	42.6	23.4
Common Mode Power (dBm)	-30.3	-34.7	-41.3	-35.5	-44.7	-47.6
Calculated CMC (dBuA)	41.6	39.5	35.2	44.0	33.7	30.1
S21 EFIELD @ 10m (dBuV/m)	60.4	62.1	67.2	72.7	51.3	52.4
k Factor (dBuV/m-dBm)	70.7	70.2	79.2	77.5	62.2	70.4
Gain(dBi)	-24.5	-25.1	-16.0	-17.7	-33.0	-24.8
Calculated EFIELD via CMC (dBuV/m)	66.4	66.3	53.2	56.2	58.5	74.4
Gain relative to calculated field (dB)	-11.3	-10.1	12.8	8.5	-9.2	-19.6

Table 4.24.1 Table of Average Parameter Values for Circuit Type

A summary of the average values, as recorded for each of the individual circuit tests is given as Table 4.24.1 above and we see that the overall transfer of power remains remarkably constant, irrespective of the circuit type, application

of loads or physical arrangement. This is also reflected in the differential and common mode impedances that both demonstrate nominal 100Ω impedances Combination of these parallel circuits is seen to reduce the overall differential impedance to Bramble whilst a smaller reduction in common mode impedance confirms the combination of series and parallel connections between the CBN.

The conversion loss is seen to vary strictly in accordance with TCL, as shown below in Figure 4.24.2 and we can see that conversion loss for all circuits remains within the order of 30-50dB. Calculation of the common mode power can be approximated directly via the application of TCL to the absorbed power.

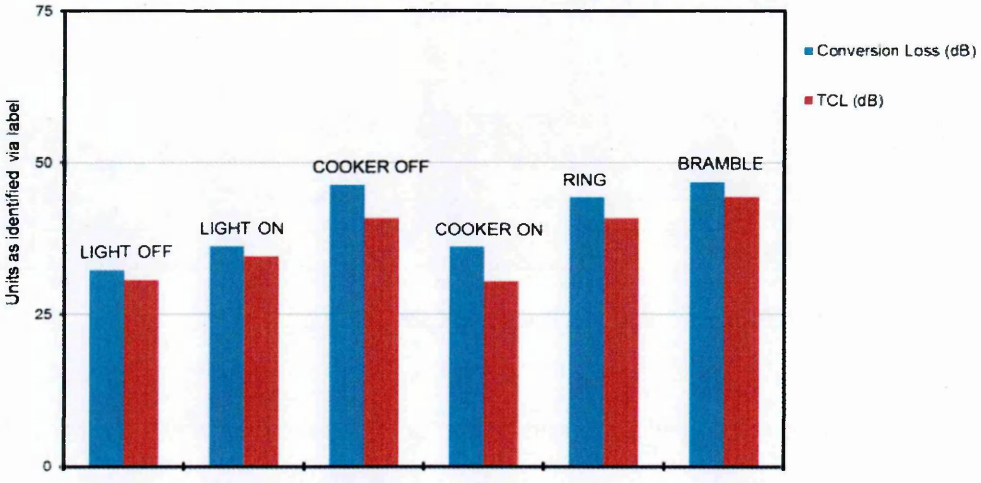

Figure 4.24.1 TCL to Conversion Loss Comparison per circuit type

Given the relative variation in common mode impedance the application of TCL has shown that common mode current cannot be calculated. Equally use of the measured common mode current to determine the radiated field has also proven to result in a large magnitude of error.

Whilst use of the k factor and gain (dBi) as given in Table 4.24.2 to describe the overall circuit transfer factor are shown to provide relative use when comparing the change of condition on a single circuit their use is limited when relating the performance of different circuits, as the two transfer factors combine both the changes in the electrical and antenna parameters into a single figure.

When comparing Bramble to the lighting circuit this becomes evident as we note that all circuits have a k factor of approximately 70dBµV/m-dBm. However, reference to the gain (dBi CM) shows that this is a coincidence, as the decrease in common mode power seen at Bramble, i.e. as a result of the 10dB increase in TCL, is directly negated by the improved gain, which increases from 6 to 16dB.

	LIGHT OFF	LIGHT ON	COOKER OFF	COOKER ON	RING	BRAMBLE
k Factor (dBuV/m-dBm)	70.7	70.2	79.2	77.5	62.2	70.4
Gain(dBi)	-24.5	-25.1	-16.0	-17.7	-33.0	-24.8
Gain (dBi CM)	5.0	6.2	23.0	14.3	8.4	16.1

Table 4.24.2 Gain Comparison per circuit type

Finally, we can summarise the combined circuit tests to the overall LVDN performance. We note that the lowest value of TCL recorded for the complete LVDN is 25dB despite the individual tests recoding values as low as 18dB.The gradual tendency for decreased TCL to the higher frequencies reflects in the increased common mode power and radiated isotropic power density as shown in Figure 4.24.2 above.

The combined effect of the individual circuit common mode paths produces a gain (dBi CM) which approximates the average gain of the individual circuits. It is interesting to note that the despite the cooker circuit measurement showing a high relative gain when tested via the overall LVDN this is no longer noted. The influence of the total earth network and the distribution of the common mode power across the CBN results in the reduced but more constant gain profile as observed below.

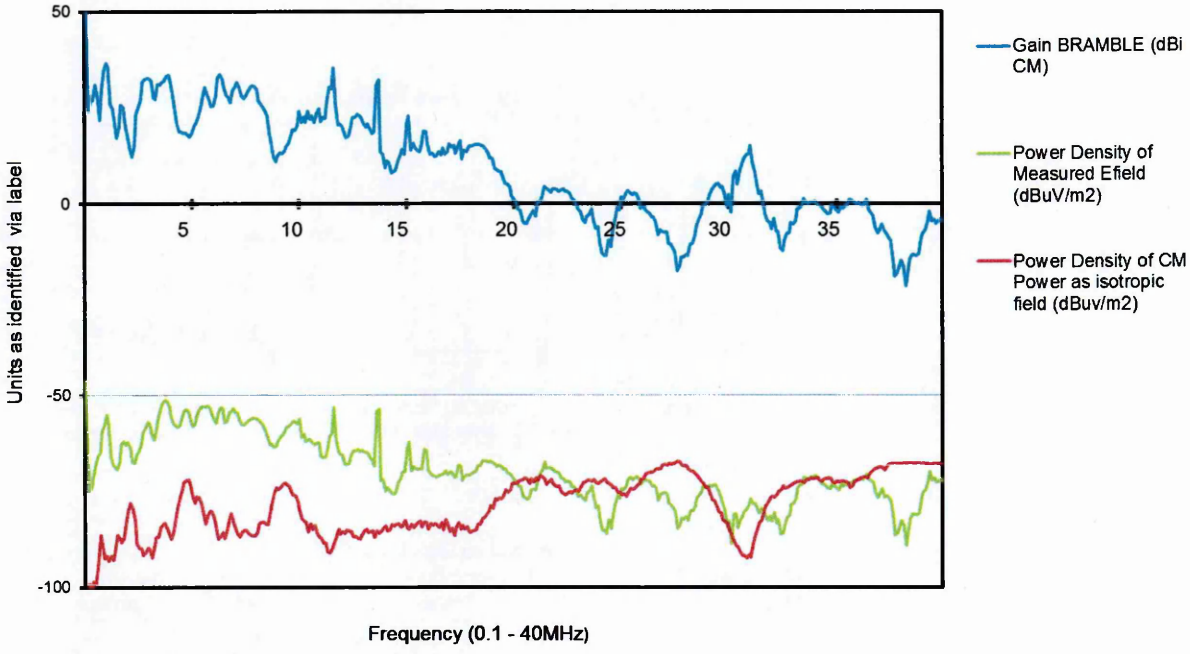

Figure 4.24.2 Gain Graph for Bramble

Reference to Table 4.24.2 above shows that the average gain, when comparing the cooker circuit to Bramble, reduces 7dB and we can suggest this is as a result of the more extensive CBN, as described above.

4.25 PLT Measurements

As described in Chapter 2 the default powerline device for the domestic UK market circa 2006 was the Comtrend 902 unit. This was marketed by British Telecom who engaged the EMC test house Messrs Blackwood Compliance Laboratories to undertake emission testing of the device prior to its use within the UK.

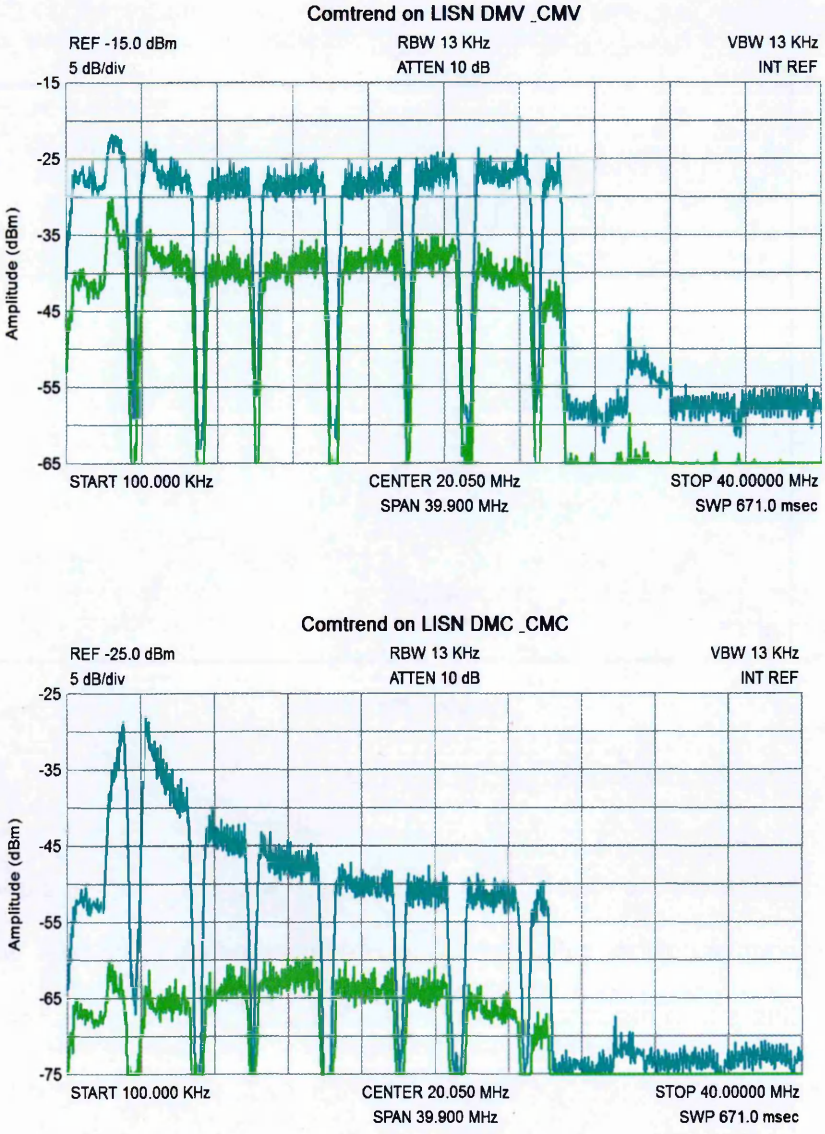

Figure 4.25.1 Comtrend Conducted Voltage and Current Measurements

The conducted emissions are shown in Figure 4.25.1 and the PLT signal is seen to comprise a broadband signal spanning from 0.5 -26.5MHz interspaced with a series notches. Each notch is shown to be approximately 30dB deep, with respect the signal level, and arranged to avoid frequencies between 3-3.7MHz, 6.8-7.4MHz, 9.8-10.3MHz, 13.7-14.5MHz, 18-18.3MHz(17m) and 20.7-21.7MHz(15m).

On activating the Comtrend units and arrange them to poll, i.e. provide communication to establish an Ethernet connection but not to transfer data, we observe that the conducted emission from the mains port, as shown above, displays a minor variation in signal strength between polling and full data transfer. Therefore unless stipulated all tests are arranged with modems in polling mode only.

4.26 L-ISN – PLT Measurements

To measure the performance of the Comtrend modems they are energised via the L-ISN and as noted above in Figure 4.25.1 the differential mode voltage is seen to be order of 10dB greater than the common mode voltage. This agrees with the previous TCL measurement for the L-ISN, Figure 4.12.1, where an average value of 11dB was found.

Measurement of the current confirms the power absorbed by the circuit and we note from Table 4.26.1 below that the power delivered to the differential mode circuit is -20.1dBm.

Parameter	Peak Calculated Value
DMV	85.34dBµV
DMC	54.47dBµA
DMZ	30.87dBΩ
Power Absorbed	-20.09dBm
CMV	74.11dBµV
CMC	34.48dBµA
CMZ	39.63dBΩ
Common Mode Power	-35.7dBm

Table 4.26.1 Values of Comtrend conducted parameters via L-ISN

As noted previously the modem has a declared power of -58dBm/Hz at 9kHz and this should reflect on a 100Ω system as an absorbed load of -19dBm. The variation in actual absorbed power due to mismatch, i.e. of the L-ISN with differential impedance of 100Ω in parallel with the two modems and the overall impedance is shown to be 30.87dBΩ. This indicates that the modems have an internal impedance of 105Ω and results in the mis-match described above.

Due to the series, i.e. 25Ω asymmetric impedance of the L-ISN the combined common mode impedance is seen to be greater than the DMZ at 39.63dBΩ (95.8Ω), which corresponds with the general circuit results shown in Table 4.24.1 but is significantly higher than the overall LVDN.

In Chapter 2 the proposed CISPR/I/257/CD standard, which aims to restrict the common mode current in the same manner as the Japanese PLC regulations to 22dBµA for the 1.6–5MHz and 18dBµA for 5–30MHz range, when operating the modem via a L-ISN was described. This limitation to the common mode current presupposes (Kitigawa, 2008) that the noise floor at a

distance of 10 metres from the source will not be increased as a result of the radiated Efield.

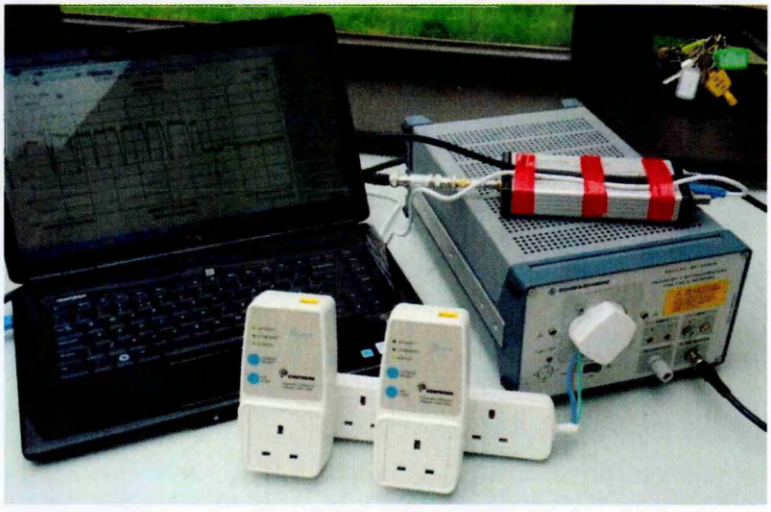

Figure 4.26.1 Image of the Comtrend modems operating via the L-ISN

It is seen from Table 4.26.1 that the average recorded CMC for the Comtrend unit is far greater than this and application of this limit would prohibit the use of the Comtrend modem. It is to be noted however that the TCL of the L-ISN used in the above measurement is 5dB less than that required by the proposed Japanese limit and provides an asymmetric impedance of 50Ω in lieu 25Ω. If we correct for these variables we see that the Comtrend would generate a common mode current as given in Equation 4.26.1.

$$CMC = DMV\ (dB\mu V) - TCL - (20\log(95.8 - 25\Omega)$$

$$CMC = 85.34dB\mu V - 16dB - 37dB = 32.34dB\mu A$$

Equation 4.26.1

Having observed from the LVDN measurement of Bramble above that the minimum recorded value of TCL is in the order of 25dB it would be reasonable

to increase the L-ISN to this value and we can show that in order to operate the Comtrend modems within this limitation the minimum TCL required is given as Equation 4.26.2.

$$TCL = 85.34dB\mu V - 18dB\mu A - 37dB = 30dB$$

Equation 4.26.2

This suggests that use of the Comtrend modems to the UK typical LVDN, as represented by Bramble will result in a common mode current exceeding 18dBμA at certain frequencies with the creation of a subsequent increase to the ambient noise floor. Confirmation of whether this level of current to the common mode circuit would result in an increased noise floor can be estimated by placing the modems on the LVDN, with a known TCL and comparing to the modems whilst operating via the L-ISN.

Figure 4.26.2 indicates the S_{21} trace recorded at 3metres from the L-ISN/modem and we apply regression, as described by Equation 4.10.3 to allow calculation of the field strength at 10 metres.

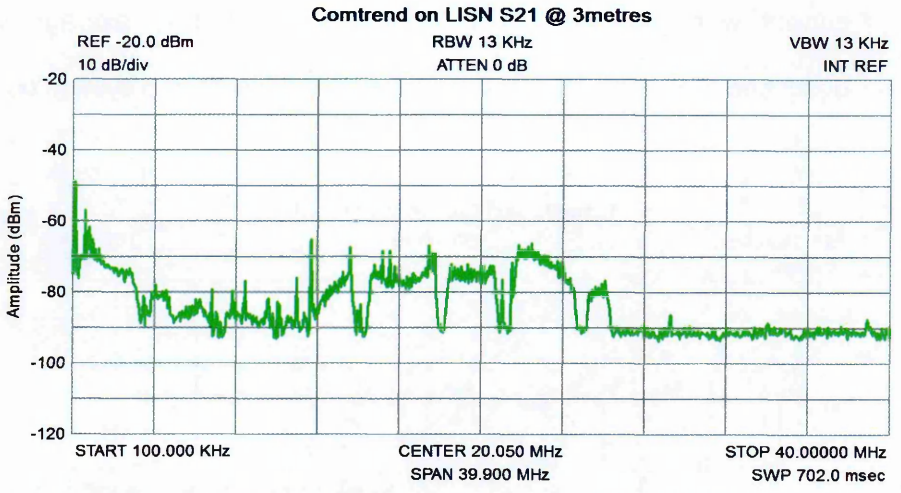

Figure 4.26.2 Profile of Comtrend radiated field via L-ISN

The average values for the measured Efield are given in Table 4.26.2 and we note that the magnitude of the radiated field is lower than expected from the common mode power recorded on the other tests. This may demonstrate that radiated emissions are distorted by testing via the L-ISN and we shall confirm the radiated values by testing the modems on the LVDN.

Parameter	Peak Calculated Value
Efield @ 3metres	43.27dBµV/m
Efield corrected to 10metres	32.18dBµV/m

Table 4.26.2 Comtrend S_{21} via L-ISN

4.27 BRAMBLE – PLT Measurements

The modems are now energised via the LVDN with all other circuits, as described above, connected and live.

Figure 4.27.1 below indicates the traces for the Comtrend modems operating (polling) on the ring main at Bramble. Both the differential mode voltage and

current were recorded as PEAK and converted to average values, as described in Section 4.6 above to allow calculation of the system power.

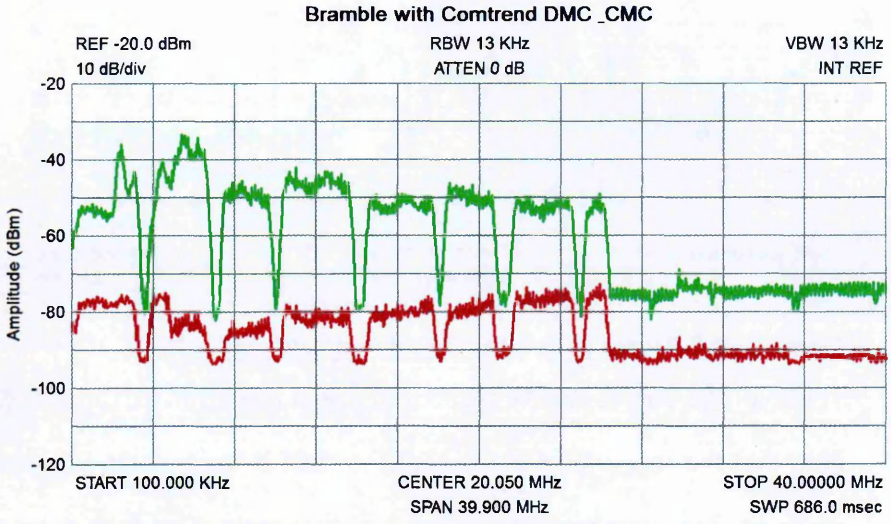

Figure 4.27.1 DMC & CMC for Comtrend on Bramble

When we compare the figures for Bramble as shown in Table 4.27.1, i.e. an injected swept signal and the Comtrend modem, we note that despite the variation in absorbed power the conversion loss remains nominally equal with the conversion of absorbed to common mode power un-influenced by the change in the LVDN. However, when we compare the radiated loss the LVDN is seen to produce less EMI when live and operating the modems. The radiated losses increase under the modem operation by 10dB and the gain relative to the equivalent isotropic radiation of the common mode power reduces by 10dB.

We can deduce that because the LVDN is now live with the phase and neutral conductors connected via the supply cable a proportion of the common mode power is circulated along the supply cable and reduces the energy being dissipated by the radiating elements of the LVDN.

	BRAMBLE	Bramble - Comtrend
Power Absorbed PA (dBm)	-11.2	-26.1
DMC (dBuA)	71.6	42.9
TCL (dB)	44.3	44.3
CMC (dBuA)	30.2	12.6
Conversion Loss (dB)	40.9	36.0
Common Mode Power (dBm)	-47.6	-64.4
S21 EFIELD @ 10m (dBuV/m)	52.4	27.0
Power Density via Efield (dBuV/m2)	-60.4	-87.0
Radiated Loss (dB)	14.9	24.7
Power Density via CM power (dBuV/m2)	-78.6	-95.4
Gain (dBi CM)	16.1	6.4

Table 4.27.1 Bramble Average Values

Equally we see, that the radiated field at 10 metres is clearly observed to be greater than the ambient noise floor and we can conclude that the Efield is 4dB higher than the noise floor across the 1-30MHz range. This agrees with the results of laboratory and field testing by the CRC (2009) who found that the maximum emissions from PLT devices in a typical residential house exceeded the average ambient noise levels by more than 30dB at distances of 3 metres and by 5 to 10dB at 10 metres from the outer wall of the house.

Recommendation ITU-R BS.703 stipulates that wanted radio signal at the location of HF radio broadcast receiver is either at or above the minimum usable field strength level of 40dBμV/m and we can note that this is not exceeded at 10 metres by the modem operation on any frequency.

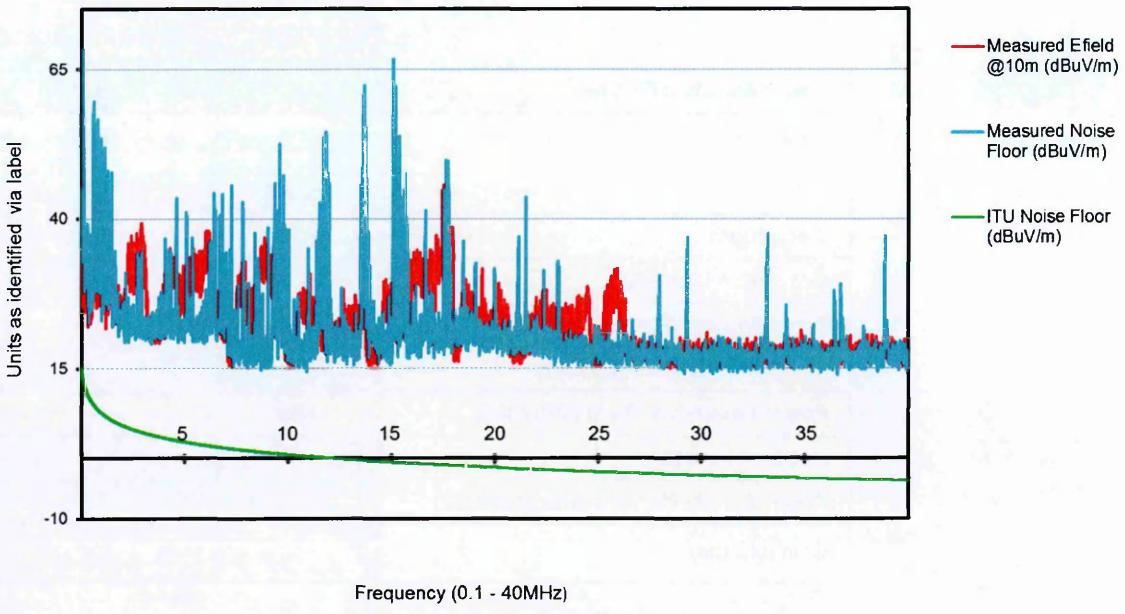

Figure 4.27.2 Graph of Efield with Noise Floor

The ITU noise floor figure, corrected for 9kHz bandwidth as described in Chapter 3, is also shown in Figure 4.27.2 and we can note that this is typically 20dB below the measured value at all frequencies. We also note that the common mode current recorded with the above Efield measurement was 12.6dBμA, as Table 4.27.1 and it therefore clearly demonstrates that values of CMC lower than that proposed under CISPR/I/257/CD remain capable of realising increases in the ambient noise floor. The proposed method for regulation of PLT based on either a noise floor or CMC limit appears not to be valid for the UK, given the inability to currently define this relationship.

4.28 Measurement Uncertainty

Whilst efforts have been made at each stage of the measurement and analysis to reflect on the results and compare values to other researchers a level of error may still exist within these figures.

Generally most equipment has been calibrated against Open University laboratory equipment, which is fully calibrated and has demonstrated that the probes and modems operated with approximately 1dB of error across the frequency range of interest.

As the swept signals are automatically recorded and exported to the Excel spreadsheet, as indicated in Appendix A there is little opportunity for error in calculation, however it is likely that a minimum of 3dB difference would exist in the event of repeating these measurements and calculations.

All measurements stated are average and not worst case, which are often quoted in EMC trials.

5.1 Introduction

As described in Chapter 2, despite the several hundred thousand powerline devices sold by BT there were surprisingly few complaints reported to OFCOM, and we therefore conclude with the analysis of this data via an overall model to describe some of the mitigation effects that have been observed from the measurements. In addition we shall also consider the further stated aims of this thesis and provide commentary on the following;

- Can a cohesive approach be provided to determine the RF properties of the typical domestic property?
- Is it possible to accurately determine the RF performance of the LVDN through a number of discrete and unobtrusive measurements?
- Can a LVDN transfer factor be confirmed within a proposed model? Is the commonly accepted figure of -30dBi appropriate to the UK housing stock?
- Finally, can those parameters which most significantly influence the EMI generated be determined and are we able to determine technical benefit for the use of conducted or radiated limits?

5.2 Model

It was described in Chapter 2 that many researchers have undertaken field trials on PLT systems and despite having completed significant measurement campaigns no overarching model of the LVDN has been produced to facilitate the need of the standards and regulatory bodies.

In order to progress this situation Chapter 4 describes the measurements carried out at a UK residential property and the individual circuits contained within.

When operating the Comtrend 902 modems via the LVDN we have shown that the radiated field equates to a gain of -29.7dBi at 10metres from the wall of the property and this not only verifies the use of this figure for general emissions. Studies but confirms that Bramble's RF signature represents that of a standard UK domestic property. Equally under this situation we have shown that with modems operating at -58dBm/Hz the LVDN produces a current to the common mode circuit of 18.6dBμA and this reflects in a radiated field 4dB above the measured ambient noise floor for a semi-rural location.

Therefore, we can conclude that application of the combined Japanese, CISPR/I/257/CD methodology would not achieve the proposed limitation on powerline derived radiated fields from a typical UK property.

Equally in order to understand how to minimise the radiated field and to what degree the common mode current and circuit configuration could influence such propagation, the following methods have been considered;

1. The derivation of power within the common mode circuit, via measurement of return loss and TCL, to allow calculation of the equivalent power density of an isotropic radiator at 10metres

2. The calculation of the Efield via measurement of the common mode current through use of the equations derived in Section 3.13. This

supposes that the phase and neutral conductors radiate as dipoles to produce a field directly proportional to the current.

These methods have resulted in a need to consider the power flow through the circuit as a whole and determine the associated losses, namely conversion and radiated losses, which relate directly to the above methods and are discussed below.

5.3 Conversion Loss

In order to calculate the common mode power we have utilised the measurement of return loss and TCL. The variation in these measurements together with the variation of impedance between the circuit types is reflected in the overall Conversion Loss, which relates the conversion from input power to common mode power. It was noted previously that Conversion Loss varies strictly in accordance with TCL and we note from Table 4.24.1 that the Conversion Loss for the overall LVDN is 38dB, with those circuits having low values of TCL showing a minimum Conversion Loss of 26dB.

We can therefore propose that irrespective of the makeup of the LVDN, in terms of the connected circuit types, the power delivered to the common mode circuitry will not be greater than the Absorbed Power less 26dB Conversion Loss.

The profile for the Conversion Loss, as demonstrated by Figure 5.3.1, will be unique and TCL dependant.

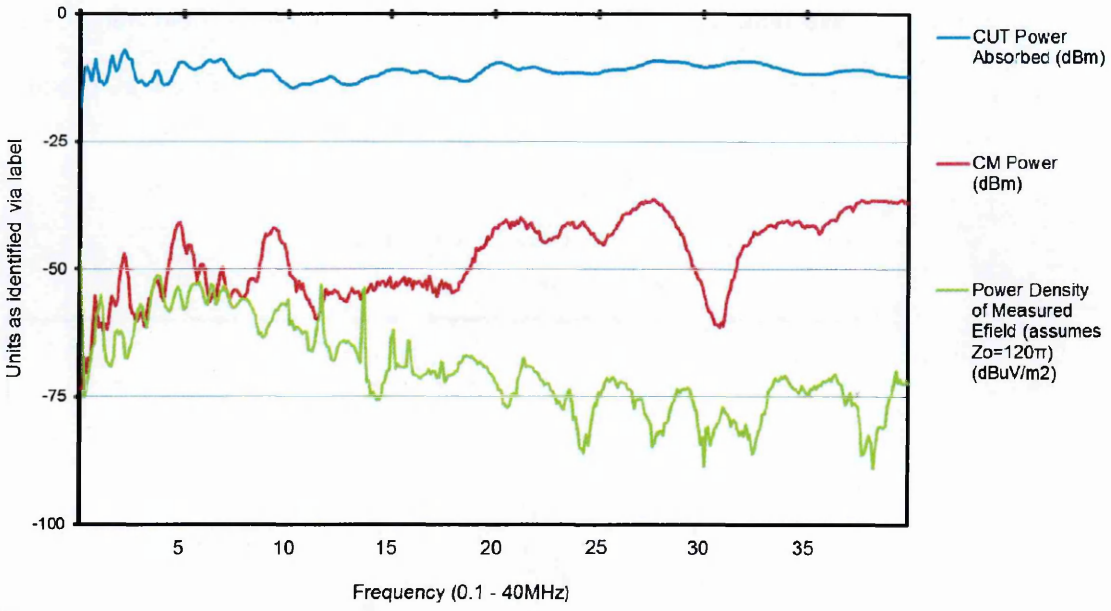

Figure 5.3.1 Power Graph for Bramble

Use of the Conversion Loss in this manner allows direct comparison of different circuit types and facilitates international discussion on PLT regulation. Clearly different circuit arrangements, constructed of different cabling will produce differing values of Conversion Loss. However, this would not only provide a bounding case for the injected power but also introduce a direct means to engineer better powerline circuitry, i.e. is metallic cable containment or newer cabling types preferable for example?

5.4 Radiated Loss

Figure 5.3.1 above indicates the power density of the measured field and we can compare this to the power density of the fields produced by the common mode power and common mode current as described above and shown in Figure 5.3.2.

We note that at the low frequencies the radiated field adheres to the theory given in Section 3.13 and mirrors the Calculated Efield as produced from the common mode current.

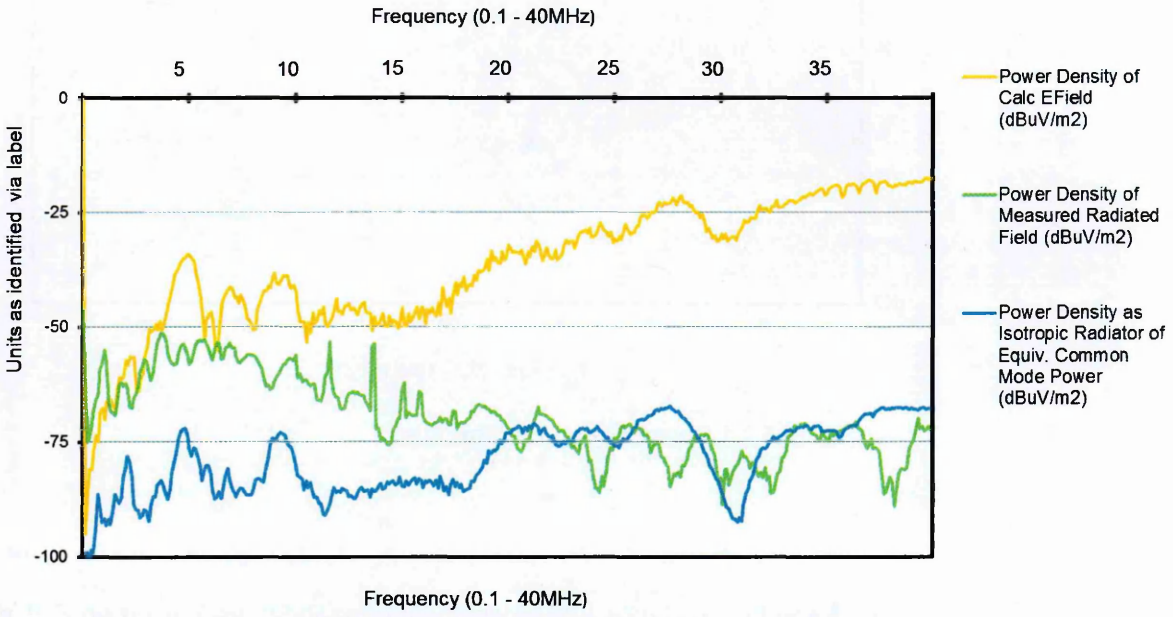

Figure 5.4.1 Power Density Graph for Bramble

At a frequency whereby the wavelength is comparable to the circuit length the circuit commences to radiate less effectively than a dipole and reduces in gain such that at 20MHz it is seen to radiate as an isotropic source of the equivalent common mode power. This arrangement is seen to occur to each of the individual circuits, with the exception of the cooker radial, as discussed earlier.

Given the general advances in powerline system bandwidth and the corresponding increase in the modem operating frequencies an inherent mitigation, or reduction, of the radiated field may result from the above effect. Further work may consider the optimum operating frequency vis-á-vis, typical

circuit lengths to demonstrate a radiated field strength at all frequencies representative of the equivalent isotropic field from the common mode power.

Also, more importantly, when the Comtrend modems are operated via a live circuit, with the LVDN connected to the phase and neutral conductors of the supply cable, we note that the radiated field at all frequencies approximates that of the isotropic common mode equivalent, as shown by Figure 5.4.2. Therefore, as confirmed by Hosoya (2009), who modelled and measured OFDM signal propagation through a switchboard, the circuit length now remains comparable to the signal wavelength at all frequencies.

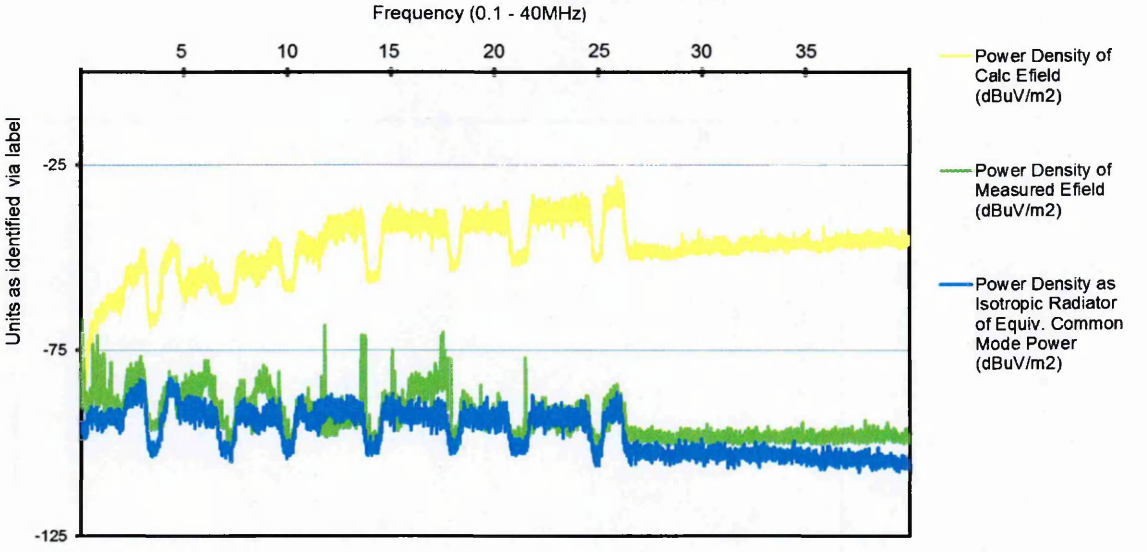

Figure 5.4.2 – Power Density Graph for Comtrend

We can therefore propose that the LVDN, when connected to the CBN and supply cable will radiate power from the common mode circuitry which will not be greater than the Common Mode Power less 27dB Radiation Loss.

5.5 Earthing

The measurements above, as Figure 5.4.1 indicate that the measured field reduces to provide a power density of magnitude equal to the isotropic equivalent of the common mode power. However, when we consider this with the current measured on the PME connection as shown in Figure 5.5.2 we note the following correlation.

It is demonstrated that as TCL decreases an increased common mode current will circulate via the multiple parts of the CBN and we note a direct inverse correlation between the TCL and current on the PME connection. This indicates that towards the higher frequencies a greater proportion of the CMC is circulated via the CBN.

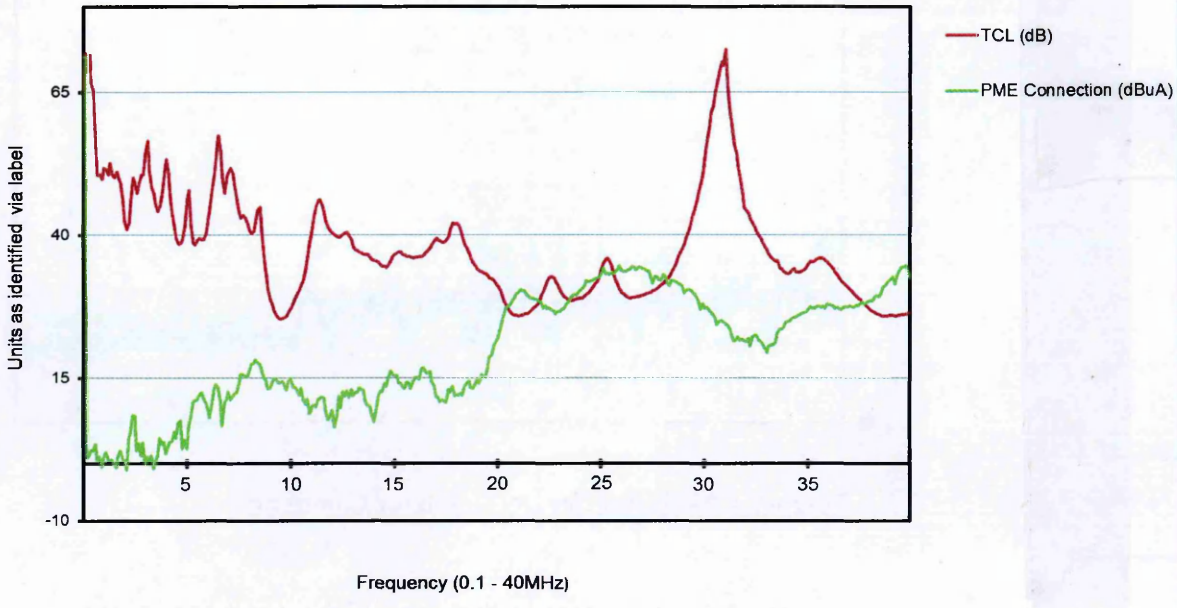

Figure 5.5.1 TCL and PME current for Bramble

Such an increase, when compared to the CMC measured on the LVDN, as the blue trace in Figure 5.5.2, shows that currents of a similar magnitude are seen to exist beyond 20MHz.

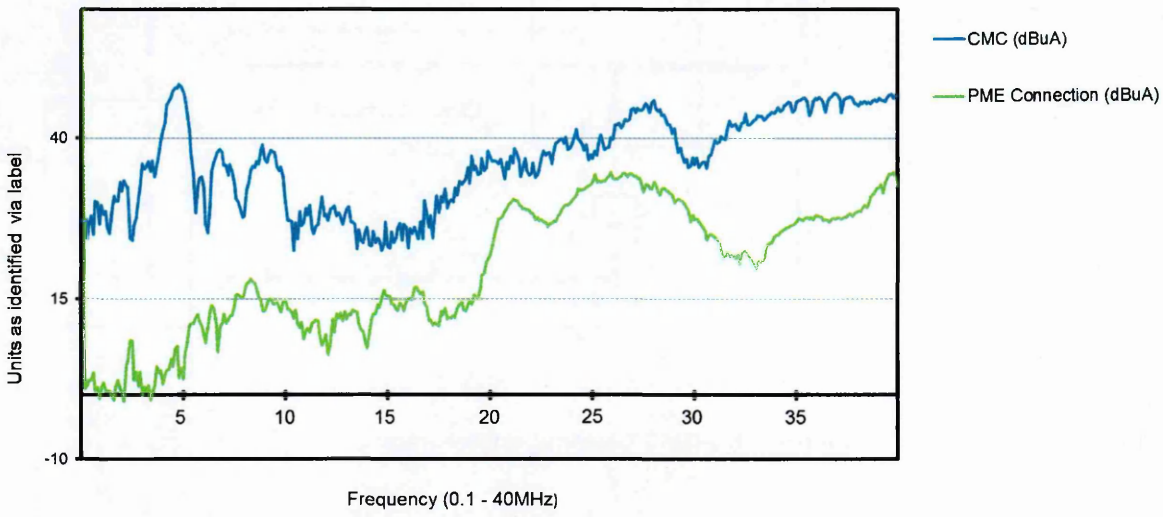

Figure 5.5.2 Comparison of LVDN CMC & PME CMC

Equally if we consider the circulation for these currents, which is shown in Figure 5.5.3 it is clear that the current within the CBN circulates generally within the equipotential bonding and earthing conductors towards the PME connection and therefore may produce a radiated field in anti-phase to that generated from the CMC in the phase and neutral conductors. Given that neither the dispersion of the current within the CBN, nor the physical arrangement of such conductors is known it is extremely difficult to model the interaction of these fields, however we can conclude that given the correlation of current to radiated field, as shown on the above graphs that this is the mechanism that is seen to reduce the radiated field from the theoretical calculated value to the isotropic value.

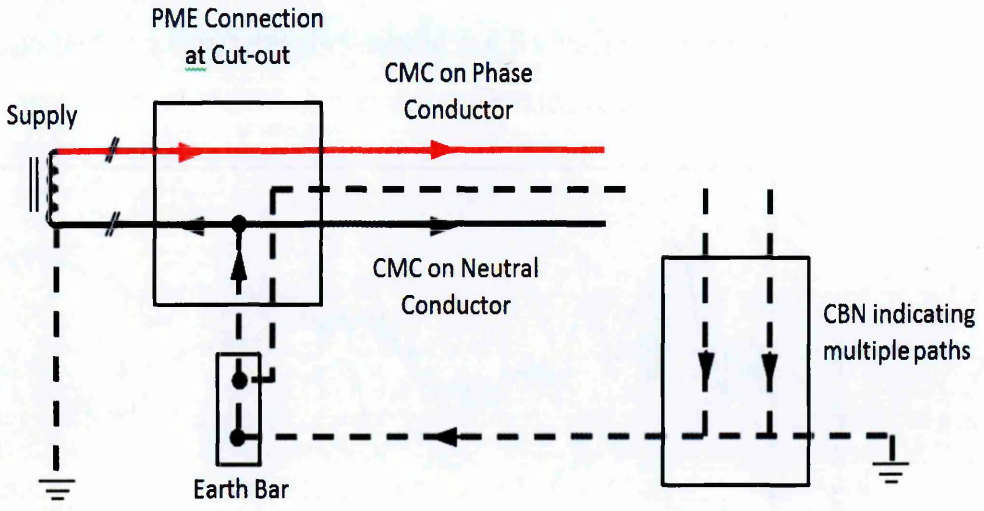

Figure 5.5.3 CMC Distribution Diagram

Arnautovski-Toseva (2011) using Method of Moments analysis demonstrated that a model of the radiated field from a short length of cable located within the fabric of a structure agreed with the measured radiated fields but to fully model the interactions of the complete CBN and LVDN is beyond current modelling abilities.

However, it is suggested that further work to model the unique property of the transmission line forming the LVDN i.e. that of the centrally located earth conductor, and the impact this may have on returning common mode currents and field cancellation is considered.

5.6 Overall Conclusion

We have seen that historically the powerline community has relied on k factor and gain (dBi) to describe the overall performance of PLT installations. This has been shown to provide limited use as both variation to the electrical

properties and antenna properties are combined with the single parameter. Through the measurement of limited parameters it has been shown in this thesis that the electrical and antenna properties relating to the LVDN can be found.

In order to therefore resolve the enigma of regulation and in which manner this is to be addressed we can confirm the following;

1. As described by the NSOs the measurement of the radiated fields from individual LVDNs does not appear appropriate given the increasing difficulty of achieving far field measurements and the unknown radiation patterns

2. Measurement of the common mode current alone has also been shown to be insufficient as direct correlation to the radiated field is not viable.

3. Modelling the radiated field is too complex due to the interaction of the LVDN and CBN.

It is therefore suggested that empirical modelling of further powerline installations be conducted, as described in this thesis, for different structures allowing the general development of a model as this approach. Such data will further our ability to consider the overall interaction of the LVDN with the CBN to determine the radiated field.

We can conclude by stating that the typical UK domestic property provides a maximum radiated field power density at 10 metres from the property which is 53dB less than the injected power. This figure reflects the current 1-30MHz

powerline spectrum and, as discussed in Chapter 6, defining such benchmarks will also benefit with the inevitable rise in modem frequencies.

6.1 Introduction

In considering the inevitable increase in the operating frequency of powerline technology the (ITU, 2010) have stated;

> *'it is very important to describe the physical generation mechanisms of the common mode current on the power line network' as this current is viewed as the principal source of radiated emission.*

This thesis has considered these mechanisms and related the distribution of power from injection of the HF signal applied to the LVDN to the radiation created by the common mode circuitry..

6.2 Areas of further study

Throughout this thesis the measurement of TCL has been recorded, and use of OU Macfarlane probe also allows measurement of LCL via the same probe, given the ability to reduce the impedance to the common mode port. As stated above most researchers have assumed reciprocity of the voltage creation between the differential and common mode circuits. However, the measurements undertaken above have noted subtle variation, i.e. 1-5dB at particular frequencies only. This suggests that full reciprocity is not provided and further study is required to resolve this conflict.

Equally, as stated above, the process for the measurement of TCL is currently ill-defined and there is little research to demonstrate that the ratio of differential to common mode voltages at the point of measurement reflects the

overall circuit, particularly where the point of measurement is some distance from the principal imbalance or load on the circuit. Further research into this area may be achieved via the modelling of the ring circuit, whilst imbalanced with known impedances connected at known locations, to allow validation of the waveforms in Figure 4.23.2 and allow a defined methodology to be developed for the measurement of TCL.

It is clear that the full effects of the radiation pattern resulting from the LVDN are little understood and that with further deployment of powerline products, as discussed below due to the smart grid will increase the density of such radiations. More works will be required to understand the radiation behaviour of the LVDN.

The general acceptance thus far of the PLT community to employ near field measurements whilst applying far field conditions will become more problematic, as the increasing frequency of powerline devices will result in the Raleigh distance exceeding the distance at which radiated signals can be measured.

6.3 Future Design

Despite the fact that powerline technology relies on an imperfect transmission line the evolution of powerline performance appears to adhere to Moores Law and bandwidth continues to increase. A feature of this increased bandwidth is a requirement for signal carriers to be spread across a greater portion of the spectrum and recent Comtrend products, achieving 500Mbps with advanced security encryption, are already operating at frequencies in excess of 100MHz.

As stated by the ITU (2010), this continuation of the use of higher frequencies will require the PLT community to understand some of the areas described above in order to allow development of the international regulation that has currently remained un-acceptable to NSOs and un-adopted by practitioners.

Equally without this understanding the expectation of the electrical industry to design the electrical distribution systems of the future, to aid the use of the LVDN as a medium for HF or even VHF transmission, is unrealistic and will not benefit the full realisation of the Smart Grid.

6.4 Smart Grid and Powerline of the Future

The Department of Energy and Climate Change (DECC), in response to the UKs requirement to reduce greenhouse gases, has conducted an analysis which suggests that there could be significant changes to both electricity generation and electricity demand which will impact electricity networks and system balancing. Such changes will include locally embedded generators, such as solar panels and wind turbines, and financial incentives to influence 'time of day' demand and achieve stable base loads for the suppliers.

To meet these challenges, the electrical distribution system needs to become more integrated while remaining flexible. Integration of both the generation and distribution of electricity with consumption will require 'smart' technology to be provided within the consumer's premises as the bridging technology between the RECs and the home network. The home network as a result will become more extensive including connection of the appliances as well as the fixed loads of lighting and heating in order to provide an effective and efficient control of energy consumption.

The expansion of powerline technologies within both distribution control and the home network arena will result in a far greater deployment of powerline products, which may consequently result in the need for a fully defined RF model of the LVDN.

Arnautovski-Toseva, V El Khamlichi Drissi, K Kerroum, K (2011). Antenna Mode Currents and Radiated Emissions of in-door PLC line within wall structure. IEEE International Symposium on Power Line Communications and its Applications, Udine, Italy, 3-6 April 2011, pp 231-236

Barclay L. (2012) Propagation of Radiowaves. 3rd Edition, Stevenage, UK: IET. ISBN 1849195781.

Brannon R, Haq T, Newbury, J, Morris K, Robertson F, Wills L and Summers I. (2005). Evaluation of key parameters for determining the efficiency of signal propagation in broadband PLT systems. IEEE International Symposium on Power Line Communications and its Applications, ISPLC 2005, Vancouver, 6-8 April, pp 228 – 232.

BSI (2007) Information technology equipment - Radio disturbance characteristics - Limits and methods of measurement. BS EN 55022:2006 +A1:2007

Butler L. (1989) Transmission Lines and Measurement of their Characteristics. Amateur Radio (Wireless Institute of Australia), October 1989, p1-11. (Available at http://users.tpg.com.au/users/ldbutler/TransLines.pdf accessed 22/01/14)

Carr, J. and Hippisley, G. (2011). Practical Antenna Handbook. New York: McGraw-Hill ISBN 0071639586.

Catrysse J. (2008). Correlation between unbalance and radiated fields in BPL structures. International Symposium on Electromagnetic Compatibility – EMC Europe 2008, Hamburg, 8-12 Sept 2008, pp 1-5.

Chandna V and Zahida M. (2010). Effect of varying topologies on the performance of broadband over power line. IEEE Transactions on Power Delivery Vol. 25, No. 4, 2010, pp 2371-2375

CISPR (2003). Initial results of FCC tests related to in-house Power Line Communications (PLC). CISPR/I Working Group 3 ISN Task Force 2003.

CISPR (2008). COMMITTEE DRAFT (CD) for EMC of Information technology, multimedia equipment and receivers CISPR/I/257/CD Document Number CISPR 22 am3 f1 Ed. 5.0.

Communications Research Centre Canada (2009) Measurement of In-house Power Line Telecommunication (PLT) Devices Operating in a Residential Environment Version: Draft 2.3 March 2009

Degauque P, Laly P, Degardin V, Lienard M and Diquelou L (2010). Compromising electromagnetic field radiated by in-house PLC lines. IEEE Global Telecommunications Conference (GLOBECOM 2010), Miami, 6-10 December, pp 1-5.

Denovo AG (2009) http://www.devolo.co.uk/consumer/dlan-200-av-wireless/pictures/image-picture-dlan-200-av-wireless-uk-livingroom-xl.jpg (accessed 02/06/10)

Donohoe (2012). Radiated emissions and susceptibility. Mississippi State University Department of Electrical and Computer Engineering. http://www.ece.msstate.edu/~donohoe/ece4323radiated_emissions.pdf (accessed 08/06/13)

Dostert, K. (2001). Powerline Communications. Upper Saddle River, NJ: Prentice-Hall ISBN 0130293423

Eland Cables (2009) http://www.eland.co.uk/electricalcable/fixedwiringcable/cable266/624-y-twin-and-earth.html (accessed 15/11/11)

ETSI (2003). Powerline telecommunication (PLT); basic low voltage distribution network (LVDN) measurement data. TR 102 270 V1.1.1 (2003-12).

ETSI (2008) PowerLine Telecommunications (PLT); Coexistence between PLT Modems and Short Wave Radio broadcasting services. ETSI TS 102 578 V1.2.1 (2008-08)

European Commission (2001). Standardisation mandate addressed to CEN, CENELEC and ETSI concerning electromagnetic compatibility (EMC), Telecommunications Networks; M/313, 07.08.2001.

European Union (2003), questionnaire relating to the draft Product Family emission standard for telecommunication networks - (03)10_04 July 2003

Favre P, Candolfi C, Schneider M, Rubeinstein M, Krahenbuehl P and Vukicevic A. (2007). Common mode current and radiations mechanisms in PLC Networks. IEEE International Symposium on Power Line Communications and its Applications, Pisa, 26-28 March 2007, pp 348-354

Ferreira HC, Lampe L, Newbury J and Swart TG (eds.) (2010). Power Line Communications: theory and applications for narrowband and broadband communications over power lines. Chichester, Sussex: Wiley ISBN 0470740302.

Hansen, D (2002). Update on power line telecommunication (PLT) activities in Europe. IEEE International Symposium on Electromagnetic Compatibility, Minneapolis, Minnesota, 19th-23rd August 2002, pp 17-22.

Haq T (2012). Investigation into the impedance and communication requirements for the low voltage distribution line in the high frequency spectrum. PhD thesis, The Open University.

Hrasnica H, Haidine A and Lehnert R (2004). Broadband Powerline Communications: Network Design. Chichester, Sussex: Wiley. ISBN 0470857412.

Hosoya S and Tokuda, M. (2009). OFDM Signal Transmission Characteristics through a Switchboard for a Power Line Communication. IEEE International Symposium on Power Line Communications and Its Applications, ISPLC 2009, Dresden, 29 March - 1 April, pp 119-124

IET/BSI (2008). BS 7671:2008 Requirements for Electrical Installations 17th Edition.

Ishigami S, Gotoh K and Matsumoto Y (2007), Effect of structure and materials of building on EM fields generated by indoor power line communication systems. EMC Europe Workshop 2007, Paris; 14-15 June, 2007.

ITU (1996) ITU-T Recommendation G.117 Transmission Aspects of Unbalance about Earth (02/96)

ITU (2009) Commentary on work in ITU-R on Power Line High Data Rate Telecommunication Systems 2009, Doc. PT46(09)044

ITU (2010) Impact of power line telecommunication systems on radiocommunication systems operating in the LF, MF, HF and VHF bands below 80 MHz. Report ITU-R SM.2158-2.

ITU (2011) SERIES K: Protection Against Interference - Method for measuring longitudinal conversion loss (9 kHz - 30 MHz) Recommendation ITU-T K.86

Jia, J, Rinas, D and Frei, S (2012). Predication of radiated fields from cable bundles based on current distribution measurements. 2012 International Symposium on Electromagnetic Compatibility, EMC Europe, Rome, 17-21 September 2012, pp 1-7

Kitagawa M. and Ohishi M. (2008). Measurement of the radiated electric field and the common mode current from the in-house broadband PLC in

residential environment. International Symposium on Electromagnetic Compatibility, EMC Europe 2008, Hamburg, 8-12 September, pp1-6.

Kitagawa M. (2009) LCL and common mode current at the outlet do not tell the common mode current generated at the remote unbalanced element on the power-line. 20th International Zurich Symposium on Electromagnetic Compatibility, Zurich, 12-16 January 2009, pp 1-4.

Koch M (2009) Average Reduction of the PLC mask by PLC Management. CISPR/I/PT PLT, June, 2009

Lauder DM and Sun Y (2005). Modelling and measurement of radiated emission characteristics of in-building and telecommunication cables. Proceedings of the IEE Seminar on EMC and Broadband for the Last Mile, London, May 2005.

Luo W, Tan S and Tan B. (2005) Effects of the ground on power-line communications. IEEE Transactions on Microwave Theory and Techniques, Vol. 53, No. 10, 2005 pp 3191-3197

Macfarlane IP (1999). A probe for the measurement of electrical unbalance of networks and devices. IEEE Transactions on Electromagnetic Compatibility, 41 (1), pp 3-14.

Magesacher T, Henkel W, Tauböck G and Nordström T. (2002) Cable Measurements supporting XDSL Technologies. e&i Elektrotechnik und Informationstechnik. February 2002, **119** (2), pp 37-43

Mahbub Ar Rashid AKM, Kuwabara N, Maki M, Akiyama Y and Yamane H. (2003). Evaluation of longitudinal conversion loss (LCL) for indoor AC mains line. 2003 IEEE International Symposium on Electromagnetic Compatibility, Boston, 18-22 August, Volume 2 pp 771-776.

Miyoshi K, Kuwabara N, Akiyama Y and Yamane H. (2005) Calculation of radiating magnetic field from indoor AC mains cable using four-port network. IEEE International Symposium on Electromagnetic Compatibility, Chicago, 8-12 August 2005, Volume 3 pp 1002-1007

NATO (2008) Potential Effects of Broadband Wire-Line Telecommunications on the HF Spectrum (2008) Document Reference RTO-MP-IST-083

Newbury J, Fenton D, Brannon R, Robertson F. (2007). The assessment and measurement of the signal regression of broadband power signals in the frequency range 1.6MHz to 30MHz over the low voltage distribution network. IEEE International Symposium on Power Line Communications and its Applications, 2007. ISPLC '07, Pisa, 26-28 March, p 10

OFCOM (2010). Powerline telecommunications (PLT). http://stakeholders.ofcom.org.uk/enforcement/spectrum-enforcement/plt/ (accessed 08/06/13)

OFCOM/PA Consulting Group (2010). The likelihood and extent of RFI from in-home PLT devices.

http://stakeholders.ofcom.org.uk/market-data-research/other/technology-research/research/emerging-tech/PLT (accessed 08/06/13)

Oka N, Kanda M, Konishi Y, Morita A, Kato M. and Nitta S. (2007). Reduction of radiated emission from PLC systems by studying electrical unbalance of the PLC device and T-ISN. IEEE International Symposium on Electromagnetic Compatibility, EMC 2007, Honolulu, 9-13 July, pp 1-5.

Okugawa Y,Mokushi K, Yoshioka H, Abe T, Takaya K and Toyonaga M (2009). Investigation on the influence of VDSL transmission speed and radiated electric field strength due to unbalance in metallic communication lines. 2009 IEICE EMC, Kyoto, 20-24 July 2009, pp 641-644

Pang T, So P, See K, Kamural A (2008). Modelling and Analysis of Common-Mode Current Propagation in Broadband Power-Line Communication Networks IEEE Transactions on Power Delivery, Vol. 23, No. 1, 2008 pp 171-178

Pascagaza JFH and Martin DH (2011). Measurement of longitudinal conversion loss (LCL) in semi anechoic chambers from 150kHz to 300MHz. 10th International Symposium on Electromagnetic Compatibility (EMC Europe 2011), York, UK, September 26-30, 2011, pp 240-244.

Paul C (2006) Introduction to Electromagnetic Compatibility. Hoboken, NJ: Wiley-Interscience ISBN 0471758140

Pink, J. (2012). Draft standard 50561-1 receives a positive vote'. Southgate Amateur Radio News, 21 November 2012 http://www.southgatearc.org/news/november2012/draft_standard_50561_1_receives_a_positive_vote.htm#.ULy0h4PeQQg (accessed 3 December 2012)

Rodriguez-Morcillo C, Rubinstein A, Rubinstein M, Rachidi F and Vukicevik A. (2009). Experimental verification of common-mode current generation in home electrical wiring in the powerline communications band. IEEE International Symposium on Powerline Communications and its applications, ISPLC 2009, Dresden, 29 March - 1 April, pp58-61.

Rohde & Schwarz (2008). ENY81 coupling network data sheet. http://www.rohde-schwarz.co.uk/file/ENY_81_dat_en.pdf (accessed 08/06/13).

RSGB (2012). The RSGB position on powerline adapters and the proposed European standard FprEN 50561-1. Radcom, October 2012, pp 7-8.

Salehian K, Wu Y, Lafleche S, Gagnon G and Einolf C. (2011). Field measurements of EM radiation from in-house power line telecommunications (PLT) devices. IEEE Transactions on Broadcasting, 57 (1), pp 57-65.

Schmitt R. (2002). Electromagnetics Explained. Amsterdam, Boston: Newnes. ISBN 0750674032.

Schwager (2010) PhD Thesis Powerline Communications: Significant Technologies to become Ready for Integration University of Duisburg-Essen.

See KY, Kamarul A and So PL (2005). Longitudinal conversion loss of power line network for typical Singapore household. 7th International Power Engineering Conference, IPEC 2005, Singapore, 29 Nov - 2 Dec, pp 1-6

Semtech International AG (2007). TN1200.04 Calculating radiated power and field strength for conducted power measurements. http://www.semtech.com/images/datasheet/semtech_acs_rad_pwr_field_strength_ag.pdf (accessed 08/06/13)

Shannon CE (1949). Communication in the presence of noise. Proceedings of the IRE, 37 (1), pp 10-21.

Vukicevic A, Rubinstein M, Rachidi F. and Bermudez, J-L. (2006) On the mechanics of differential-mode to common-mode conversion in the broadband over power line (BPL) frequency band. 17th International Zurich Symposium on Electromagnetic Compatibility, EMC-Zurich, Singapore, 27 Feb - 3 March, pp 658-661.

Verpoorte J. (2003) Application of the LCL method to measure the unbalance of PLC equipment connected to the low-voltage distribution network. CISPR, Sub Committee I, Working Group 3.

Wellbrook (2012) Wellbrook ALA1530 Antenna Factor Chart http://www.wellbrook.uk.com/pdf/ALA1530AntennaFactorChart.pdf (accessed 26/06/13)

Williams T. and Armstrong K. (2000). EMC for Systems and Installations. Oxford, Boston: Newnes. ISBN 0750641673.

Williams T. (2009). Why broadband PLC is bad for EMC. EMC Journal Issue No. 80 (Jan 2009) pp 25-34.

Wirth (2003) Radiated Impact of Signals on the Mains, CISPR CISPR/I/TFISN (Wirth) 03-01 (CISPR committee paper)

Wright, M (1990) Common mode Current Measurements and Radiated Emissions from long cable systems. IET Conference Publications Seventh International Conference on Electromagnetic Compatibility 1990, Washington DC, 21-23 August, pp 19-23

Wu I, Ishigami S, Gotoh K and Matsumoto Y. (2008). Attenuation effect of the wall structure on the electric field generated by indoor power line communication system. 2008 International Symposium on Electromagnetic Compatibility - EMC Europe, Hamburg, 8-12 September, pp 1 – 5.

Wu L, Su D, Chen J and Wu N (2010). Radiated emission analysis of wires. 9th IEEE International Symposium on Antennas Propagation and EM Theory, Guangzhou, China, 29 Nov - 2 Dec 2010, pp 998-1001

Yuichiro O, Kentaro M, Hiroshi Y, Tsutomu A, Kazuhiro T and Masanobu T. (2009). Investigation on the Influence on VDSL Transmission Speed and Radiated Electric Field Strength due to Unbalance in Metallic Communication Lines. IEICE EMC Conference 2009, Kyoto, 20-24 July, pp 641-644

Zhang M. and Lauber W. [2008] Evaluation of the interference potential of in-home power line communication systems. IEEE International Symposium on Power Line Communications and its Applications, ISPLC 2008, Jeju Island, Korea, 2-4 April, pp 263-268.

Zheng T, Yang X, Zhang B. (2006) Broadband transmission characteristics for power-line channels. IEEE Transaction on Power Delivery, Volume 21, No. 4, October 2006 pp 1905

Zimmermann M. and Dostert K. (2002). A multipath model for the powerline channel. IEEE Transactions on Communications, Volume 50 (Issue 4), April 2002 pp 553-559.